Cranfield University

School of Aerospace, Transport and Manufacturing

Muttuswamy Sivakumaran

'Towards the development of Molecularly Imprinted Polymer (MIP) for lineage specific cell surface antigens used in cancer diagnosis'

MSc by Research

Academic Year: 2016-2018

Supervisors

Dr Iva Chianella, Professor Ibtisam Tothill & Dr Gregory Bizarri

Cranfield University

School of Aerospace, Transport and Manufacturing

Muttuswamy Sivakumaran

‘Towards the development of Molecularly Imprinted Polymer (MIP) for lineage specific cell surface antigens used in cancer diagnosis’

MSc by Research

Academic Year: 2016-2018

Supervisors

Dr Iva Chianella, Professor Ibtisam Tothill & Dr Gregory Bizarri

ABSTRACT

Immunohistochemistry using antibodies plays a pivotal role in the diagnosis of various solid cancers and haematological malignancies such as leukaemias, lymphomas and myelomas. However, antibodies have a number of disadvantages including its high cost, requirement for refrigeration for transport and storage and its limited shelf life. Hence, the search for a sensitive and specific diagnostic platform that is robust and reproducible and one that utilises a capture ligand which is easy and cheap to manufacture and is stable at room temperature with a long shelf life. Such diagnostic platform would be particularly useful in developing countries, where facilities for storage and transportation at sub-zero temperatures are limited. Molecularly Imprinted Polymers (MIPs), one of the rapidly advancing technologies for nanodiagnostics, may offer such a solution in cancer diagnostics.

This exploratory study was undertaken to investigate whether MIP nanoparticles synthesised using the solid-phase approach and epitope imprinting method have potential to replace antibodies in cancer diagnosis. The common leucocyte antigen or CD45 protein which is universally expressed on haemopoietic cells was chosen as the candidate for molecular imprinting because the expression of this antigen can differentiate blood cancers from other neoplasia. In order to make the process cost-effective, a custom-made peptide template with the amino acid sequence that is widely used for anti-CD45 antibody production was used for imprinting. A modification to the amino acid sequence of the template was made by adding the amino acid cysteine which has a thiol group, to the carboxyl end of the CD45 template peptide and anchored to silica nanoparticles to improve the homogeneity of the imprinted polymers. Synthesis of MIPs was carried out using two different compositions of functional monomers, one with a 'standard' mix of monomers and the other one containing a fluorinated monomer. The characterisation of the synthesised nanoMIPs and the binding of the target protein to the MIPs were studied using dynamic light scattering (DLS) and tunable resistive pulse sensing (TRPS).

The results of this study prove that the solid-phase synthesis using a custom made polypeptide as the template (segment imprinting) is a logical approach. One important technical refinement is the immobilisation of the template protein to the silica beads in a single orientation *via* the amino acid cysteine. This modification resulted in the production of

more uniform nanoMIPs with low polydispersity. Another significant observation of this study is that the use of fluorinated monomer in combination with the 'standard functional monomers' for the MIP synthesis has improved the quality of the nanoMIPs produced. Furthermore, this study has successfully explored, for the first time, the usefulness and applicability of the technique of tunable resistive pulse sensing (TRPS) for the characterisation of nanoMIPs. The preliminary results obtained in this study indicates that this technique may be superior to dynamic light scattering (DLS) for not only measuring the size and size distribution of the particles but also to study MIP-target interactions. The TRPS analysis of the changes in the zeta potential of the nanoMIPs has shown that the CD45 epitope imprinted nanoMIPs bind to the CD45 protein.

Key words: Cancer diagnosis, Common Leucocyte antigen, CD45 protein, Molecularly Imprinted Polymers, NanoMIPs, Solid Phase synthesis, Epitope printing, Dynamic Light Scattering, Tunable Resistive Pulse Sensing.

ACKNOWLEDGEMENTS

There are several individuals and departments I should thank for their kind support, help and guidance with this project but first and foremost I would like to thank Dr Iva Chianella, my Supervisor, for her continuous support and guidance throughout the course of this research which I must add has not always been smooth running. It would not be an overstatement to state that without the help and encouragement of Dr Chianella, this research project would not have been completed. I would also like to thank Professor Ibtisam Tothill who was my chief supervisor at the beginning for her kind support, advice and guidance and Dr Gregory Bizarri for his support.

I am indebted to Professor Sergey Piletsky (University of Leicester) for providing me unrestricted facilities to carry out synthesis of nanoMIPs in his laboratory under the expert guidance of Dr Francesco Canfarotta. I would also like to thank Dr Tom Bedwell in the same laboratory for his technical advice and help.

I am very grateful for Dr Mark Platt and Mr Rhush Maughi at Loughborough University Chemistry department for their assistance and advice with TRPS analysis.

My sincere thanks to the Peterborough City Hospital Haematology Research fund for funding the purchases of CD45 protein and CD45 epitope peptides. Finally, I would like to say a big 'thank you' to the Laxton Library team at Peterborough City Hospital, Peterborough for their help with obtaining article reprints and book loans for this project.

TABLE OF CONTENTS

LIST OF FIGURES

LIST OF TABLES

APPENDICES

LIST OF ABBREVIATIONS

AAc	Acrylic acid
AAm	Acrylamide
ABC	Avidin-Biotin Conjugate
AFP	Alpha Feto Protein
ALK	Anaplastic Lymphoma Kinase
AMACR	Alpha-methylacyl-CoA Racemase
AMP	Adenosine Monophosphate
APAAP	Alkalinephosphatase-antialkaline phosphatase
APMA	*N*-(3-Aminopropyl)methacrylamide hydrochloride
APS	Ammonium persulfate
APTES	3-Aminopropyltriethoxysilane
ATP	Adenosine Triphosphate
BCA	Bicinchoninic acid
BCL-2	B Cell Lymphoma-2
BCR-ABL	Breakpoint Cluster Region-Abelson
BET	Brunauer-Emmett-Teller
BIS	N,N′-Methylenebisacrylamide
BSA	Bovine Serum Albumin
CALLA	Common Acute Lymphoblastic Leukaemia Antigen
cAMP	Cyclic Adenosine Mono Phosphate
CaTe	Cadmium Telluride
CCR-4	Chemokine Receptor Type 4
CD	Cluster of Differentiation
CEA	Carcino Embryonic Antigen
CEC	Capillary Electrochromatography
CK	Cytokeratin
CLC	Capillary Liquid Chromatography
DAB	diaminobenzidine
DFT	Density Functional Theory
DLS	Dynamic Light Scattering
DNA	Deoxyribose nucleotide
dsDNA	Double Stranded DNA
EDTA	Ethylene diamine tetraacetic acid
EGDMA	Ethylene glycol dimethacrylate
ELISA	Enzyme Linked Immunosorbent Assay
FISH	Fluorescent In-Situ Hybridisation
FITC	Fluorescein Isothiocyanate
FRET	Fluorescence Energy Transfer
5 FU	5 Fluouracil
GP	Glycoprotein
GPTMS	Glycidoxypropyltrimethoxysilane
H&E	Haematoxylin&Eosin
HEMA	2-Hydroxyethyl methacrylate
HPLC	High Performance Liquid Chromatography
HIV	Human Immunodeficiency Virus
HSP	Heat Shock Protein
ICC	Immunocytochemistry

IHC	Immunohistochemistry
IPTS	3-isocyanatopropyl triethoxysilane
LDL	Low Density Lipoprotein
MAA	Methacrylic acid
MGG	May-Grunwald-Giemsa
MIP	Molecularly Imprinted Polymer
MISPE	Molecularly Imprinted Solid Phase Extraction
MMA	Methyl methacrylate (MMA)
MMIPs	Magnetic MIPs
MPO	Myeloperoxidase
MPTS	Methylacryloxyprolyl trimethoxysilane
MVDS	Methylvinyldiethoxysilane
NaCl	Sodium chloride
NaOH	Sodium hydroxide
NFP	Neurofilament protein
NIPAm	*N*-Isopropylacrylamide
NMR	Nuclear magnetic resonance
PAD	Pulsed Amperometric Detection
PAP	Peroxidase-Antiperoxidase
PBS	Phosphate buffered saline
PCS	Photon Correlation Spectroscopy
PDI	Polydispersity index
PML-RARA	Promyelocytic leukaemia-retinoid receptor alpha
PrEST	Recombinant Protein Epitope Signature Tag
ProGRP	Pro Gastrin Releasing Peptide
PSA	Prostate Specific Antigen
PSMA	Prostate Specific Membrane Antigen
PTPRC	Protein tyrosine phosphatase receptor type C
QCM	Quartz Crystal Microbalance
QELS	Quasi Elastic Light Scattering
RNA	Ribose nucleotide
RPS	Resistive Pulse Sensing
SEM	Scanning Electron Microscopy
SERS	Surface Enhanced Raman Scattering
SIA	N-hydroxysuccinimide ester
SPE	Solid-Phase Extraction
SPR	Surface Plasmon Resonance
TBAm	*N*-tert-Butylacrylamide
TDT	Terminal Deoxynucleotidyl Transferase
TEM	Transmission Electron Microscopy
TEMED	*N*,*N*,*N*′,*N*′-Tetramethylethylenediamine
TFMAA	Trifluoromethyl acrylic acid
TGA	Thermogravimetric analysis
TLC	Thin Layer Chromatography
TRPS	Tunable Resistive Pulse Sensing
VEGF	Vascular Endothelial Growth Factor
VP	Vinylpyridine
VSM	Vibrating Sample Magnetometer

CHAPTER 1 INTRODUCTION

1.1 Background

Currently cancer diagnosis relies on conventional cytochemistry/histochemistry for initial morphological evaluation and immunocytochemistry/immunohistochemistry for more precise analysis of the tumour characteristics including its lineage, subtype, prognostic markers and malignant potential (Bain BJ, 2017 ; Dabbs D, 2018). In the former, cells or tissue specimens are stained with chemical dyes such as haematoxylin/eosin or Giemsa stain and examined microscopically. Immunocytochemistry (ICC) and Immunohistochemistry (IHC) are, on the other hand, specialised techniques used to detect the presence of a specific protein or antigen in cells by use of a specific antibody that binds to it. ICC and IHC are valuable tools to study the presence and sub-cellular localisation of proteins. The antigen-antibody binding is detected by using either fluorescent labels or traditional enzymatic conversion of dye substrates (Dabbs D, 2018; Merighi and Lossi, 2015). ICC and IHC using monoclonal or polyclonal antibodies against various cell surface or cytoplasmic antigens play a pivotal role in the diagnosis of various solid cancers and haematological malignancies such as leukaemias, lymphomas and myelomas (Bain BJ, 2017).

Whilst antibody based techniques have become a routine diagnostic modality in most Pathology laboratories, it must be emphasised that antibodies (hence antibody based techniques) have a number of disadvantages. These include high cost, mostly require the use of animals for their production, which is unethical, require special storage conditions (refrigeration), with limited shelf life and require specific and often restricted conditions for optimum antigen binding. Most antibody based tests often require an additional step using secondary antibodies (fluorescent labelled or enzyme linked) to improve their sensitivity. For these reasons, a sensitive and specific diagnostic platform that is robust and reproducible and one that utilises a capture ligand which is easy and cheap to manufacture and is stable at room temperature without special storage conditions and a method that doesn't require any additional steps for signal amplification would be a valuable introduction to the diagnostic armamentarium of any clinical laboratory. Such diagnostic platform would be particularly

useful in developing countries, where facilities for storage and transportation at sub-zero temperatures are limited. Molecularly Imprinted Polymers (MIPs), one of the rapidly advancing technologies for nanodiagnostics, may offer such a solution in cancer diagnostics.

1.2 Cancer Diagnosis

Cancer diagnosis is a highly specialised process involving several disparate techniques and technologies. The initial step is to obtain a suitable diagnostic material. In the case of solid cancers where the malignant cells form a tumorous growth (or lump), the diagnostic material is often obtained by a large bore needle or a ‘truecut’ biopsy using a purpose made contraption or an open biopsy where a surgeon obtains a piece of the tissue by surgery. In blood cancers, however, the diagnostic materials are often peripheral blood and bone marrow aspirate/trephine biopsy. The biopsy material obtained from a solid tumour is then 'fixed' in a fixative such as formalin to preserve the integrity of tissues and cells in the sample. The fixed biopsy sample is then embedded in paraffin wax and cut into thin slices by a microtome and placed on glass microscope slides prior to staining (Babbs D, 2018; Svarna et al, 2018; Swerdlow *et al*, 2017).

'Liquid tumour' samples such as blood, bone marrow aspirate, cerebrospinal fluid and effusions (e.g. ascitic fluid, pleural fluid) are collected and processed differently. Blood is routinely collected into an anticoagulant medium (e.g. EDTA, citrate) to prevent clotting. A tiny drop of anticoagulated blood is directly placed on a glass microscope slide and immediately smeared using another glass slide. The slide with the smear is left to dry completely and 'fixed' in a fixative such as ethanol to preserve the integrity of the cells before staining (Bain BJ, 2016).

Bone marrow aspirate samples can be processed in two ways. The aspirate is treated like a blood sample i.e. collected in an anticoagulant tube and marrow smears are made on glass slides and fixed prior to staining. However, the more commonly used practice is to make a smear using fresh non-anticoagulated sample i.e. drops of bone marrow aspirate samples placed on glass microscope slides immediately upon collection (before it clots) and smeared using another glass slide, dried and fixed using a fixative (alcohol) prior to staining (Bain BJ, 2016).

Because the cell content of specimens such as cerebrospinal fluid, ascitic fluid and pleural effusions tend to be low, they are first centrifuged to sediment the cells and remove the supernatant prior to preparing smears (so-called cytospin prep).

1.2.1 Laboratory Techniques for Cancer Diagnosis

A variety of techniques are routinely used for the laboratory diagnosis of various diseases including malignant and non-malignant conditions. The most commonly used diagnostic techniques are listed below (Babbs D, 2018; Bain BJ, 2016; Svarna et al, 2018; Swerdlow *et al*, 2017)

- Morphological evaluation of cell smears stained with conventional dyes using light microscopy (Cytochemistry).
- Morphological evaluation of tissue biopsy specimens stained with conventional dyes using light microscopy (Histochemistry).
- Microscopic analysis of the expression of various cellular antigens using specific antibodies (immunocytochemistry/immunohistochemistry).
- Flow cytometric analysis of the expression of various cellular antigens using specific antibodies.
- Fluorescent in-situ hybridisation (FISH).
- Molecular analysis of genetic abnormalities (gene mutations, deletions, rearrangements, translocations etc).
- Gene sequencing.

1.2.1.1 Cytochemistry in Cancer Diagnosis

Morphological examination of blood and bone marrow aspirate smears is an essential step in the diagnosis of haematological malignancies such as acute/chronic leukaemias, lymphomas and myelomas (Bain BJ, 2016 & 2017). The most widely used cytochemical stain used for microscopic evaluation of blood/marrow smears is May-Grunwald-Giemsa (MGG) stain. This stain produces excellent definition of cellular features such as cell membrane, cytoplasm, cytoplasmic contents and nucleus. Examples of images of MGG stained blood smears of

patients with acute myeloid leukaemia, chronic lymphocytic leukaemia, high grade Non Hodgkin's lymphoma and multiple myeloma are shown in Figure 1.1 (A-D).

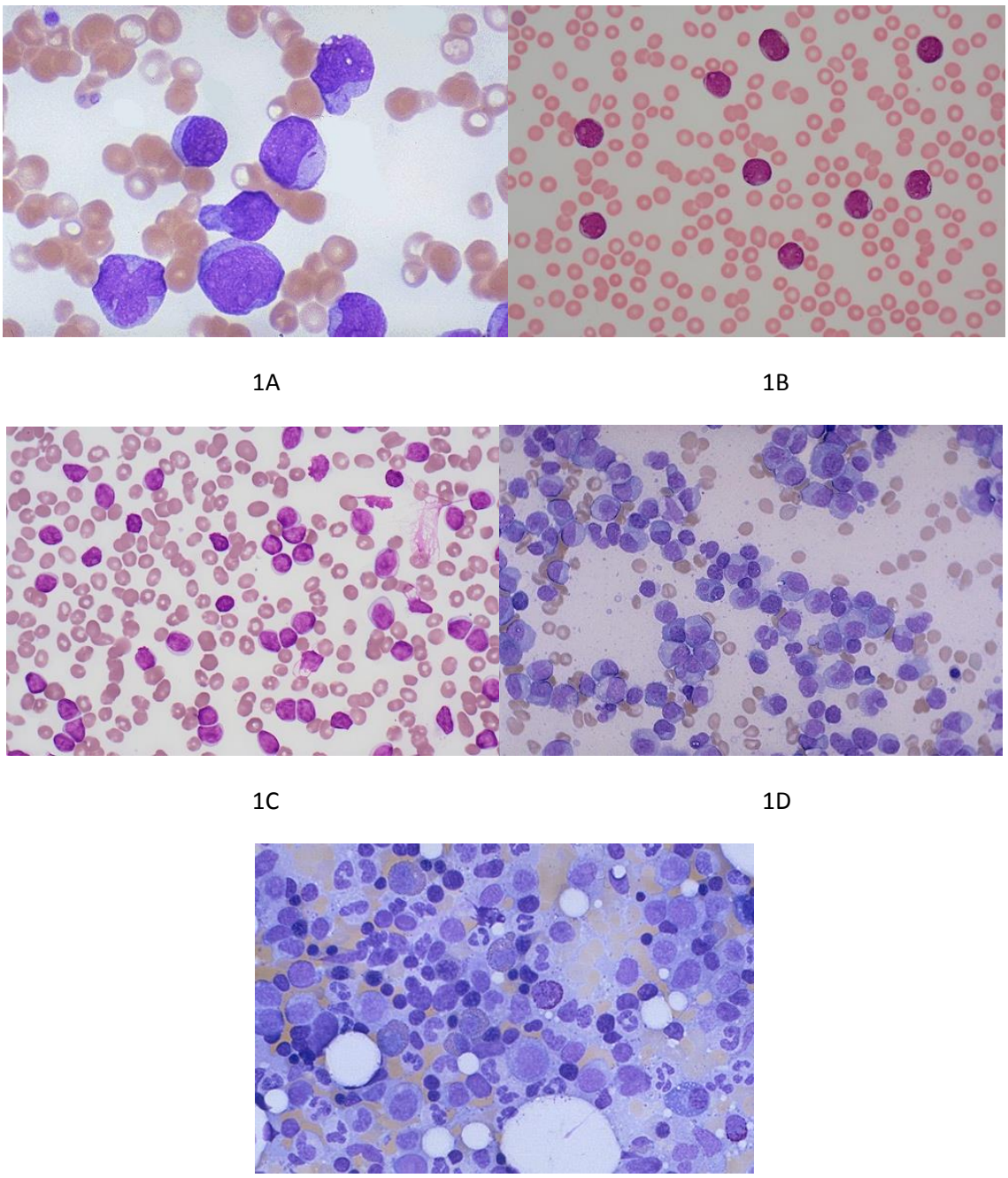

1A 1B

1C 1D

1E

Figure 1.1 Cytochemistry in Cancer Diagnosis. Light microscopic evalution of blood/bone marrow smears stained with May-Grunwald-Giemsa (MGG) stain

A- Acute Myelod Leukaemia
B- Acute Lymphoblastic Leukaemia
C- Chronic Lymphocytic Leukaemia
D- Multiple myeloma
E- Normal bone marrow aspirate smear

(images from www.webpath.med.utah.edu)

1.2.1.2 Histochemistry in Cancer Diagnosis

Light microscopic evaluation of stained biopsy sections is an essential step in the diagnosis of solid cancers including lymphomas (e.g. Hodgkin's disease), carcinoma (eg. breast cancer), sarcoma (eg. osteosarcoma) and variety of other neoplastic tumours. Although several stains are available for histochemistry, Haematoxylin and Eosin (H&E) is by far the most commonly used histochemical stain at present. Haematoxylin stains nucleus blue while eosin stains cellular cytoplasm and extracellular matrix pink (Svarna et al, 2018). Examples of images of H&E stained tissue biopsy specimens patients with different types of solid cancers are shown in Figure 1.2.

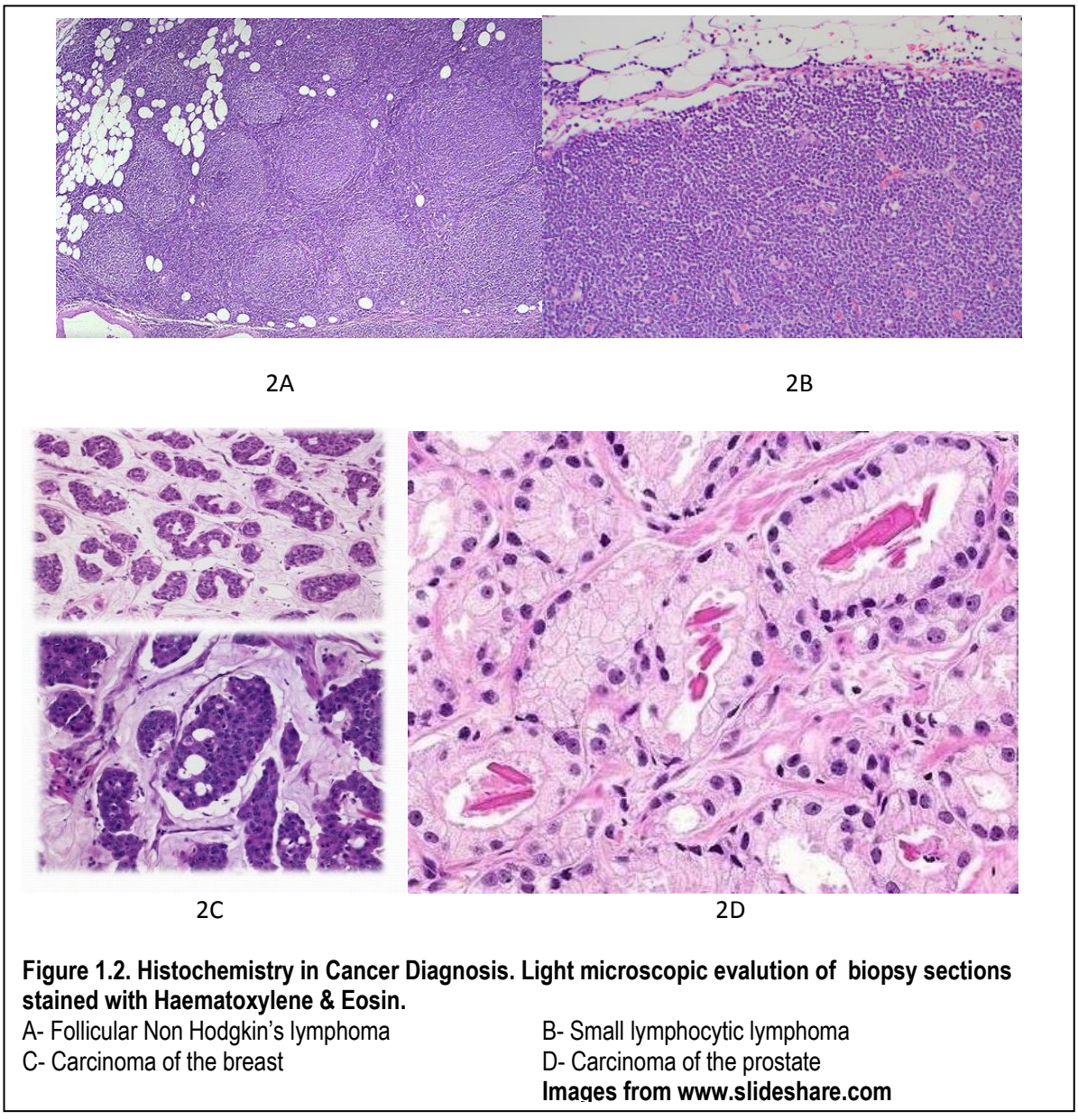

Figure 1.2. Histochemistry in Cancer Diagnosis. Light microscopic evalution of biopsy sections stained with Haematoxylene & Eosin.
A- Follicular Non Hodgkin's lymphoma
B- Small lymphocytic lymphoma
C- Carcinoma of the breast
D- Carcinoma of the prostate
Images from www.slideshare.com

1.2.1.3 Immunocytochemistry/Immunohistochemistry in Cancer Diagnosis

All living cells express numerous proteins, lipids and carbohydrates on their cell surface and within the cytoplasm. Because most of these biomolecules have the potential to generate antibody response, they are collectively called 'antigens'. The expression of these antigens has given Pathologists an invaluable opportunity to develop various antibody based techniques (immunocytochemistry for separate cells and immunohistochemistry for tissues) for the diagnosis of diseases, biotechnology research and drug development (Dabbs D, 2018; Tuffaha *et al*, 2018).

Cellular antigens can be grouped in to several types;

a) Lineage-specific antigens.

Based on the expression pattern on cells, antigens can be divided into either lineage-specific or non-specific. The lineage specific antigens are expressed on one line of cells. For example, all leucocytes express common leukocyte antigen (CD45) but various white cell subsets express different specific antigens. Myeloid cells, monocytes, B lymphocytes and T lymphocytes are distinguished by the expression of CD33, CD14, CD19 and CD2 respectively. Examples of lineage specific antigens are shown in Appendix 1.

b) Disease-associated antigens

Some antigens are disease related i.e. expression of these antigens are associated with a particular pathological condition. These antigens are very useful markers in histological diagnosis of various diseases. In most cases, these antigens are the products of disease associated genetic changes (gene mutations and translocations) or over expression of the antigen gene. Well known examples are BRCA antigen in breast cancer and hybrid BCR-ABL antigen in chronic myeloid leukaemia. Examples of disease associated antigens are given in Appendix 2.

C) Prognostic marker antigens

Expression of certain antigens by the cancer cells may be associated with prognosis (good or poor). For example, high expression of the proliferation marker Ki67 is associated with poor prognosis in Non Hodgkin's lymphoma (NHL) and over expression of P53 protein is

associated with poor prognosis in a variety of cancers including acute myeloid leukaemia, chronic lymphocytic leukaemia and multiple myeloma.

Cancer diagnosis is often involves studying the composite expression pattern of various lineage specific, disease specific and prognostic marker antigens by immunocytochemistry (for cells) and immunohistochemistry (tissue sections).

1.2.1.4 Techniques of Immunocytochemistry/Immunohistochemistry

Immunocytochemistry (ICC) and Immunohistochemistry (IHC) are techniques developed to localise and visualise specific antigens (surface or cytoplasmic) in cells and tissues based on antigen-antibody recognition ((Dabbs D, 2018; Tuffaha *et al*, 2018). IHC was developed in 1940s by Coons to detect antigens in frozen sections (Coons *et al*, 1941). However, the technique gained general acceptance much later when a number of technological developments enabled efficient detection of the antigen-antibody binding. One significant advance was the development of enzymatic label (horse radish peroxidase) in combination with a colorogenic substrate that allowed visualisation of the bound antibody by light microscopy (Avrameas, 1972; Nakane & Pierce, 1967). Further advances were made to enhance the sensitivity of detection by multi-step methods amplifying the original signal using secondary antibodies. The novel approaches included the use of peroxidase-antiperoxidase (PAP) (Sternberger et al, 1970), alkaline phosphatase (Engwall & Perlman, 1971), avidin-biotin conjugate (ABC) (Hegeness & Ash, 1977), avidin-biotin with peroxidase (Guesdon *et al*, 1979), alkaline phosphatase-antialkaline phosphatase (APAAP) (Cordell *et al,* 1984) biotin-streptavidin (Adams JC, 1992) and polymer based labelling systems (Vyberg & Nielson, 1998).

Originally the antibodies for diagnostics were obtained from animal sources and were polyclonal. However, the landmark development of hybridoma technology by Kohler and Millstein in 1975 to produce monoclonal antibodies in large amounts revolutionised this field. Another major advance was the introduction of techniques to enable IHC to be carried out on paraffin fixed tissue sections (Taylor & Burns, 1974; Pinkus GS, 1982). Further improvements in the sensitivity of detection took place when the technique of antigen retrieval was

introduced in early 1990s (Shi et al, 1991). This simple technique of heating the paraffin sections at high temperature significantly enhanced the sensitivity of detection.

While the basic principle of IHC and ICC remains the same, a variety of detection systems have been developed to study the antigen expression profile of cells. These include

1. Immunocytochemistry/Immunohistochemistry using chromogenic detection system
2. Immunocytochemistry/Immunohistochemistry using fluorescence detection system by fluorescent microscopy or confocal microscopy
3. Immunocytochemical analysis using flow cytometry.

1.2.1.5 Immunocytochemistry/Immunohistochemistry using chromogenic detection system

An advantage of this detection system is that the cells/tissues could be counterstained with MGG or H&E to reveal the morphological details. A variety of chromogenic substances are used to visualise the antigen-antibody reaction in ICC and IHC. The most popular chromogen is diaminobenzidine (DAB) which produces a dark brown colour. Several alternatives are available (e.g. 3-amino-9-ethylcarbazole, 4-chloro-1-naphthol and alpha-naphthol pyronin).

Two types of approaches are available for ICC/IHC, namely direct technique and indirect technique. In the former, the primary antibody is directly conjugated to the label. It has the advantage of being simple but it lacks sensitivity. In the indirect technique, the unconjugated primary antibody is used to bind the target antigen but then another antibody directed against the first antibody that is tagged with a label is then applied to amplify the signal ((Dabbs D, 2018; Tuffaha *et al*, 2018) (Figure 1.3).

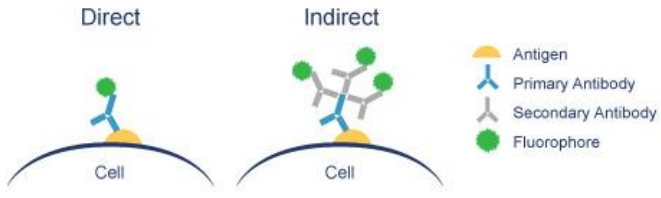

Figure 1.3. Schematic diagram illustrating the basis of Direct and Indirect Immunocytochemistry/ Immunohistochemistry

Examples of the use of immunocytochemistry and immunohistochemistry in cancer diagnosis are shown in Figures 1.4 and 1.5 respectively.

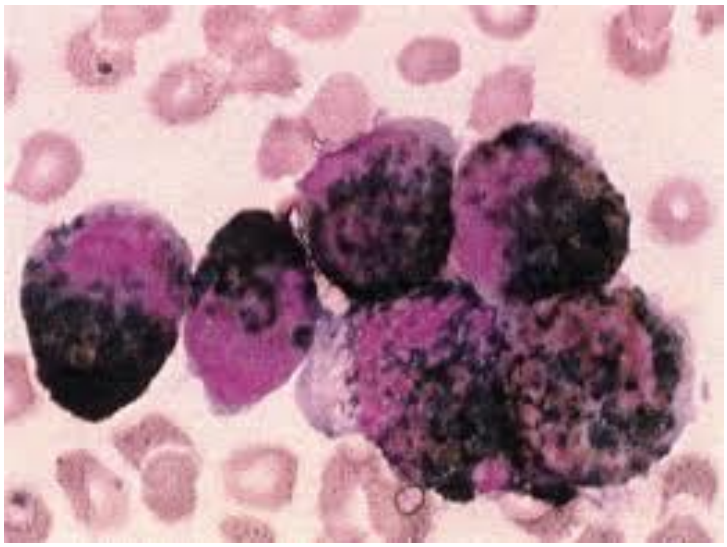

Figure 1.4. Immunocytochemical analysis of the expression of myeloperoxidase on Acute Myeloid Leukaemia cells (image from www.researchgate.com**)**

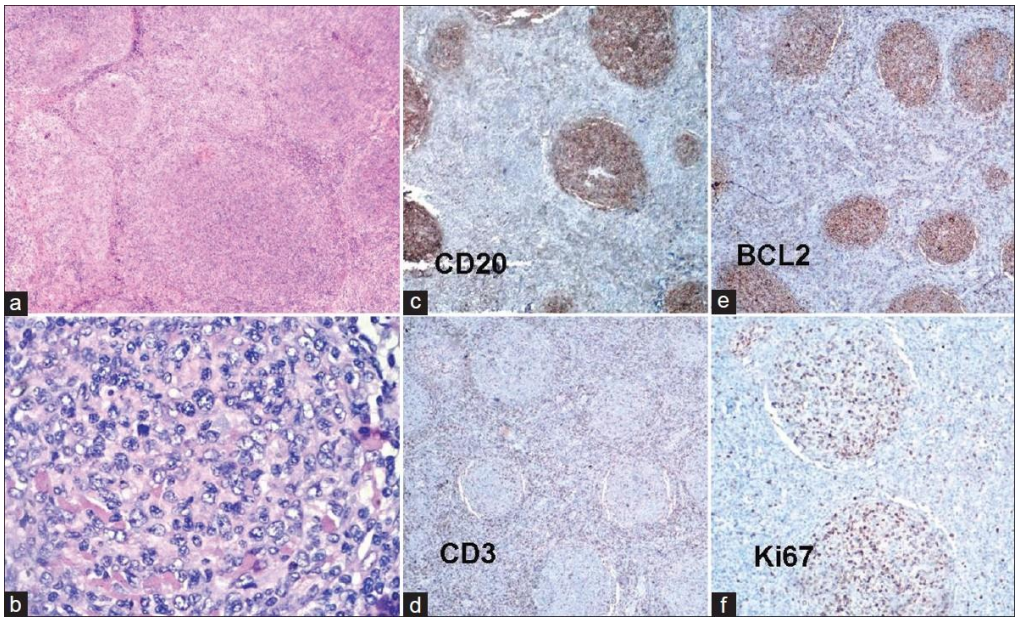

Figure 1.5. Immunohistochemical analysis of follicular Non Hodgkin Lymphoma.

A H&E stain (low power)

B H&E stain (high power)

C IHC with anti-CD20 antibody (positive expression)

D IHC with anti-CD3 antibody (negative expression)

E IHC with anti-BCL2 antibody (positive expression)

F IHC with anti-Ki67 antibody (positive expression)
(images from Dr Sivakumaran's personal collection)

1.2.1.6 Immunocytochemistry/Immunohistochemistry using fluorescence detection system

Immunofluorescence techniques have been used as a diagnostic tool of diseases including cancer for more than 40 years. As in the case of chromogenic techniques, immunofluorescence techniques can be direct in which the primary antibody against the antigen of interest is labelled with a fluorophore or indirect where a fluorescent labelled secondary antibody targeting the primary antibody is used to enhance the sensitivity of the test. There are several fluorophores available for Immunofluorescence technique (Dabbs D, 2018; Tuffaha *et al*, 2018). The most popular fluorophores are fluorescein isothiocyanate, rhodamine, phycoerythrin, Fluor X and DyLight 633.

Visualisation of the antigen-antibody reaction in Immunofluorescence based ICC/IHC is made using a fluorescent microscope or confocal microscope. Examples of Immunofluorescence based IHC of cancer tissues are shown in Figure 1.6 and 1.7.

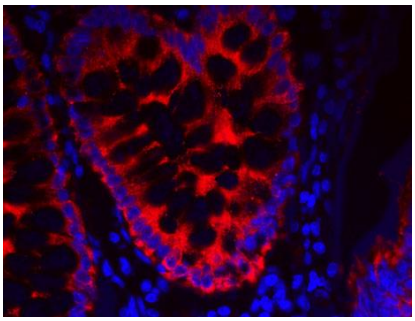

Figure 1.6. Immunohistochemical detection of cytokeratin 18 in human colon carcinoma by Immunofluorescence technique.

Tissue sections were treated with biotinylated anti-cytokeratin 18 antibody and detected using a commercial fluorophore (DyLight 633) which produces a red fluorescence. The sections were counterstained with Hoechst stain to visualise nuclei (blue) (image from www.thermofisher.com)

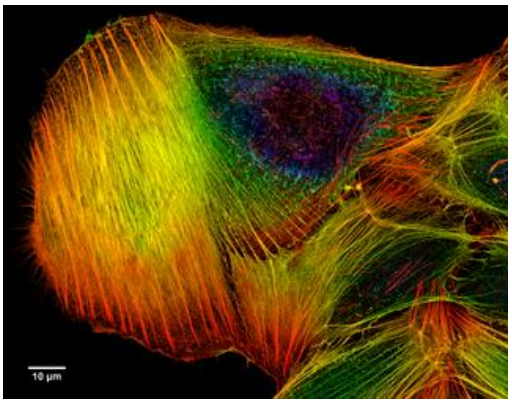

Figure 1.7. Immunohistochemical detection of actin filaments in osteosarcoma cells.

The cells were stained with anti-phalloidin antibody to visualise actin filaments. (image from www.thermofisher.com)

1.2.2 CD 45 antigen

CD 45 antigen is one of the most informative lineage specific antigens presented in Appendix 1. The CD45 antigen, which was originally called Leucocyte Common Antigen (LCA) is a member of the protein tyrosine phosphatase receptor type C (PTPRC) family of enzymes. These enzymes regulate a variety of cell functions including cell growth, differentiation and cell division. It has been shown to be a regulator of T and B cell antigen receptor signalling (Hermiston *et al*, 2003; Holmes N, 2006). The CD45 protein is 200-220 kDa in size and is present in various isoforms in all mature blood cells except erythrocytes (Arendt *et al*, 1997). It contains an extracellular domain, a transmembrane domain and two intracytoplasmic catalytic domains. Because this protein is present in most of the haemopoietic cells (except erythrocytes) but absent in most non-haemopoietic cells, detection of CD 45 antigen expression is extensively used to delineate cells of haemopoietic origin from the others. Hence, the detection of CD45 antigen expression on malignant cells is a crucial part in the diagnostic work up of cancers to identify and separate haemopoietic malignancies such as leukaemias and lymphomas from non-haemopoietic cancers such as carcinomas and sarcomas (Bain *et al*, 2017; Svarna *et al*, 2018; Swerdlow *et al*, 2017) (Figure 1.8).

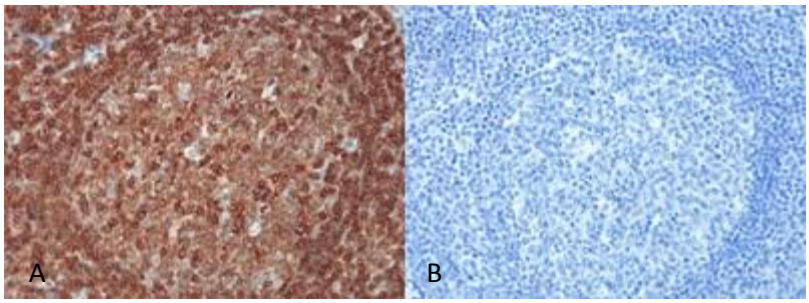

Figure 1.8. Immunocytochemistry of formalin fixed tissue section with anti CD45 antibody and DAB.
(A) Test sample showing strong CD45 antigen expression. (B) Negative control without anti CD45 antibody.
(image from Dr Sivakumaran's personal collection)

Detection of CD45 antigen on cells is carried out by immunocytochemistry or immunohistochemistry or flow cytometry (depending on the nature of the sample material) using monoclonal or polyclonal anti-CD45 antibody. Anti-CD45 antibody is included in all the leukaemia, lymphoma and solid cancer diagnostic panels. As discussed in section 1.2.1.5, detection of CD45 antigen is achieved by using a chromogenic substance such as diaminobenzidine (DAB) or a fluorescent molecule such as fluorescein isothiocyanate (FITC).

1.3 Molecularly Imprinted Polymers

Molecularly Imprinted Polymer (MIP) is a synthetic receptor created against a target analyte (template) using a variety of functional monomers that align on the surface of that template to form a temporary 'mould' which is then polymerised with cross-linking polymers (Wulff, 1993; Haupt & Mosbach, 2000). The interaction between the monomers and the template may involve covalent, non-covalent, semi-covalent, metal ion or non-polar interactions. Subsequent removal of the template results in a strong cast like shell containing the imprint of the template. Such imprint will selectively bind the original analyte with high sensitivity (Figure 1.9).

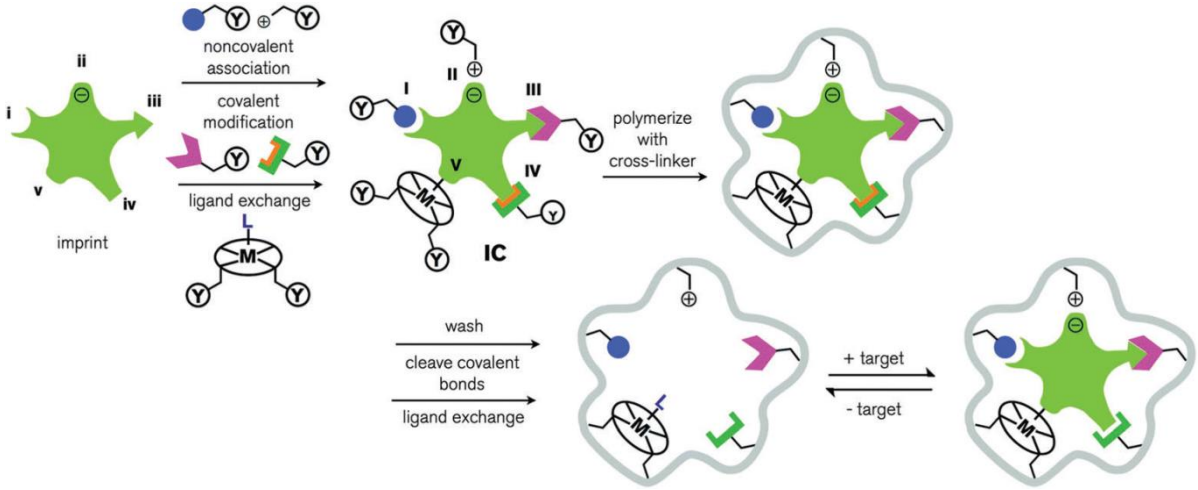

Figure 1.9. The Basic Principle of Molecular Imprinting

The interaction between the template and the functional monomers may involve (i) noncovalent, (ii) electrostatic/ionic, (iii) covalent, (iv) semicovalent, and (v) metal centre coordination (Lofgreen and Ozin, 2014).

The imprinted polymer is strong and robust and resistant to high temperatures, pressures, acids, bases and organic solvents (Bedwell & Whitcombe, 2016; Chen *et al*, 2016; Ye & Turner, 2009). Because molecularly Imprinted Polymers (MIPs) exhibit two important features of antibodies namely molecular recognition and binding, they are sometimes referred to as 'plastic antibodies (Hoshino *et al*, 2008), 'artificial antibodies' or 'enzyme mimics'.

The concept of molecular imprinting technology was originally put forward by Polyakov in 1931. However, the technology remained largely unexplored until early 70's when Wulff and colleagues pioneered the development of the technique of molecular imprinting (Wulff & Sarhan, 1972). Initially this technology was largely applied for the chromatographic

separation of enantiomers. However, it was the seminal work of Mosbach and colleagues in early 90's (Vlatakis *et al*, 1993) that pioneered the use of MIPs as antibody mimics for drug assay that truly reignited interest in this field. Due to their favourable attributes of high sensitivity and specificity, exquisite recognition ability, mechanical and chemical stability, low cost of synthesis and manufacture and reusability, MIPs are attracting considerable attention in wide ranging disciplines like sensor technology, medical diagnostics, solid-phase extraction, separation technology including chromatographic separation, purification, catalysis, drug development and delivery (Antuna-Jimenez *et al*, 2012; Bedwell & Whitcombe, 2016; Chen *et al*, 2016; Chen & Ye, 2013; Del Bruno *et al*, 2019; Ge *et al*, 2013). So far MIPs have been synthesised against a wide range of templates that include drugs, chemicals, toxins and small biomolecules such as sugars, lipids, amino acids and peptides, and incorporated into various devices (Antuna-Jimenez *et al*, 2012; Bedwell &Whitcombe, 2016; Chen *et al,* 2016; Chen & Ye, 2013; Del Bruno *et al*, 2019; Ge *et al,* 2013). More recently, several researchers have successfully developed MIPs against larger biomolecules such as whole proteins (Shi *et al,* 1999), viruses (Altintas *et al,* 2015, Haydon & Dickert, 2001) and cells (Haydon et al, 2003; Eersels *et al*, 2015).

1.3.1 Synthesis of Molecularly Imprinted Polymers

The molecular imprinting process involves the copolymerisation of a functional monomer and a cross-linking monomer in the presence of a template molecule and a porogenic solvent. The functional monomers initially form a complex with the template. After polymerisation, their functional groups are held in position by the cross-linked polymer structure. Subsequent removal of the template results in MIPs with binding site complementary in size, shape and chemical functionality to the template (Zhang, 2013).

Various approaches have been utilised for molecular imprinting. When Wulff and co-workers pioneered the technique of molecular imprinting in the early 1970s (Wulff & Sarhan,1972), they employed a covalent imprinting process in which the interaction between the template and the functional monomer was covalent. This covalent binding permitted the use of polar solvents for subsequent polymerisation. However, this approach has a number of drawbacks. Firstly, covalent binding is limited to particular functional groups (e.g. amine-aldehyde, diol-

ketone, acid-amine) and it is generally directional. Furthermore, the covalently imprinted polymers have slow binding kinetics that restricts its analytical applications.

In order to overcome the drawbacks of covalent imprinting, Mosbach and colleagues introduced the technique of non-covalent imprinting (Arshady and Mosbach, 1981; Vlatakis *et al,* 1993). Non-covalent interactions involve hydrogen bonds, electrostatic forces (e.g. ion-dipole, dipole-dipole), van der Waal's forces, ionic interactions, hydrophobic forces, charge transfer and metal-ion chelating interactions for both the imprinting process and the subsequent template rebinding. One advantage of this method is that the template molecule is easy to remove by solvent extraction. Because of the simplicity and flexibility of this technique and the availability of a broad range of functional monomers, it has become the method of choice for MIP synthesis. It must, however, be noted that the average affinity of the binding site created by non-covalent interactions are generally weaker than those synthesised using covalent interactions. In addition, selectivity of this method is relatively poor compared to the covalent binding method.

To circumvent the drawbacks of both covalent and non-covalent imprinting techniques, Whitcombe and colleagues introduced the technique of semicovalent imprinting (or hybrid imprinting) in which covalently imprinted polymers bind target molecules through non-covalent interactions (Whitcombe *al*, 1995; Alexander *et al*, 2006).

Although a wide selection of functional monomers is available, Methacrylic acid has been the most commonly used monomer, especially for non-covalent molecular imprinting. It interacts with amides, carbomates and carboxyl groups through hydrogen bonds and with amines via ionic interactions. Other established functional monomers for non-covalent imprinting are methacrylamide, 4-vinyl benzoic acid, 4-vinyl pyridine, p-aminostyrene, itaconic acid, diethylaminoethyl methacrylate, 1-vinylimidazole, 2,6-bis-acrylamidopyridine and 2-hydroxyethyl methacrylate. The commonly used functional monomers are given in Table 1.5.

Table 1.1 Commonly used functional monomers for molecular imprinting

Covalent	Non-covalent	Semi-covalent
4-vinyl benzene boric acid 4-vinyl benzaldehyde 4-vinyl aniline tert-butyl p-vinylphenylcarbonate	acrylic acid (AA) methacrylic acid (MAA) trifluoromethyl acrylic acid (TFMAA) methyl methacrylate (MMA) p-vinylbenzoic acid itaconic acid 4-ethylstyrene 4-vinylpyridine (4-VP) 2-vinylpyridine (2-VP) 1-vinylimidazole acrylamide (AAm) methacrylamide 2-acrylamido-2-methyl-1-propane sulfonic acid 2-hydroxyethyl methacrylate (HEMA) trans-3-(3-pyridyl)-acrylic acid 3-aminopropyltriethoxysilane (APTES) Methylvinyldiethoxysilane (MVDES) 3-methylacryloxyprolyl trimethoxysilane (3 MPTS) Glycidoxypropyl trimethoxysilane (GPTMS).	3-isocyanatopropyl triethoxysilane (IPTS)

Cross linking monomers also play a vital role in the imprinting process. They stabilise and strengthen the imprinted cavities. Ethylene glycol dimethacrylate (EGDMA) is the most widely used cross linking monomer in molecular imprinting. Other cross linkers used for this purpose are trimethylolpropane trimethacrylate, divinyl benzene, 1,4-diacryloyl piperazine and pentaerythritol triacrylate. It should also be noted that the molecular imprinting process is significantly influenced by number of factors including molar ratios of the components, amount of the solvents, reaction temperature and reaction pressure.

MIPs can be fabricated in various physical forms. At the beginning, MIPs were synthesised by 'bulk' polymerisation in which the porogenic solvent constitutes more than 50% of the reaction mix and it yields monolithic macroporous product that has to be mechanically ground and sieved to obtain particles of desired size for their final applications (Ye and Yilmaz, 2005). This process is tedious and time consuming and results in particles of irregular shape

and wide size distribution. Furthermore, this fractionation step results in considerable loss of MIPs. The yield is typically less than 50%. Because of the disadvantages of this technique, efforts were made to synthesise spherical micro/nano MIP beads. Subsequently, several research groups successfully synthesised MIP beads of controlled diameter by alternative methods such as precipitation polymerisation (Ye *et al,* 1999), solution polymerisation (Biffis *et al,* 2001), mini-emulsion polymerisation (Vaihinger *et al*, 2002), micro-emulsion polymerisation (Ki and Chang, 2006; Zeng *et al*, 2010), non-aqueous emulsion polymerisation (Dvorakova *et al*, 2010), core-shell emulsion polymerisation (Perez et al, 2001), two step polymerisation (Yang *et al,* 2009), seed polymerisation, aqueous two step swelling procedure, grafting approaches (grafting to and grafting from) (Gao *et al,* 2007; Sulitzky *et al,* 2002), sol gel process (Wang *et al*, 2009), surface deposition (Zhou *et al,* 2010), dispersion polymerisation, suspension polymerisation, swelling and thermal polymerisation (Arshady R, 1992).

It should be noted that the above techniques can be used to synthesise MIPs with varying sizes ranging from hundreds of microns (microMIPs) down to few nanometres in diameter (nanoMIPs) by varying the conditions of polymerisation. However, for a number of reasons, nanoMIPs are preferred to microMIPs in the field of diagnostics, in particular for assays and sensors; (1) the high surface to volume ratio of nanoMIPs provides greater total active surface area per weight unit of polymer, (2) nanoMIPs offer homogenous affinity and specificity of binding, (3) due to their small size, the imprinted cavities are more easily accessible to the templates, (4) nanoMIPs exhibit superior binding kinetics compared to microMIPs, (5) nanoMIPs speed up mass transfer which is a very desirable feature in sensor technology and finally (6) the template molecule can be easily removed from nanoMIPs.

Precipitation polymerisation is a simple yet powerful method to prepare MIP micro/nanoparticles with a high yield (>85%) and narrow size distribution. In addition, this method can be employed for imprinting biomolecules such as water soluble small molecules, peptides and proteins (Hoshino et al, 2008) and also for synthesising MIPs with catalytic activity (Cutivet *et al,* 2009). Solution polymerisation, on the other hand, has been shown to be suited for the synthesis of soluble microgel/nanogel (Biffis *et al,* 2001). Soluble imprinted microgels/nanogels with hydrolytic catalytic activity have been synthesised using this method (Maddock *et al,* 2004; Wulff *et al,* 2006). For the synthesis of core-shell nano MIPs, two-step

precipitation polymerisation has shown to be a simpler process compared to core-shell emulsion polymerisation. Furthermore, two-step precipitation polymerisation process is very amenable to post-modification of the nanoparticles to introduce any additional functionality. Due to its favourable physical properties including stability and ease of derivatisation, silica is the most widely used material for the synthesis of MIPs by grafting process. However, other materials such as magnetite, gold, polystyrene nanoparticles and quantum dots can also be used depending on the intended application(s) (Chen & Ye, 2013).

One of the drawbacks of non covalent MIPs is their heterogeneous binding affinity sites. In order to reduce the heterogeneity of MIPs, Zimmerman and co-workers developed an ingenious method of imprinting inside dendrimers which produced soluble MIPs with nearly homogeneous imprinting sites (Zimmerman *et al,* 2002).

Over the last decade, the above methods have successfully been employed to synthesise nanoMIPs for a variety of applications. For instance, precipitation polymerisation has recently been used to synthesise nanoMIPs to hemozoin to develop an assay for malaria diagnosis (Rifai-Graham *et al*, 2019). Mendez and colleagues recently employed mini-emmulsion polymerisation to encapsulate an anti-leukaemic plant extract *Piper Cabralanum* in poly methyl methacrylate nanoMIPs (Mendez *et al*, 2017). Micro-emulsion technique was used to prepare powdery polymer aerogel as the stationary phase for high resolution gas chromatographic separation (Zheng *et al*, 2016). The core-shell emulsion polymerisation technique has recently been used to synthesise nanoMIPs for a point of care diagnostic assay for rapid and sensitive detection of cardiac troponin I (Cai *et al,* 2018). Two-step polymerisation has been used to develop surface imprinted cryogel for lysozyme purification (Erol *et al*, 2016). Recently, sol-gel surface imprinting technique has been employed to synthesise MIPs for the plant toxin, gossypol (Wang *et al,* 2019). Zimmerman's approach to MIP synthesis using dendrimers has recently been exploited by Baimani and colleagues (Baimani et al, 2019). The researchers fabricated a photoresponsive MIP incorporating a dendrimer in order to increase the number of binding sites for separation of methylprednisolone.

1.3.2 Fluorinated Monomers for Molecular Imprinting

It is known that the incorporation of fluorine confers highly desirable properties to polymethacrylate polymers such as low surface energy, chemical and weather resistance, thermal stability, low refractive index, oil and water repellency and excellent inertness to solvents, acids and alkalis (Liu *et al*, 2012; Patel & Ameduri, 2013; Yao *et al*, 2014). Because of these properties, fluoropolymers are widely used in chemical-resistant and antifouling coatings, non-corrosive materials, leather, textile and dental re-line resins (Liu *et al*, 2012; Yoshida *et al*, 2013). Co-polymerisation of fluorinated monomers with common hydrocarbon monomers results in polymers with improved physico-chemical properties (Yao *et al*, 2014). For these reasons, several researchers have incorporated fluorinated monomers such as alkyl 2,2,2-(trifluoromethyl) acrylic acid (TFMAA), 2,2,2-trifluoroethyl acrylate (TFEA), 2,2,2-trifluoroethyl methacrylate (TFEMA), 2,2,2-trifluoroethyl α-fluoroacrylate (TFEFA), 2,3,5,6-tetrafluoro-4-iodostyrene (TFIS), 1,1,1,3,3,3,-hexafluoroisopropyl methacrylate (HFIPMA), 1,1,1,3,3,3-hexafluoroisopropyl acrylate (HFIPA), 2-sulfoethyl methacrylate (SEMA) and hexafluoropropylene for molecular imprinting (Takeuchi *et al*, 2016). Takeuchi and colleagues (Takeuchi *et al*, 2005) synthesised MIPs for 4-dimethylaminopyridine (DMAP) by co-polymerising 2,3,5,6-tetrafluoro-4-iodostyrene (TFIS), styrene and divinylbenzene. The synthesised MIP exhibited preferential binding between the MIP and the template. A photoresponsive MIP for a model template 2,3,4,5,7,8,9,10-octafluorophenazine was successfully synthesised by Tang and colleagues using a photoresponsive fluorinated monomer 4-methacryloyloxy nonafluoroazobenzene (MANFAB) (Tang *et al*, 2011). Tamayo and co-workers prepared a new selective MIP by precipitation polymerisation for the extraction of phenylurea herbicides using methacrylic acid (MAA) or TFMAA as the functional monomers. The study showed that TFMAA based MIP was superior to the MAA based polymer for the extraction of phenylurea herbicides (Tamayo *et al*, 2005).

Fluorinated monomers have also been used by the Piletsky group at Cranfield and Leicester. In their bid to synthesise a biotin-specific synthetic receptor, they tested the ability of various functional monomers to generate specific binding sites. Their molecular modelling and computational screening indicated that MAA, TFAA and 2-acrylamido-2-methyl-propanesulfonic acid (AMPSA) were the most promising monomers to form a strong complex with the template molecule in water. Furthermore, the MIPs synthesised with MAA and TFAA were stable while MIPs with AMPSA gradually lost their affinity for the template (Piletska *et*

al, 2004). In another study, the group synthesised anti-melamine MIP nanoparticles using solid-phase approach (Moczko *et al*, 2013) using a monomer mix containing TFMAA.

Although the published data on fluorinated monomers in molecular imprinting is encouraging, it should, however, be noted that the target templates have been small molecules. There is sparse data available on the utility of these monomers for molecular imprinting of more complex molecules such as peptides and proteins. Hence, further investigations are warranted to establish the usefulness of these monomers for molecular imprinting of macromolecules including proteins.

1.3.3 Molecularly Imprinted Nano/Micro fabrications

In addition to bead forms, MIPs have also been fabricated as thin films which are particularly useful for sensors. Schmidt and colleagues developed an effective method by first spin-coating of a MIP prepolymerisation mixture and then UV curing (Schmidt *et al*, 2004) while Li and colleagues have fabricated MIP membranes through a water assisted method (Li *et al,* 2007). Piacham and colleagues successfully fabricated 50 nm thick MIP film on a gold surface by surface initiated free radical grafting polymerisation for quartz crystal microbalance (QCM) analysis (Piacham *et al*, 2005). Li and colleagues developed an efficient method to produce surface imprinted monodisperse nanowires of 100 nm diameter for protein recognition (Li *et al*, 2006). Molecular imprinted surface bound nanofilaments with enhanced binding capacities have been developed by Vandevelde and colleagues (Vandevelde *et al*, 2007). A successful fabrication of molecular imprinted nanofibers was carried out using an electrospinning approach (Chronakis *et al,* 2006). An effective approach to synthesise MIPs in the form of soluble single-molecule nanogel with catalytic activity has been described by Wulff and colleagues (Wulff *et al,* 2006).

1.3.4 Composite Nanomaterial-incorporated Molecularly Imprinted Polymers

With the increasing popularity of nanomaterials in sensor technology, a number of research groups have succeeded in molecular imprinting directly onto various nanomaterials. As described by Xie and colleagues, nanosized MIP materials have superior properties compared to normal MIPs. The extremely high surface to volume ratio facilitates (1) easy

removal of template molecules, (2) higher binding capacities due to the presence of more recognition sites on the surfaces and (3) faster template binding kinetics due to easy accessibility of binding sites (Xie *et al*, 2006). Furthermore, incorporation of certain nanomaterials such as carbon nanotubes, graphene and quantum dots greatly enhances the sensitivity of MIP based sensors/assays. A variety of nanomaterials including gold nanoparticles (Huang *et al,* 2011; Matsui *et al*, 2005), superparamagnetic nanoparticles (Ansell & Mosbach, 1998), silica nanoparticles (Shen & Ye, 2011; Xia *et al*, 2013), nanowires, carbon nanotubes (Cai *et al*, 2010; Gian *et al,* 2014), graphene (Mao *et al*, 2011; Yanez-Sedeno *et al*, 2017), aptamers (Bai et al, 2013; Zhang & Liu, 2016) quantum dots (Lian *et al*, 2012; Zor *et al*, 2015) have been shown to be effective in MIP based sensing (Tokonami *et al*, 2009; Dai *et al,* 2015).

1.3.5 Synthesis of Molecularly Imprinted Nanoparticles by Solid Phase Polymerisation

In order to overcome the drawbacks of the traditional imprinting techniques, Piletsky and co-workers developed a versatile method ('solid-phase polymerisation') using silica microparticles to immobilise the template prior to imprinting (Poma *et al,* 2013). As illustrated in Figure 1.10, the template is immobilised in a pre-determined orientation onto a column packed glass beads before polymerisation. After polymerisation and particle synthesis, elution at low or room temperature results in the removal of the lowest affinity MIPs together with unbound monomers and impurities. Subsequent high temperature elution yields high affinity MIPs. The immobilisation of the template enabled synthesis of MIPs with limited variations in the binding characteristics (affinity and specificity). Hence, they are dubbed 'monoclonal MIPs' by the authors. Piletsky and co-workers also reported that this synthetic approach was compatible with automation and the process parameters were under computer control requiring minimal manual intervention and notably, the template was reusable. In this study, the researchers synthesised MIPs with low polydispersity index to melamine.

Similar strategy has also been used by other researchers. Haupt and co-workers synthesised thermoresponsive MIPs to trypsin using solid-phase polymerisation (Ambrossini *et al*, 2013).

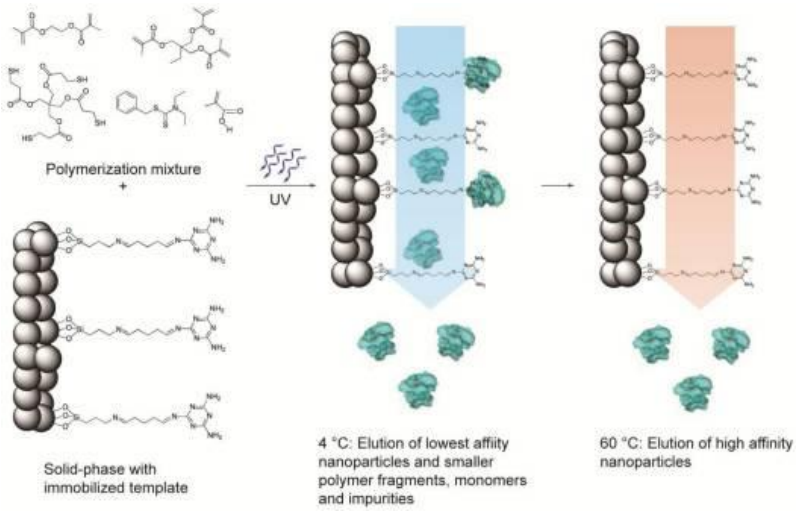

Figure 1.10. Schematic representation of the solid-phase synthesis of MIP nanoparticles.

The monomer mixture is injected onto the column reactor with immobilized template and polymerization is initiated by UV-irradiation. The low-affinity particles, as well as unreacted monomers, are eluted at low temperature. The temperature is then increased and high-affinity particles are eluted from the column for collection (Poma *et al*, 2013)

Solid phase imprinting technology developed by Piletsky's group has had a significant impact on MIP based diagnostics and drug delivery systems. Using this method, Piletsky's group have succeeded in imprinting a number of toxic chemicals, drugs, biological molecules (Canfarotta *et al*, 2017; Chianella *et al*, 2013; Smolinska-Kempisty *et al*, 2017), proteins (Mahajan *et al*, 2019), tumour markers (Cecchini et al, 2017), viruses (Altintas *et al*, 2015). This technique has paved the way for fabricating a number of robust, specific, low-cost electrochemical and optical sensors (Ahmad *et al*, 2019; Moczko *et al*, 2016: Munawar *et al*, 2018; Piletsky *et al*, 2017; Smolinska-Kempisty *et al*, 2016). This technology has also been adopted to develop drug delivery systems (Canfarotta *et al*, 2018; Piletska *et al*, 2015).

1.3.5.1 Epitope/Segment Imprinting

Traditionally, whole molecules are used for imprinting. However, in certain situations, the use of whole molecule may be problematic. For instance, it may be difficult to obtain the whole molecule in sufficient quantities either due to its cost or limited availability or to the fact that it may be toxic or biologically hazardous to handle. In the case of proteins or DNA imprinting, if the whole molecule is used, due to the 'fluctuation' of the molecular structures, only a number of specific conformations might be imprinted, resulting in receptors with low affinity and specificity. Minoura and colleagues (Rachkow A & Minoura N, 2000) introduced an imprinting

strategy using only a segment or fragment of the whole molecule. The researchers first synthesised an artificial receptor that was capable of binding to an exposed domain of the peptide hormone oxytocin in aqueous media. Since then, several research groups have successfully adopted this technique to imprint macromolecules like proteins. Lu and colleagues (2012) has developed a sensor using an epitope imprinted polymer coated quartz crystal microbalance for the detection of human immunodeficiency virus type I related protein 41. The researchers synthesised a peptide of 35 amino acid residues analogous to residues 579-613 of the gp41, immobilised onto the surface of a QCM and polymerised using dopamine as the functional monomer. The detection limit of gp41 was 2ng/ml. Yang *et al* (2014) fabricated a sensor for the detection and quantification of bovine serum albumin by coating CdTe quantum dots with epitope imprinted polymer. The researchers synthesised a peptide with the sequence derived from the surface exposed C-terminus of BSA (residues 599-607) and used as the template for imprinting.

1.3.6 Smart Molecularly Imprinted Polymers

In living cells, interactions between receptors and ligands are heavily influenced by the ambient conditions such as temperature, pH and other biomolecules. In order to enable the molecularly imprinted polymers ('synthetic receptors') to simulate natural receptors, several researchers have successfully developed so-called 'Smart MIPs' that respond to various stimuli. The Smart MIPs that have been developed so far include temperature responsive, pH responsive, magnetic responsive, salt responsive, dual-stimuli responsive and multi-stimuli responsive MIPs (Ge et al, 2003; Chen et al, 2016). These Smart MIPs have great potential in a number of fields such as chemical sensors, bioassays, biotechnology, drug delivery, separation science and solid phase extraction. Examples of Smart MIPs are summarised in Appendix 3.

1.3.7 Characterisation of MIPs

It is imperative to perform detailed analysis of MIPs especially if they are intended for the use in medical diagnostics and therapeutics. A number of parameters such as size, charge, structure, surface properties, porosity, thermal stability, magnetic property and monomer-template interactions might be analysed. Dynamic light scattering (DLS) is widely used to

measure the size of ‘nano scale’ MIPs. Determination of the size and dispersity is also measured by scanning and transmission electron microscopes. Atomic Force microscopy is used to study the surface characteristics of MIPs. Surface properties and pore sizes of ‘micro scale’ MIPs can be studied by Brunauer-Emmett-Teller (BET) analysis by nitrogen adsorption studies. Thermogravimetric analysis (TGA) is used to study the thermal stability ‘micro scale’ MIPs. Magnetic properties of MIPs can be analysed by vibrating sample magnetometer (VSM). The interactions between monomers and template can be studied by a variety of methods including nuclear magnetic resonance (NMR), Infra-Red and UV-Vis spectroscopies (Chen *et al*, 2016).

1.3.7.1 Dynamic Light Scattering

Dynamic Light Scattering (DLS) is one of the most widely used techniques to characterise nanomaterials. It is also known by various names such as Photon Correlation Spectroscopy (PCS), Diffuse Light Scattering, 3-D Dynamic Light Scattering, Quasi Elastic Light Scattering (QELS), Beating Spectroscopy, Intensity Fluctuation Spectroscopy and Homodyne Spectroscopy (Kulkarni SK, 2014). DLS technique can be used to determine the size and size distribution of nanoparticles dispersed in liquid. The basis of this technique relies on the measurement of intensity fluctuations of visible light scattered from the particles while they make random motion (Brownian motion) in liquid as a result of buffeting by the solvent molecules. The time-dependent fluctuations in the scattered light are measured by a photon counter. The fluctuations are directly related to the diffusion coefficient of the particles which in turn is related to their size (Berne BJ & Pecora R, 2000; Goldburg WI, 1999).

Stokes-Einstein equation relates particle size to particle motion. The equation most often used in particle size analysis is given below

$$D_h = \frac{k_B T}{3\pi\eta D_t}$$

D_h - hydrodynamic diameter of the particle (i.e. size)
D_t - diffusion coefficient (measured by dynamic light scattering)
k_B - Boltzmann's constant
T - temperature of the liquid

η - viscosity of the liquid

The instrument set up of standard DLS technique is given in Figure 1.11

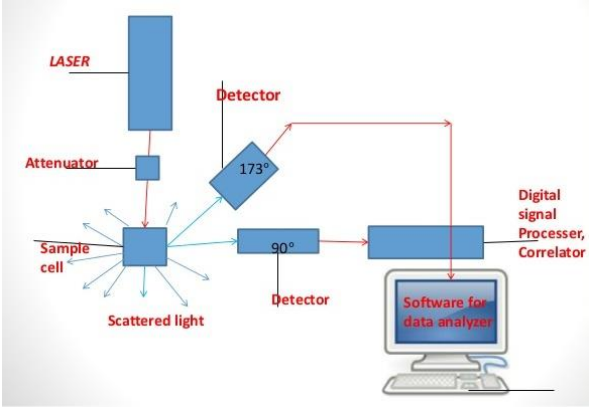

Figure 1.11. Schematic diagram illustrating the instrument set up of a DLS analyser.

Light from the light source (laser) illuminates the sample in the cell. The scattered light signal is received by detectors either at a 90 degrees or 173 degrees. The received optical signal is processed in real time with a digital signal processing device known as a correlator. The correlator compares the scattering intensity at time intervals to derive the rate at which the intensity is changing. A software is then used to derive the size and size distribution of the particles from the data obtained by the correlator. (Technical information from Malvern Instruments Ltd (Malvern, UK), Wyatt Technology (Santa Barbara, USA) and Horiba Scientific (Japan).

It must be noted that a number of factors can influence the results of particle size analysis by DLS. They include viscosity, temperature, ionic strength of the sample and the shape and surface structure of the particles. The viscosity of the sample can significantly influence the results because it can affect the motion of the particles. Similarly temperature can influence the results because it affects the viscosity of the sample. Hence the importance of recording the temperature of the sample accurately and maintaining it stable during analysis. The ions in the medium and their concentration can affect particle diffusion speed by changing the thickness of the electric double layer around the particle. A low conductivity medium will result in a larger apparent hydrodynamic diameter while high conductivity medium will have the opposite effect. The size analysis of particles by DLS can also be affected by surface

characteristics of the particles due to their effect on diffusion speed. The shape of the particles and presence of aggregates also can affect the analysis.

1.3.7.2 Resistive Pulse Sensing

The technique of resistive pulse sensing (RPS) to enumerate particles in solution was first developed by Wallace. H. Coulter in early 1950s (Coulter WH, 1953). This technique is based on the principle that when a particle traverses through a channel filled with aqueous electrolyte solution, there is a transient change in the channel's ionic resistance known as a 'resistive pulse'. Coulter applied this technology to count particles in biological fluids in particular in the field of Haematology where it is extensively used for enumeration of blood cells.

The main attraction of the RPS technology is its ability to analyse individual particles. It can provide valuable information on individual particles examined. A variety of parameters such as concentration, size and charge of particles can be measured by RPS. It can be applied to a variety of particles including peptides, proteins, nucleic acids, exosomes and organic/inorganic nanomaterials (Henriquez *et al*, 2004; Kozak *et al*, 2011).

1.3.7.3 Tunable Resistive Pulse Sensing (TRPS)

TRPS is an adaptation of RPS technology. It utilises a conical tunable elastomeric pore that can be stretched or relaxed to change the pore size to suit the sample (Kozak *et al*, 2011; Roberts *et al*, 2010). The concept of tunable nanopore membrane was first developed by Sowerby *et al* (2007). The membrane can be stretched in a biaxial direction to alter the pore size.

The standard TRPS equipment commercially available in the United Kingdom has two fluid reservoirs for conducting electrolyte solution. The pore membrane is mounted horizontally between the two reservoirs. The test sample is typically placed into the top reservoir, see Figure1.12.

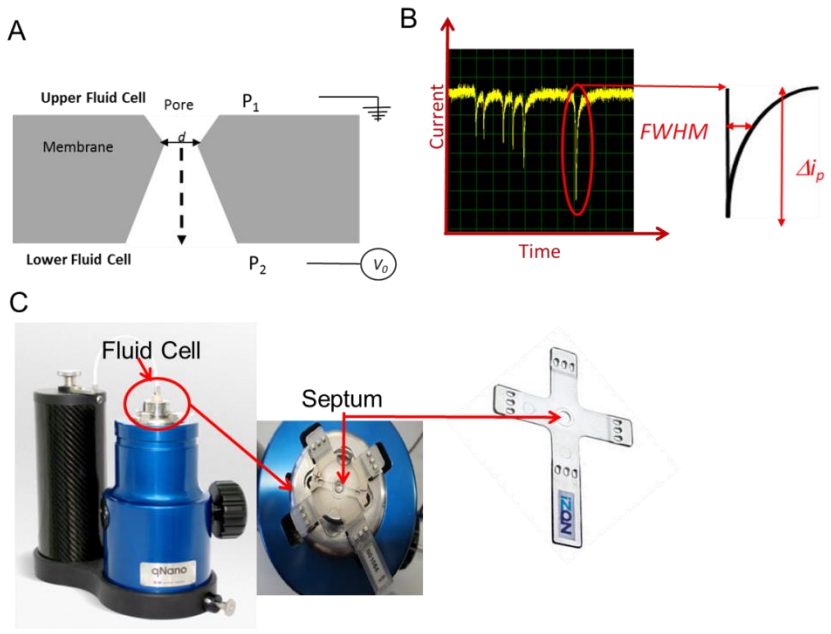

Figure 1.12 Tunable Resistive Pulse Sensor

(A). Schematic diagram of a pore.The sample is placed into the upper fluid cell. (B). Illustration of baseline current and "blockade" events (current dips) that are each caused by an analyte traversing the pore. Each event is analysed for full width half maximum (FWHM) duration and Δi_p. (C). The Izon qNano instrument, showing the fluid cell and location of crucifix plastic membrane. As particles/analytes translocate the pore they temporarily occlude ions, leading to a transient decrease in current known as a "blockade event", examples of which can be seen in figure 3B.

TRPS technology is versatile with a number of remarkable features. The pore tunability permits analysis of particles of broad size range (40nm-10µm). In addition, it enables particle by particle measurement of size and surface charge of individual particles simultaneously. It can also analyse particle aggregation and stability. It is relatively inexpensive as it requires few consumables and works with physiological strength buffers.

TRPS has several applications including analysis of particle parameters such as size, size distribution, shape and surface charge. In addition, this technique can also be used to study particle aggregation, particle-plasma protein interactions ('protein corona formation'), particle-DNA/RNA/Aptamer interactions and analysis of extracellular vesicles, liposomes and micelles. An exciting application of TRPS is in the field of drug delivery and drug development. Other potential areas of interest are in the fields of microbiology where TRPS is successfully applied to enumerate and size microorganisms including viruses and bacteria and in toxicology where it has been used to study the cytotoxic effects of nanoparticles

(Kozak *et al*, 2011; Sivakumaran & Platt, 2017; Weatherall & Willmott, 2015). In this work, TRPS together with DLS will be used to characterise the morphology (e.g. size) and the recognition capabilities of the MIP nanoparticles produced.

1.3.8 Applications of MIPs

As previously alluded, MIPs are being investigated as recognition ligands in wide ranging disciplines such as sensor technology, medical diagnostics, solid-phase extraction, separation technology including chromatographic separation, purification, catalysis, drug development and delivery. So far MIPs have been synthesised against a wide range of templates that include drugs, chemicals and small biomolecules such as sugars, lipids, amino acids and peptides and incorporated into various devices (Bedwell & Whitcombe, 2016; Chen & Ye, 2013; Chen *et al*, 2016; Ge & Turner, 2009). More recently, several researchers have successfully developed MIPs against larger biomolecules such as whole proteins, viruses and cells.

1.3.8.1 MIPs in Separation& Extraction

One of the very first applications of MIPs has been analytical separations. They have been mainly used in chromatographic separations such as high performance liquid chromatography (HPLC) (Kempe, 1996), capillary electrochromatography (CEC) (Schweitz *et al*, 2001; Spegel *et al*, 2003), capillary liquid chromatography (CLC) and thin layer chromatography (TLC) (Ansell, 2005). Their main utility was as packing materials or monolithic column materials as the stationary phases of chromatography. Both forms have been widely used in HPLC, CEC, CLC and TLC for the separation of a variety of molecules in diverse scientific fields such as biotechnology, medicine, environmental science and food technology.

Walshe and co-workers pioneered the use of MIPs that were prepared by bulk polymerisation for CEC (Walshe *et al*, 1997). They synthesised MIPs to 7-hydroxycoumarin and packed them in cartridges and used as SPE sorbent. The authors reported that the extraction efficiency was linear over the range of 10-50 micrograms per ml. Subsequently Schweitz and colleagues employed precipitation polymerisation to synthesise submicron sized MIPs to s-propranolol and used for CEC separation of propranolol enantiomers (Schweitz *et al*, 2000).

One of the drawbacks of early MIP particle based CEC separations was the phenomenon of 'tailing' due to the presence of heterogeneous binding sites. This technical problem has been overcome by the use of MIP nanoparticles with homogenous binding sites. Priego-Capote *et al* prepared 30-150nm sized MIP nanoparticles using mini-emulsion polymerisation and successfully used them to separate racemic propranolol without tailing (Priego-Capote *et al*, 2008).

Monolithic columns are generally prepared *in situ* within the columns from the imprinting reactant solution, thus avoiding the need for grinding, sieving and packing (Watanabe *et al*, 2009). They have been widely used in HPLC, CEC and CLC. Liu *et al* (2010) applied this technology to synthesise macroporous molecularly imprinted polymer columns for protein recognition by liquid chromatography (HPLC). MIP for the protein cytochrome C was synthesised directly in an HPLC column by one step free radical polymerisation. Lysozyme was used as the competitive protein. The researchers demonstrated that even in a competitive environment containing both cytochrome C and lysozyme, the MIP column was able to achieve high level separation. Subsequently, Liao *et al* (2011) fabricated a MIP monolith by thermal polymerisation for the separation of anti-parasitic drug s-ornidazole by pressurised CEC. The authors reported that, under the conditions used, the enantiomers were rapidly separated within 9 minutes on the MIP based chiral stationary phase. Jang *et al* (2011) successfully performed simultaneous separation and characterisation of phospholipids in human urine by combining two powerful technologies- CEC with molecularly imprinted monolith column and electrospray ionisation tandem mass spectrometry. Remarkably, the authors were able to separate and characterise 18 molecules including phosphatIdyl serines, phosphatidylethanolamines, phosphatidylglycerols, phosphatidic acid and lysophosphatidyl glycerols based on their acyl chain length and polar head groups.

Apart from CEC separation, MIP nanoparticles are also used in solid phase extraction (SPE). The use of MIPs for SPE was first suggested in the mid 1990s. Over the last two decades numerous reports have been published in the literature describing the use of MIPs in the extraction of various chemicals, toxins, drugs and biomolecules.

While most of the published reports have focused on separation of small organic molecules such as drugs, chemical compounds and toxins, separation of large biomolecules has also

been achieved. Using magnetic MIP nanoparticles, Jing *et al* successfully separated lysozyme in biological samples (Jing *et al*, 2010).

Different structural forms of MIP nanoparticles have been used to provide solid support for affinity separation. Besides the most widely used spherical nanoparticles, nanofibres and nanofilms have also been used for this purpose. Chronakis *et al* (2006) immobilised MIP nanoparticles in to nanofibres using an electrospinning method. They were able to extract trace amounts of theophylline and 17β oestradiol using electrospun nanofibers. These authors subsequently fabricated electrospun nanofiber affinity membranes for selective adsorption of propranolol (Yoshimatsu *et al*, 2008). By combining HPLC-MS, the authors were able to separate trace amounts of propranolol (1 ng/ml) in tap water.

1.3.8.2 MIPs in Drug delivery

Another exciting area for MIPs is the field of drug delivery and control release. Hiratani and Alvarez-Lorenzo (2002) were among the first to propose the use of MIPs in the form of a contact lens for ocular drug delivery of timolol.

Nanocapsules for the control delivery of drugs were fabricated by Ki and Chang (2006) using a semi-covalent polymerisation approach. The researchers used oestrone as the template in this experiment. Because the imprinted nanocapsules exhibited fast uptake and binding capacity for the target molecule, they were considered to be potentially useful as drug carriers. Kan and co-workers (2009) developed a magnetic MIP for the recognition and controlled release of aspirin.

A molecularly imprinted nanoparticle for controlled release of the cancer drug 5-fluouracil (5-FU) was developed by Cirillo and co-workers (2009). The nanoparticles were synthesised by precipitation polymerisation. A sustained release of 5 FU was observed over a period of 50 hours in-vitro.

A novel approach to remove melitin, a 26 amino acid peptide, bee venom toxin, using melitin imprinted hydrogel nanoparticles has been reported by Hoshino and co-workers (2010). The MIP nanoparticles were synthesised by precipitation polymerisation. The imprinted nanoparticles exhibited high binding selectivity for melitin. The melitin imprinted nanoparticles

were shown to be effective in neutralising the toxin in vivo. Intravenous administration of the melitin imprinted nanoparticles into mice reduced mortality following exposure to melitin by 50%.

1.3.8.3 MIPs as Enzyme Mimics

Molecularly imprinted polymers are sometimes dubbed 'enzyme mimics' because of their ability to function like an enzyme. The synthesis of MIPs with catalytic activity was first reported by Resmini and colleagues (Maddock *et al*, 2004). They synthesised catalytic nanogels with hydrolytic activity employing a non-covalent approach, using a phosphate transition state analogue as template and polymerisable tyrosine and arginine units as functional monomers for catalysing a carbonate catalysis reaction (Pasetto *et al,* 2005). The same research group subsequently developed a MIP nanogel with aldolase type I activity (Carboni *et al*, 2008). Subsequently, Wulff and co-workers developed hydrolytically active nanogels (Wulff *et al*, 2006). The active sites were imprinted using a diphenyl phosphate template as transition-state analogue for carbonate hydrolysis reaction.

Chen and co-workers 2007 developed 'smart MIP' in the form of a stimuli responsive catalyst as a mimic of the enzyme horse radish peroxidase. MIP was synthesised by precipitation polymerisation using homovanillic acid as the template. The hydrogels produced using the above MIPs exhibited significant pH-dependant catalytic activity.

1.3.8.4 MIP based Sorbent Assays and Sensors

Traditionally binding assays have relied on antibodies for the recognition of the target analyte, but because of its cost of production, limited shelf life and requirement for special storage and transport conditions, a search for an alternative recognition element was vigorously pursued. The research team of Mosbach and co-workers at the University of Lund, Sweden was the first to develop a binding assay using a molecularly imprinted polymer in 1993 (Vlatakis *et al*, 1993). They reported the first MIP based radioimmunoassay for the drugs theophylline and diazepam in human serum. The authors reported a satisfactory selectivity and high detection sensitivity and proposed that MIPs could be an alternative for antibodies in binding assays. The same group subsequently reported the first immunoassay using MIPs. They synthesised microspheres bearing binding sites by precipitation

polymerisation (Ye *et a*l, 1999). Using this approach, the researchers successfully fabricated an assay for the detection of estradiol and theophylline.

Following on from the above pioneering work of Mosbach and colleagues, several research groups around the world have embarked on developing new assay platforms using MIPs. The target analytes are diverse ranging from drugs, chemicals and environmental toxins to small biomolecules and even cells and unicellular organisms such as viruses and cells (Table 1.8).

Table 1.2. Types of target molecules for molecular imprinting

Type of target molecule	**Examples**
Metals (ions)	Pb, Hg, Sr, Hg, Cd, Cu, Cr, Fe, Ni, Th, Eu, As
Drugs	tetracyclins, quinolons, propranolol, digoxin, sulphonamides, vancomycin, enalapril, lisinopril, mitoxantrone, fluconazole, salicylic acid, 5-fluouracil, chloramphenicol, tamoxiphene, metformin, gemcitabine, diclofenac, ciprofloxacin, ifosfamide, penicillin, phenytoin, theophylline, diazepam, erythromycin, zidovudine, theophylline, indomethacin, amoxicillin, paracetamol, frusemide, carbamazepine, tramadol
Organic molecules	pesticides (atrazine), fungicides (benzimidazole), explosives (TNT), cannabinoids, cocaine, methamphetamine
Biomolecules	cAMP, ATP, lysozyme, endotoxins, histamin, beta 2 microglobulin, CEA125, PSA, troponin T, AFP, ferritin, creatinine, uric acid, bilirubin, dopamine, ascorbic acid, serotonin, corticosteroids, folic acid, oestradiol, oestrone, testosterone, glucose, fructose, galactose, LDL, cholesterol, phospholipids, lactose, maltose, Tyrosine, alanine, tripeptides, glycoproteins, BSA, haemin, red cell antigens, haemoglobin, bovine leukaemia virus proteins, HIV p24, myoglobin, albumin, dengue virus protein
Viruses	Bacteriophage, tobacco mosaic virus, dengue, H5N1, human rhinovirus, food and mouth disease, picorna virus, hepatitis A, adenovirus
Bacteria	Nisseria meningitidis

The following section will briefly discuss the developments in the field of binding assays and biosensors.

1.3.8.5 MIP based Assays and Sensors for Biomolecules

MIP based assays for the detection of a variety of molecules has been published. These biomolecules include vitamins, hormones, neurotransmitters, metabolites, biomarkers, sugars, lipids, amino acids and proteins. (See Appendix 4). As outlined in the section 1.7 (MIP Platforms), several different techniques have been employed for capture of the target molecule and their detection.

1.3.8.6 MIP based Assays and Sensors for Drugs

Numerous reports have been published in the literature describing developments of MIP based assays for the detection and quantitation of several groups of drugs that are widely used in clinical medicine. They include different classes of antibiotics, antivirals, antiprotozoals, anticancer drugs, antidiabetics, bronchodilators, tranquilisers, antidepressants, antiepileptics, analgesics, cardiotropic drugs, hormone analogues, immunomodulators, narcotics, antihypertensives, anticoagulants, anti-inflammatory drugs and others (see Appendix 5). As in the case of MIP based assays for biomolecules, a diverse array of technologies has been employed for capture and detection of target molecules.

1.3.8.7 MIP based Assays and Sensors in Microbiology

Diagnosis of several infectious diseases relies on antibody based immunological tests. In order to find an alternative to these expensive tests, several research groups have embarked on developing MIP based assays for the detection of microorganisms or antigens or other specific molecules expressed on pathogens. In 2001, Haydon and Dickert reported development of MIPs against the cell surfaces of yeast and bacteria for enriching these microorganisms (Haydon & Dickert, 2001). The same research group subsequently developed MIP based sensor layer for the detection of cells, viruses and enzymes (Haydon *et al*, 2003).

Subsequently a MIP based test for the diagnosis of dengue virus infection was developed by Tai and co-workers (2006). They developed the sensor by coating quartz crystal microbalance (QCM) chip with MIPs for non-structural protein 1 of flavivirus. Serum samples from confirmed cases of dengue were analysed using the MIP sensor and a standard ELISA test. The results obtained with the MIP sensor correlated with the ELISA results.

Gupta and colleagues (2016) developed a piezoelectric sensor for the diagnosis of Nisseria meningitidis by detecting a protein from the outer membrane of the bacterium. Employing computational approach, they identified a peptide sequence for imprinting. The epitope imprinted sensor was able to bind N meningitidis proteins in patients suffering from meningitis.

Zhou and colleagues (2014) developed a rapid and cost effective sandwiched electrochemiluminescence immunosensor for ultrasensitive detection of HIV-1 using magnetic MIPs (MMIPs) as capture probes and antigen conjugated horseradish peroxidase as labels. The imprinting was achieved on the surface of silicate-coated magnetic iron oxide nanoparticles. The recognition and enrichment of ultra trace levels of anti-HIV1 by the MMIPs was followed by a sandwich electrochemiluminescence immunosensor. The detection limit of this assay was 1:60,000.

A comparison between a MIP based recognition and quantitation of adenovirus with an antibody based detection system was undertaken by Altintas and colleagues (2015). They employed a solid phase synthesis method for the production of MIP for adenovirus. The MIPs were immobilised on a SPR and the detection of adenovirus was investigated in the concentration range of 0.02 pM. The results were compared with those obtained from antibody based detection assays. The authors concluded that the MIP based SPR sensor was suitable for the detection of viruses.

Altintas and colleagues adopted an interesting strategy for the detection of blood borne viruses (Altintas *et al,* 2015).They developed an SPR biosensor incorporating a high affinity MIP targeting bacteriophage MS2 as the template. The authors reported that their biosensor provides an alternative approach for the detection of waterborne viruses. They also suggest that this technology may enable removal of waterborne viruses.

More recently, Ma and colleagues developed an electrochemical sensor for rapid detection of human immunodeficiency virus by using a MIP against HIV-p24 protein on the surface of multi-walled carbon nanotubes modified glassy carbon electrodes (Ma *et al*, 2017). The sensor exhibited specific recognition of HIV-p24 protein with good selectivity, reproducibility and an exquisite sensitivity. The detection limit was reported to be 0.083pg per cm^{-3}.

MIPs have also been developed to detect pathogen derived toxins in the treatment of severe infections. Altintas and colleagues (2016) fabricated MIP for E.coli endotoxin using computational modelling. Based on the binding interactions between the template and 21 different monomers, they chose itaconic acid, methacrylic acid and acrylamide as functional monomers. The synthesised nanoMIPs with functional groups on the outer surface were immobilised on to SPR sensor surfaces. The endotoxin MIPs displayed high affinity and selectivity. The limits of detection was 0.44 ± 0.02 ng $mL^{(-1)}$when itaconic acid was used as the functional monomer. The authors were able to regenerate the MIP surface more than 30 times without any significant loss of binding activity.

1.3.9 Pitfalls and Challenges of Molecular Imprinting

Even though the MIPs have obvious merits, it should, however, be stated that there are number of challenges that will have to be met before they can be adopted for more general uses in the biomedical arena. As discussed in the preceding sections, molecular imprinting has been proven successful for small molecules, in particular, for those that are hydrophobic and chemically inert templates but the process is much more challenging when it comes to imprinting complex polypeptides and proteins with tertiary and quarterinary structures and those that undergo conformational changes due to ambient conditions (Flavin & Resmini, 2009; Janiak & Kofinas, 2007).

In biological systems, molecular recognition occurs in aqueous media. It is, therefore, important that synthesis of MIPs that recognise their target molecules in water is carried out in aqueous media (Janiak & Kofinas, 2007; Verheyen *et al*, 2011). The synthesis of high affinity MIPs in aqueous media remains a challenge and their performance is low compared to antibody-based assays (Chen & Ye, 2013; Ge & Turner, 2009). The availability of monomers for imprinting in aqueous media is also limited. Another problem with imprinting in aqueous media is that the hydrogen bonding interactions that play important role in non-covalent molecular imprinting performed in organic solvents are hampered in water (Verheyan *et al*, 2011).

There are other difficulties with imprinting macromolecules such as proteins. It has been shown that the structure of protein templates is adversely affected by exposure to monomers and cross linkers used in imprinting (Janiak & Kofinas, 2007). Furthermore, Hjerten's group has shown that the use of highly charged monomers for macromolecular imprinting results in non-specific binding (Ghasemzadeh *et al*, 2008). In addition, the Piletsky group showed that the monomers with multiple interaction points can also lead to non-specific binding (Bonini *et al*, 2007) The poor penetration of macromolecular templates such as proteins into the polymer network to access the binding sites can also create difficulties. The complexity of these macromolecules also creates non-specific and heterogeneous binding sites (Ge & Turner, 2008). The polymers carrying charged monomers can non-specifically bind to the targets thus impeding specific binding between the MIPs and the target molecules (Whitcombe *et al*, 2011). It should also be noted that the charge and hydrophobicity vary greatly across different domains of a protein surface and, similar sites (eg. conserved domains) are likely to be present in other proteins resulting in non-specific binding and cross-reactivity.

Another issue with imprinting macromolecules is that, due to high cross linker densities, template removal and rebinding may be hindered or even lead to entrapment of the template in the polymer network due to immobilisation (Verheyen et al, 2011). The method of template removal can also be an issue. It has been shown that certain commonly used detergents such as SDS and acetic acid can induce artefacts in MIPs for macromolecules such as bovine serum albumin (Fu *et al*, 2008; Janiak *et al*, 2009).

The quantification of rebinding of the template to the synthesised MIP and the reproducibility of the results can also be problematic in molecular imprinting of macromolecules (Guo *et al*, 2005; Verheyan *et al*, 2011). There is an unmet need for standardised methods to validate the results of MIP-target interactions (sensitivity and specificity).

The homogeneity of the MIPs in terms of size, charge and binding affinity will need to be improved to fabricate standardisable diagnostic assays and drug delivery systems (Ge *et al*, 2013; Ge & Turner, 2008). Furthermore, the adoption of MIPs for various diagnostic assays is being hampered due to the lack of generality in the sensor format (Bedwell & Whitcombe, 2016). Hence, more work is needed to synthesise uniform and high affinity MIP nanoparticles

to fabricate diagnostic assays that are comparable to antibody based assays in terms of sensitivity and specificity.

The development of MIPs for drug delivery is even more problematic due to lack of biocompatible/bioavailable systems (Chen & Ye, 2013; Ge *et al*, 2013). It has to be said that the development of non-toxic and biocompatible MIP nanoparticle based drug delivery systems are in its infancy at present. Finally, it must be emphasised that any MIP based diagnostic assay or a drug delivery vehicle will need to meet the standards set by the various regulatory authorities such as FDA (USA) and MHRA (UK).

1.4 Aims and Objectives of the study

In this project, the ability of molecularly imprinted polymer nanoparticles to replace antibodies in cancer diagnosis will be investigated. Specifically MIP nanoparticles for a lineage-specific antigen or a disease associated antigen will be synthesised using the solid phase polymerisation approach. The imprinting will be performed using the 'epitope' method. Once produced the MIPs nanoparticles will be characterised using techniques such as DLS and TRPS.

The aims and objectives of this study are outlined below.

Aim of the study

To investigate whether MIP nanoparticles synthesised using the solid-phase approach and epitope imprinting method have potential to be used as recognition ligands in cancer diagnosis.

Objectives

- 1) Identify a suitable candidate as a reliable biomarker in the diagnosis of haematological malignancies
- 2) Identify an appropriate epitope for the synthesis of a nanoMIP
- 3) Synthesise MIP nanoparticles using solid-phase imprinting process
- 4) MIP nanoparticle characterisation by DLS and TRPS
- 5) MIP nanoparticle-CD45 binding studies by DLS and TRPS to determine affinity and selectivity of the MIPs

CHAPTER 2 MATERIALS & METHODS

2.1 Materials& Equipment

2.1.1 Reagents

N-Isopropylacrylamide (NIPAm, >97.0%), *N*-tert-Butylacrylamide (TBAm, 97%), *N*,*N*′-Methylenebisacrylamide (BIS, 99%), *N*,*N*,*N*′,*N*′-Tetramethylethylenediamine (TEMED, 99%), Acrylic acid (AAc, 99%), Ammonium persulfate (APS, >98%), Sodium hydroxide (NaOH, ≥98.5%), Glutaraldehyde (GA, 50 wt% in H2O), Sodium chloride (NaCl, ≥99.5%) and Toluene (CHROMASOLV, 99.9%) were purchased from Sigma-Aldrich, UK. *N*-(3-Aminopropyl) methacrylamide hydrochloride (APMA, >98%) was purchase from PolySciences, UK. Phosphate buffered saline (PBS) was obtained from Life Technologies, UK, Ethanol, absolute (>99.5%) from Fisher, UK and Acetone was from AnalaR, UK.

2.1.2 Equipment

Glass beads, disposable plastic syringes, sintered disc filter funnel and filter membrane (0.22µm) were obtained from Sigma-Aldrich, UK. Polypropylene solid-phase extraction (SPE) tubes (60 ml) and polyethylene frit (20 µm) was purchased from Supelco, UK. Puradisc FP 30 syringe filter was from Whatman. Buchner filter flasks and Buchner filter cones were purchased from Fisher Scientific. Dynamic Light Scattering (DLS) measurements were made on Zetasizer, Malvern Instruments, Malvern, United Kingdom and Tunable Resistive Pulse Sensing analysis was made on qNano, IZON Science, Oxford, United Kingdom

2.2 Literature Search

Extensive literature search was undertaken to (1) acquire a sound knowledge in the subjects of Molecular Imprinting and Cancer Diagnosis and (2) to gather comprehensive scientific information on the developments in the area of Molecular Imprinting over the last thirty years. In order to achieve this objective, background reading of a number of text books and review articles was undertaken. On-line literature search was carried out on PubMed database and

Google Scholar. The following search terms were used to capture the publications- 'molecular imprinting', 'molecularly imprinted polymers', 'molecularly imprinted sensors', 'MIPs' and 'MIP sensors'. My PubMed search produced over 3200 articles published since 1987. Google Scholar was used to search for publications that were not included in the PubMed search.

A separate background reading and literature search were carried to determine the most informative protein (antigen) marker in terms of clinical utility for cancer diagnosis. As alluded in section 1.2.2, one of the most widely used markers used in cancer diagnosis is CD45 antigen (common leucocyte antigen) because expression of this antigen is routinely used to differentiate blood cancers from non-haematological malignancies such as carcinoma and sarcoma (Bain *et al*, 2017; Svarna *et al*, 2018; Swerdlow *et al*, 2017). For this reason a decision was made to synthesise a MIP for this protein.

A separate search was undertaken to obtain the CD45 antigen epitope sequence for molecular imprinting. In addition to on-line PubMed search, a number of websites of antibody manufacturers/distributors (Sigma, Dako, Beckton Dickenson, AbCam and Atlas) was performed.

2.3 Purchase of CD45 antigen and CD45 epitope

Purchase of CD45 antigen and CD45 epitope was made from Peterborough City Hospital Haematology Research Fund with the approval of the Trustees of the above Charity Fund.

CD45 antigen was purchased from Sigma Aldrich (UK). CD45 antigen epitopes with the sequence LNLDKNLIKY and CGLNLDKNLIKY were custom made from Peptide Synthetics, UK.

2.4 Risk Assessment and COSH Evaluation

In accordance with the Health & Safety policy of Cranfield University, a full risk assessment of the proposed research project and COSH Evaluation were undertaken.

2.5 Synthesis of Molecularly Imprinted Polymer Nanoparticles

Since the quantity of the purchased CD45 antigen was very small (25 µg), it was insufficient for molecular imprinting. It was, therefore, decided to use the target antigen for binding assays rather than for imprinting and to synthesise a MIP against a CD45 antigen epitope sequence that has been widely used by several antibody manufacturers for the production of anti-CD45 antibody for immunocytochemistry, immunohistochemistry and flow cytometry.

Synthesis of the MIP nanoparticles was performed both at Cranfield and at the Department of Chemistry, University of Leicester, UK in Professor Piletsky's laboratory using a protocol published in the Nature Protocols by his research group (Canfarotta *et al*, 2016). This protocol describes a method for the production of MIP nanoparticles using a solid phase synthesis technique. The principle of this method is illustrated in Figure 2.1.

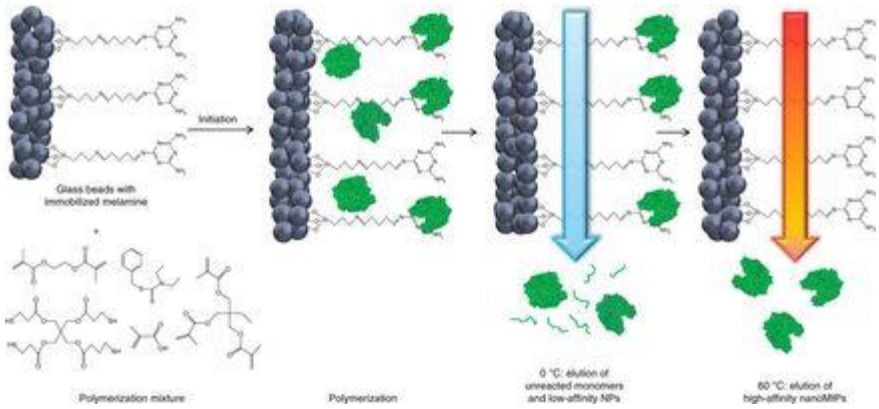

Figure 2.1. Solid-phase synthesis and separation of nanoMIPs by photo-polymerization, using melamine as a model template (Canfarotta *et al,* 2016).

2.5.1 Preparation of glass beads

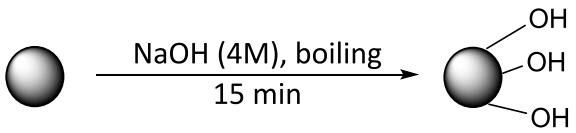

Clean glass beads (70 grams) were activated by boiling them in 4M NaOH for 15 minutes. The beads were then washed thoroughly with deionised water (ten times with 200ml of water). The beads were neutralised with 300ml of PBS and then washed three times with

deionised water to remove any salt residues. The beads were rinsed with 200ml acetone twice and allowed to dry at 80 °C for 3 hours.

2.5.2 Silanisation of glass beads

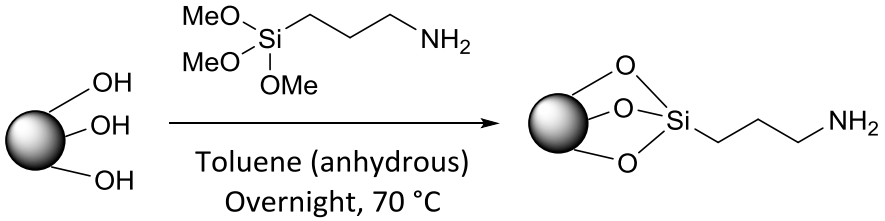

The glass beads were silanised by incubating in 2% APTMS solution in anhydrous toluene for 24 hours at room temperature in a closed bottle. The glass beads were then decanted into a sintered disc filter funnel and rinsed with eight volumes of acetone and one volume of methanol. The glass beads were then dried under vacuum. The silanisation of nanoMIPs was assessed by dansyl chloride test

Dansyl Chloride Test

The basis of this test is that dansyl chloride or 5-(Dimethyl Amino) Naphthalene- 1 -SulfonYL chloride reacts with primary amino groups to produce stable blue or blue-green fluorescent sulfonamide adducts (Walker JM, 1994). Dansyl chloride (10 mg) was dissolved in 3ml acetonitrile. Aliquots of silanised and non-silanised silica beads were added to vials containing dansyl chloride solution and kept in the dark for 2 hours. The beads were examined under ultraviolet lamp.

2.5.3 Immobilisation of template (CD45 peptide)

Glutaraldehyde (GA) method

In the initial experiments performed at Cranfield and Leicester, the option A of the Piletsky protocol was followed to immobilise the peptide on to the glass beads. This option was specifically designed to immobilise templates containing free amino groups. In this method, glutaraldehyde acts as a linker between the amine residue on the surface of the silanised glass beads and the amine groups of the template.

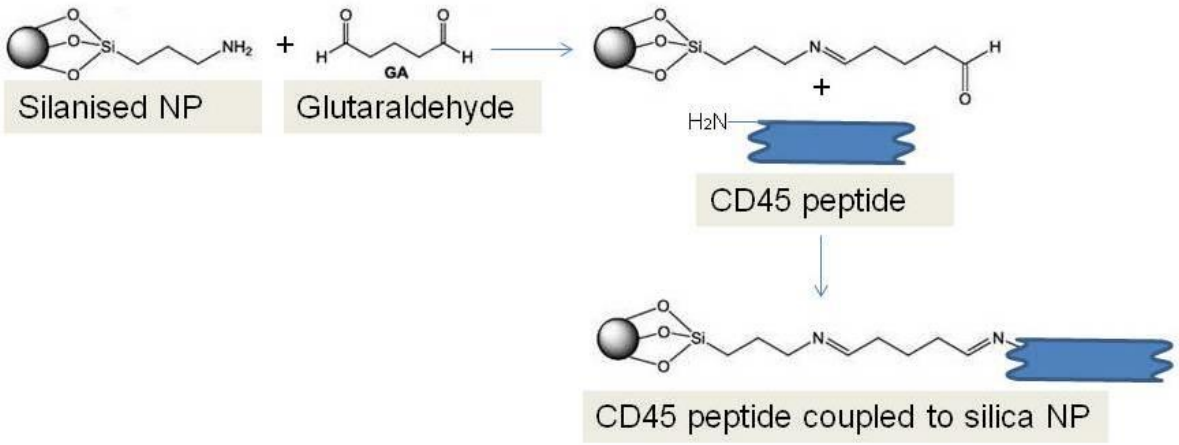

Silanised glass beads were incubated for 2 hours in a 5% (vol/vol) glutaraldehyde solution in 0.01 M PBS, pH 7.2. Glass beads were then washed with deionized water (eight volumes) in a Buchner funnel under vacuum.

In the latter experiments, the option B of Piletsky protocol was employed. In this approach, iodoacetic acid N-hydroxysuccinimide ester (SIA) was used as a linker. This option was designed by the Piletsky group to immobilise peptides containing thiol groups. In order to employ this method, one cysteine and one glycine amino acids (C-G) were added to the carboxyl end of the template.

Iodoacetic acid N-hydroxysuccinimide ester (SIA)
SIA coupling method was used to immobilise CD45 antigen peptide to silica nanoparticles to 'orientate' the template on the surface of the silica NP by coupling the amine group on the silanised NP with a -SH group on the template peptide. In order to achieve this, a new batch of polypeptide was custom made with two additional amino acids (cysteine and glycine) added to the original polypeptide (CGLNLDKNLIKY)

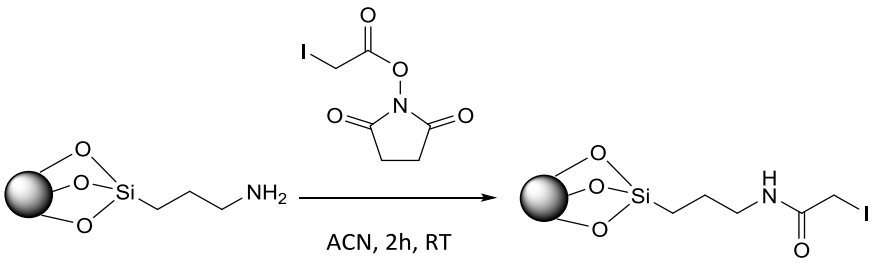

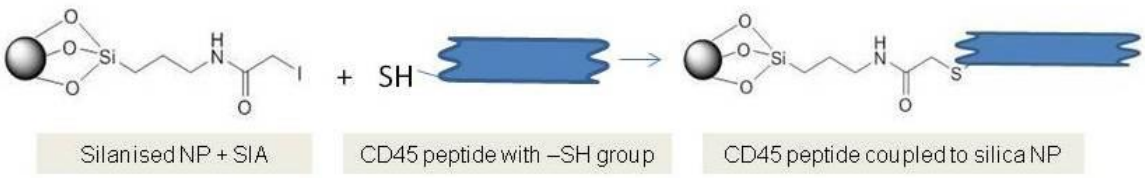

Iodoacetic acid N-hydroxysuccinimide ester (SIA) (10 ml) was added to the silanised glass beads in 50 ml anhydrous acetonitrile and incubated for 2 hours under dark. The beads were then washed with acetonitrile five times.

Coupling to peptide

The conditions used for coupling of silanised nanoparticles to peptide varied depending on the linker used. For glutaraldehyde linked beads, a PBS buffer (0.01 M, pH 7.2 (50 ml)) was used. But for the SIA linked beads, a thiol buffer (pH 8.2) consisting 50 ml phosphate buffered saline and 74 mg (5 mM) ethylenediaminetetraacetic acid (EDTA) was used. The buffer solutions were degassed and purged with nitrogen prior to addition of peptide (6.9 mg). GA treated or SIA-linked glass beads (70g) were then transferred in to that flask containing PBS buffer (for GA-linked glass beads) or thiol buffer for the SIA-linked beads. The flasks were wrapped in aluminium foil to exclude light and left overnight at room temperature. After overnight incubation, a one ml aliquot of the beads was transferred in to a vial for BCA protein assay to assess template binding.

BCA protein assay

The basis of BCA (bicinchoninic acid) assay is that the peptide bonds in protein/peptide reduce Cu^{2+} ions from $CuSO_4$ to Cu^{+}. BCA chelates with Cu^{+} and produces a purple colour (Smith *et al*, 1985). The assay was performed in accordance with the specifications of the manufacturer. Briefly, 500 µl of reagent A and 10 µl of reagent B were mixed in a vial and added to the aliquot of glass beads and incubated at 30°C for 10 minutes. Colour change was recorded.

2.5.4 Synthesis of nano MIPs (polymerisation)

In all but one experiments the functional monomers *N*-Isopropylacrylamide (NIPAm), *N*-tert-Butylacrylamide (TBAm) and acrylic acid (AAc) were used for polymerisation. *N*,*N*′-Methylenebisacrylamide (BIS) was used as the cross- linker.

In one experiment that was carried out to investigate whether addition of a fluorinated monomer may improve the quality of nanoMIPs produced, a fluorinated monomer (F1) that was kindly donated by Dr Francesco Canfarotta of MIP Diagnostics, UK was used instead of NIPAM for the synthesis of nanoMIPs.

The polymerisation mix (Protocol 1) was prepared as follows;

NIPAM (39 mg, 0.34 mmol), BIS (2 mg, 0.013 mmol) and *N*-(3-Aminopropyl) methacrylamide hydrochloride (5.8 mg) were placed in a Buchner flask and added 98 ml of water. The solids were dissolved by gentle swirling. TBAm (33 mg, 0.26 mmol) was dissolved in 1 ml of absolute ethanol (0.99.5%) in a vial. This solution was added to Buchner flask containing NIPAM and BIS and gently swirled to homogenise. In a separate vial, 22µl of AAC (0.32 mmol) was diluted in 1 ml of water. A 100 µl aliquot of this solution (corresponding to 0.032 mmol) was added to the Buchner flask containing NIPAM, BIS and TBAm and gently swirled to homogenise. The flask was sealed and connected to a vacuum and sonicated for 10 minutes and then purged with a slow stream of nitrogen gas *via* a Pasteur pipette placed into the bulk of the solution.

The composition of the polymerisation mix containing the fluorinated monomer (Protocol 2) was as follows: 0.34 mmol of fluorinated monomer (F1), 11 mg of TBAm and 0.22 mmol of hydroxyethyl methacrylate (HEMA) and BIS (2mg, 0.013 mmol). The preparation of the polymerisation mix was carried out as described above.

The template derivatised glass beads were transferred into a 250 ml sealable bottle and degassed.

For both composition, APS (30 mg, 0.13 mmol) was dissolved in 500 µl of deionised water in a glass vial and TEMED (30 µl, 0.33 mmol) was added. The degassed solution of monomers was poured onto the glass beads and the above solution (APS/TEMED) was added quickly to the glass beads suspended in the polymerisation mixture while purging the headspace with nitrogen. The bottle was sealed and incubated for 1 hour at room temperature with occasional gentle swirling by hand but without magnetic stirring to avoid abrasion of glass beads.

2.5.5 Selection of high affinity nanoMIPs

After the synthesis, the whole content of the vessel (beads and solution) were transferred into an SPE cartridge fitted with a 20 µm porosity PE frit. The solution was removed by applying negative suction. The cartridge was filled with fresh deionised water (30 ml) at room temperature to keep the glass beads wet. Any free monomers and low affinity nanoMIPs were removed by eluting the solution at room temperature and by replacing it with 30 ml aliquots of fresh deionised water each time. This step was repeated eight times. The outlet of the SPE cartridge containing the glass beads was closed with a female Luer cap and 30 ml of fresh deionised water that was pre-warmed at 65°C was added to the SPE cartridge containing the glass beads and placed this into a water bath at 65°C. After 15 minutes, the nanoMIP solution was collected by negative pressure. Fresh pre-warmed (65°C) deionised water was added and the SPE cartridge was placed at 65°C for 2 minutes. High affinity nanoMIPs were collected into a 500ml screw cap glass bottle. The nanoMIP solution was left at room temperature to cool down before being stored in a fridge at 4°C until further use.

2.6 Dynamic Light Scattering (DLS) measurements

The size and polydispersity index (PDI) of the CD45 peptide imprinted nanoMIPs were measured by Zetasizer Nano Instrument (Nano S) (Malvern Instruments Ltd, Malvern, UK). An aliquot (1 ml) of nanoMIP solution was sonicated 30 seconds and placed in a clean plastic cuvette and DLS measurements (5 runs) were made.

2.7 Determination of binding of nanoMIPs to CD45 protein by DLS

A binding assay was performed by DLS to determine whether the CD45 peptide imprinted nanoMIPs were able to bind the target CD45 protein. As DLS can assess size and polydispersity index (PDI) of nanomaterials, it can be used to determine whether the protein can bind to the nanoMIPs, as the size and PDI of the resulting complex is different to the size and PDI of the nanoMIPs alone.

Because the purified CD45 protein purchased from Sigma Aldrich was highly concentrated (0.9mg/ml), a diluted solution (40µg/ml) of the protein was prepared in water and used for the assay. The concentration of CD45 antigen used for the binding experiments was roughly similar to the antibody concentrations used in routine diagnostics (Beckman Coulter datasheet for anti-CD45 antibody). The dilute protein solution in water was added to the nanoMIP solution and sonicated for 1 minute and incubated. Initial DLS measurements were obtained after 5 minutes incubation. The measurements were repeated after 40 minutes incubation to observe any changes in the parameters (size and PDI).

2.8 Determination of size and zeta potential of nanoMIPs by Tunable Resistive Pulse Sensing

Measurement of the size and zeta potential of the nanoMIPs was carried out using the qNano (Izon Science Ltd, New Zealand). This equipment consists of two important components- (1) a tunable nanopore membrane and (2) a proprietary data capturing software (Izon Control Suite v3.1.2.53). Adopting the standard instrument set up, the lower fluid cell was filled with 75 µl of PBS buffer, ensuring no bubbles were present. The upper fluid cell was filled with 40 µL of the test sample suspended in PBS buffer. A voltage of +0.74V was applied and a stable baseline of +115nA was achieved. After each measurement, the nanopore membrane was washed several times with PBS by removing and replacing the buffer to remove any residual particles and to ensure no cross contamination between samples. The nanopore membrane NP200 which is capable of detecting particles within the size range of 100-300 nm was used for the measurements. All measurements were taken at a single stretch and voltage.

Zeta potential measurements using TRPS

To run zeta measurements a calibration dataset was run using calibration particles with a size of 200nm. To calibrate a zeta measurement, a known calibration standard with a known zeta value was made up to a known concentration ($1x10^{10}$ particles/ml). The stretch of the nanopore was kept constant for the zeta calibration datasets and for the sample measurements. The calibration and the samples were run in PBS buffer. The calibration particles were run at a given pressure (1.1mbar), using three different voltages (+0.88V, +0.74V, +0.60V). The data obtained from these calibration files were used in the Izon template to get zeta values for the samples.

2.9 Determination of binding of nanoMIPs to CD45 protein by TRPS

The basis of this assay is that the binding of peptide or protein molecule to a nanoparticle such as nanoMIP induces changes in the translocation velocity of the nanoparticle. The data generated by any changes in translocation velocities are expressed as changes in zeta potential. The method described in the preceding section (2.8) was employed to record the zeta potentials of the nanoMIPs before and after incubation with dilute preparations of CD45 antigen (40µg/ml and 0.4µg/ml) for 10 minutes.

CHAPTER 3 RESULTS & DISCUSSION

As alluded in Section 1.1, antibodies are heavily used in the diagnosis of cancers but they have a number of disadvantages such as their high cost, the need for refrigeration for transport and storage and their limited shelf life. Hence, an alternative that is easy to manufacture in large quantities at low cost, and is robust, could be stored at room temperature with long shelf life and easily incorporated into various diagnostic platforms to fabricate sensors would be a very attractive proposition. This is true, particularly in the developing countries where facilities for cold transportation and storage are limited. A number of different technologies are being actively pursued to develop artificial receptors for various molecules, but due to their desirable attributes discussed previously, molecularly imprinted polymers are the most promising candidate to challenge the dominance of antibodies in clinical diagnostics.

The aim of this study was to investigate whether MIP nanoparticles synthesised using the solid-phase approach have potential to replace antibodies in cancer diagnosis. In order to achieve this goal, a logical approach was adopted. Since the field of molecular imprinting is a highly specialised and rapidly expanding discipline, an extensive background reading was undertaken. A literature search on the subject of Molecularly Imprinted Polymers using Pubmed and Google Scholar produced more than 3200 articles published since 1987. Those articles that were relevant to this study were grouped under the headings of MIP basic principles, MIP synthesis, MIP characterisation, MIP platforms, Smart MIPs, MIP applications in separation and extraction, MIP application for drug delivery, MIP application for sensors/bioassays for biomolecules and drugs and MIPs in microbiology. Information extracted from these articles (full text and abstracts) was used to write the Introduction of this thesis and also to draft a review article titled *'Molecularly Imprinted Polymers: Potential Applications in Medicine and Biotechnology'* (Sivakumaran *et al*, 2019).

When designing this research project, special considerations were given to the following (a) identifying a suitable candidate marker (protein) for the diagnosis of blood cancers, (b) selecting or designing an appropriate template for molecular imprinting, (c) choosing the correct imprinting technique and conditions to synthesise MIPs for a protein target that is

usable in clinical diagnostics and (d) the methods of characterisation of the synthesised MIPs.

3.1 Identification of a suitable candidate marker for the diagnosis of haematological malignancies

A number of lineage specific antigens were considered as potential candidates for molecular imprinting. The list included (1) CD19 antigen (B lymphocyte antigen), which is expressed in a variety of mature B cell malignancies such as B cell Non-Hodgkin's lymphomas and chronic lymphocytic leukaemias, (2) CD3 antigen (T cell antigen), which is expressed in various T cell lymphoproliferative diseases that include large granular lymphocytic leukaemia and cutaneous lymphomas such as mycosis fungoides, (3) CD33 antigen (myelocyte antigen), which is expressed in myeloid malignancies such as acute myeloid leukaemia and (4) CD45 antigen (common leucocyte antigen), which is expressed in most haematological cancers (WHO Classification of Tumours of Haematopoietic and Lymphoid Tissues, Revised 4th Edition, 2017). Although the expression of CD19, CD3 and CD33 antigens are very useful in delineating haematological cancers originating from B cells, T cells and myeloid cells respectively, expression of CD45 antigen (‘leucocyte common antigen), a surface membrane protein that is expressed in all the bone marrow derived cells except erythrocytes, has a broader significance in that it enables Pathologists and Haematologists to differentiate 'Blood Cancers' that include leukaemias, lymphomas, myelomas and myeloproliferative diseases from those of non-haematopoietic cells such as carcinomas and sarcomas. For this reason, anti-CD45 antibody is always included in the primary antibody panel used for cancer diagnosis ((Bain *et al*, 2017; Svarna *et al*, 2018; Swerdlow *et al*, 2017); 'WHO Classification of Tumours of Haematopoietic and Lymphoid Tissues', 2017). Because of the importance of CD45 antigen expression in the diagnostic work up of cancers, a decision was made to select this protein for molecular imprinting in the current study.

3.2 Template selection for molecular imprinting

The initial plan was to imprint the whole protein. However, due to the cost of the purified CD45 protein, the plan was abandoned and a search for a suitable fragment or 'epitope' of that protein that could be synthesised in larger quantity at a reasonable cost to enable

imprinting was undertaken. On-line search on the subjects of CD45 protein and anti-CD45 antibody recognition sequence that are published on the websites of Human Protein Atlas (Human Protein Atlas : ENSG00000081237), Uniprot (Uniprot/SWISSPROT;Acc: P08575), Entrez (Entrez gene: 5788) and various antibody manufacturers revealed that the most of the commercially available anti-CD45 antibodies recognise an amino acid sequence on the extracellular domain of the CD45 protein. The amino acid sequence of this epitope is 'Leucine-Asparagine-Leucine-Asparticacid-Lysine-Asparagine-Leucine-Isoleucine-Lysine-Tyrosine' (LNLDKNLIKY), which is part of the sequence of the immunogen used to manufacture anti-CD45 antibodies. The Recombinant Protein Epitope Signature Tag (PrEST) antigen sequence of the immunogen is given below.

KLENLEPEHEYKCDSEILYNNHKFTNASKIIKTDFGSPGEPQIIFCRSEAAHQGVITWNPPQR SFHNFTLCYIKETEKDC**LNLDKNLIKY**DLQNLKPYTKYVLSLHAYIIAKVQRNGSAAMCHFTT KSAPPSQVWNMT

Therefore the CD45 antigen peptide with the amino acid sequence of LNLDKNLIKY was selected for the epitope imprinting and was custom made by a commercial company (Peptide Synthetics, UK). This peptide sequence was used initially for the synthesis of CD45 nanoMIPs. In order to investigate the hypothesis that coupling the template to the silica bead through a single-SH group of the amino acid cysteine (C) added to one end of the template may orient the peptide immobilisation and improve the homogeneity of the synthesised MIPs, thus improving the sensitivity and specificity of template binding to the target molecule (CD45), a second batch of polypeptide with the amino acid sequence of **C**GLNLDKNLIKY was synthesised and used in the latter experiments.

3.3 MIP Nanoparticle Synthesis

3.3.1 Choice of imprinting technology

A number of factors were considered before choosing the type of imprinting technique and the conditions employed. Since the primary application of this nanoMIP was going to be biological (MIP-protein/cell interaction), it was imperative that the imprinting was carried out in

aqueous medium rather than in organic solvents. Furthermore, because of the availability of the template was limited, a technique that requires minimum amount of template but produces good yield of high affinity MIPs was preferred. In this respect, some established techniques such as bulk polymerisation was considered unsuitable because of the need for large amounts of template material while producing low yield (Chin *et al*, 2016).

Another important consideration was the uniformity of the binding sites created by the imprinting process. As outlined in section 1.3.2, one of the important drawbacks of the traditional imprinting techniques is the lack of homogeneity in the recognition sites of the MIPs synthesised due to the random nature of template-monomer interaction. For this reason, the solid-phase imprinting technology that was developed by Piletsky and colleagues (Poma *et al,* 2013) in which the template molecules are 'anchored' to the surface of the silica nanoparticles in a pre-determined orientation prior to imprinting, was chosen to synthesise the MIPs in this study since immobilising the template to a solid phase in a fixed orientation facilitates, in theory, generation of MIPs with homogenous binding cavities, analogous to the 'monoclonality' of antibodies, where all the antibody molecules exhibit a single specific antigen binding characteristic. This feature would be particularly important in cancer diagnosis where 'clonality' is *sine qua non* of malignancy. In addition, the use of an immobilised template permits removal of unbound template, monomers, cross linkers and low affinity polymers yielding high affinity MIPs with uniform binding properties.

3.3.2 Selection of monomers and cross linkers

The choice of functional monomers and cross linkers (and their composition) was another important consideration. It should be noted that there is no established method of optimisation of monomer composition for imprinting peptides and proteins. That said, there is an increasing trend in using computational modelling to select functional monomers with strong binding interactions with the template and to choose the correct ratio and composition of monomers and linkers (Cowen *et al*, 2016; Nicholls *et al*, 2011). A range of computational modelling methods have been used. These include electronic structure methods such as semi empirical approaches, Density Functional Theory (DFT) and *ab initio* and Molecular Dynamics Simulations. One of the common approaches is the use of DFT in which the 'binding energy' of the polymer to the target molecule is calculated. However, such an

approach was beyond the scope of this study. For this reason, functional monomers and cross linkers that have been reported to yield MIPs for peptides and proteins with good sensitivity and specificity were selected for this study. In a landmark study, Hoshino and co-workers synthesised MIPs to melitin, a 26 residue peptide (Hoshino *et al*, 2008). They selected monomers from a combinatorial library of polymers based on their binding affinity. The monomers [N-isopropylacrylamide (NIPAm), acrylamide (AAm), N-(3-aminopropyl) methacrylamide hydrochloride (APMA), and N-tert-butylacrylamide (TBAm)] and cross linkers [N,N-methylenebisacrylamide (BIS)] used in this study have received wide acceptance and several other research groups have since used them successfully for peptide/protein imprinting. The selection of monomers and cross linkers for the current study was adapted from the Hoshino's report. In one of the nanoMIPs synthesis (protocol 2) performed at Leicester a fluorinated monomer was also used in combination with conventional monomers to study whether addition of this monomer improves the quality of the nanoMIPs synthesised.

3.3.3 NanoMIP synthesis for CD45 antigen epitope using solid-phase imprinting technology

Initial experiments to synthesise nanoMIPs for CD45 antigen epitope was conducted at Cranfield University in Professor Tothill's laboratory (Advanced Sensors Labs) under the supervision of Dr Chianella. These experiments resulted in the production of nanoMIPs that were subsequently used to study binding to CD45 protein. However, due to the unexpected organisational changes that happened in the Cranfield University (Advanced Sensors Labs), I could not continue my MIP synthesis work at Cranfield and had to utilise the facilities in the laboratory of Professor Piletsky at the University of Leicester under the guidance of Dr Francesco Canfarotta. It must, however, be noted that the methodology employed at Cranfield and Leicester was largely similar.

Certain steps in the solid-phase synthesis are critical for effective imprinting. Two such steps are (1) silanisation of derivatised silica nanoparticles and (2) template immobilisation on to the silanised particles. Appropriate tests were conducted to confirm successful silanisation and template immobilisation.

Silanisation of silica nanoparticles

The dansyl chloride test performed on the silanised silica nanoparticles confirmed satisfactory silanisation (Figure 3.1)

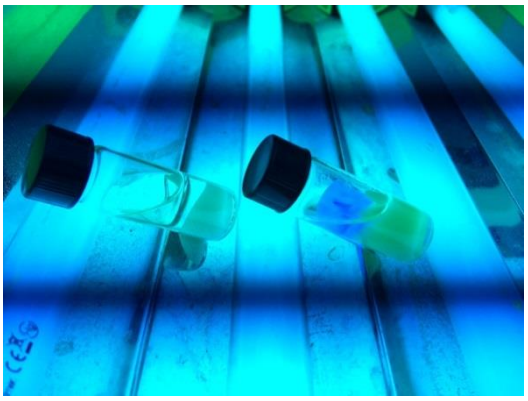

Figure 3.1. Dansyl chloride test for confirmation of silanisation.

Aliquots of silanised (right) and non-silanised silica nanoparticles were incubated with dansyl chloride and examined under ultraviolet light. The silanised particles show green fluorescence confirming presence of free amine group while the non-silanised particles show no fluorescence.

Template immobilisation

The BCA assay performed to analyse binding of CD45 peptide to glass beads confirmed that there was good protein binding (Figure 3.2). It should be stated that both methods of peptide coupling (glutaraldehyde and SIA) produced satisfactory results in BCA assay confirming that both these techniques are effective for the immobilisation of peptide templates to solid phase.

Figure 3.2. Results of BCA assay.

The CD45 peptide immobilised glass beads show intense purple colour (right) while the control glass beads show virtually no colour confirming peptide binding to the beads.

3.4 MIP Nanoparticle Characterisation

A variety of techniques have been used to study the physical and functional characteristics of MIPs. The most widely used methods to determine the size of nanoMIPs are dynamic light scattering (DLS) and electron microscopy (TEM or SEM). In addition to the size analysis, the SEM can be used to study the morphology (eg. shape) and surface characteristics such as porosity of the MIPs. Even though the DLS technique is extensively used in MIP characterisation, it must be pointed out that this method is far from ideal. The main drawback is that DLS can only give average size of a population of particles and cannot provide measurements of individual particles. The technology of tunable resistive pulse sensing (TRPS) which is based on Coulter principle, on the other hand, performs particle-by-particle analysis and is able to determine the size and size distribution of nanoparticles more accurately (Kozak *et al*, 2011; Sivakumaran & Platt, 2017; Weatherall & Willmott, 2015). That said, there has been no published report on the use of TRPS for the characterisation of nanoMIPs.

Several approaches have been used to study the interaction between the MIP and the target molecule. They include Surface Plasmon Resonance (SPR) (Abdin *et al*, 2015; Altintas *et al,* 2015; Guerreiro *et al*, 2014; Poma *et al*, 2013), Quartz Crystal Microbalance (QCM) (Diltemiz *et al*, 2017; Haydon *et al*, 2003; Tai *et al*, 2006), Surface Enhanced Raman Light Scattering (SERS) (Holthoff *et al,* 2011), Fluorescence Energy Transfer (FRET) (Yoshimatsu *et al*, 2008), Enzyme-Linked Immunosorbent Assay (ELISA) (Chianella *et al,* 2013; Smolinska-Kempisty *et al*, 2016; Tai *et al*, 2006), Fluorescent Microscopy (Zahra El-Schich *et al*, 2016), Confocal microscopy (Wang *et al,* 2016), Flow Cytometry (Zahra El-Schich *et al*, 2016), UV-VIS spectroscopy (Eersels *et al,* 2018), Spectrophotometry (El-Sharif *et al*, 2015) and various electrochemical methods such as Differential Pulse Voltametry (Sun *et al*, 2013), Pulsed Amperometric Detection (PAD) (Ramanaviciene *et al*, 2004).

In this study two techniques (DLS and TRPS) were employed to determine the sizes of the nanoMIPs. Due to logistical reasons, nanoMIP-target protein interaction could not be studied by either surface plasmon resonance (SPR) or quartz crystal balance (QCM) as originally planned. The binding of nanoMIP to target protein was, therefore, assessed by DLS and TRPS. The latter technique was chosen for the reasons that the published data and personal

experience suggest that this method is a sensitive and versatile technology to study nanoparticle-protein/peptide binding (Healey *et al*, 2019; Holton *et al*, 2018; Sivakumaran & Platt, 2017).

3.4.1 Determination of the size of MIPs by Dynamic Light Scattering (DLS) and Tunable Resistive Pulse Sensing (TRPS).

The size measurements of the MIPs synthesised at Cranfield by DLS showed that the average size of the nanoMIPs was 228±17 nm (Figure 3.3). The variation in the particle size between the measurements was considerable ranging from 198.8 nm to 295.1 nm. Although it is tempting to speculate that the size variations could have been caused by particle aggregations, this phenomenon cannot explain why the measurement 3 gave a significantly lower value (198.8 nm).

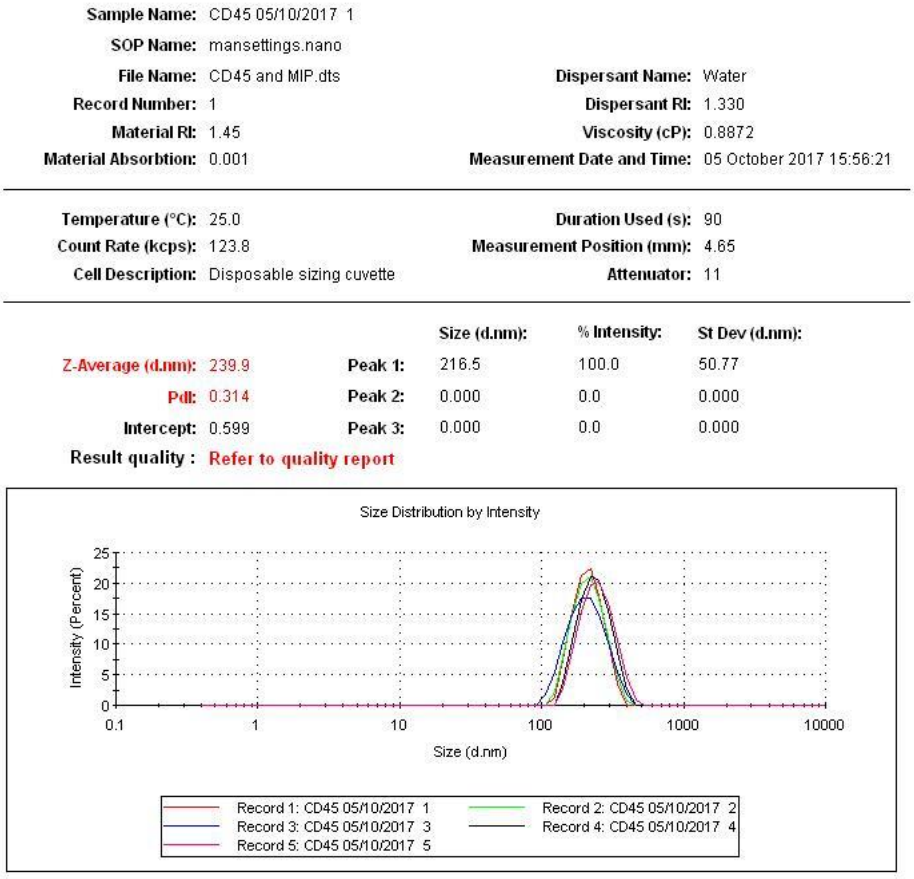

Figure 3.3. Size and polydispersity index (PDI) of nanoMIPs measured by DLS.

The mean size of the nanoMIPs derived from five measurements is 249 nm.

The mean polydispersity index (PDI), a measure of heterogeneity of the size of particles in a mixture, of the nanoMIPs was 0.330 $\pm$ 0.022 indicating that although there was variation in the particle size (Figure 3.3), this was acceptable as a value lower than 0.500 is usually desirable.

The size and PDI of the nanoMIPs synthesised in Leicester using two different protocols are shown in Figures 3.4 & 3.5. The DLS plot of the nanoMIPs synthesised using the CD45 peptide template containing amino acids cysteine and glycine but with the same monomer composition that was used in Cranfield shows that the size of the particles in the predominant peak is 187.4 nm. However, the data also shows that the PDI of the particles is 0.583 (Figure 3.4) which is higher than those synthesised in Cranfield. However, analysis of the data indicates that the high PDI of the particles is largely due to the presence of a second population with a very high diameter exceeding 1000nm. It is possible that this population (peak) represents clumps or agglomerates of MIPs or impurities.

Sample Name:	Protocol 1 peptide 6		
SOP Name:	mansettings.nano		
File Name:	180823.dts	**Dispersant Name:**	Water
Record Number:	6	**Dispersant RI:**	1.330
Material RI:	1.59	**Viscosity (mPa.s):**	0.8872
Material Absorbtion:	0.01	**Measurement Date and Time:**	23 August 2018 18:22:10

Temperature (°C):	25.0	**Duration Used (s):**	80
Count Rate (kcps):	164.2	**Measurement Position (mm):**	4.65
Cell Description:	Glass cuvette with square aperture	**Attenuator:**	11

			Size (d.nm):	**% Intensity**	**Width (d.nm):**
Z-Average (d.nm):	387.1	**Peak 1:**	187.4	71.4	14.12
PdI:	0.583	**Peak 2:**	1048	28.6	73.65
Intercept:	1.07	**Peak 3:**	0.000	0.0	0.000
Result quality :	Refer to quality report				

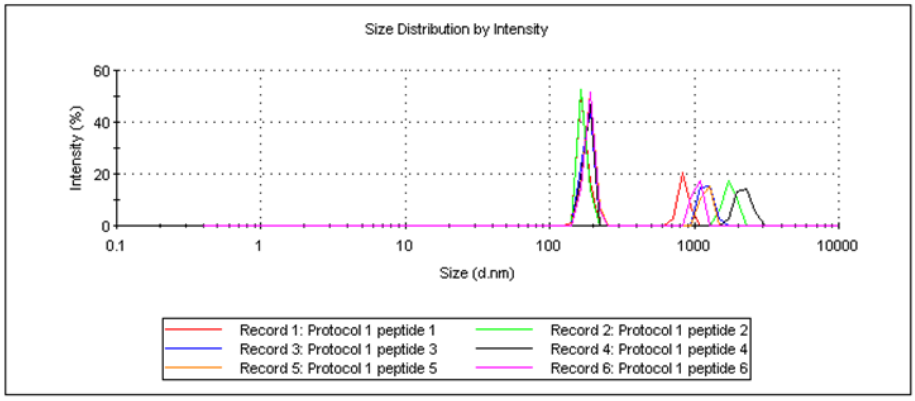

Figure 3.4. DLS analysis of nanoMIPs synthesised using the CD45 template containing cysteine and glycine and protocol 1.

The size of the dominant nanoMIP population is 187.4 nm. The second population with the larger size may represent agglomerates.

On the other hand, the nanoMIPs synthesised against the same CD45 epitope template using the protocol 2 (with added fluorinated monomer) show good results with fairly uniform particles with low PDI (0.186) but the mean size is 304.5 nm which is larger than the ones synthesised at Cranfield.

Sample Name:	protocol 2 CD45 peptide MIP 5		
SOP Name:	mansettings.nano		
File Name:	1.dts	**Dispersant Name:**	Water
Record Number:	5	**Dispersant RI:**	1.330
Material RI:	1.59	**Viscosity (mPa.s):**	0.8872
Material Absorbtion:	0.01	**Measurement Date and Time:**	24 August 2018 17:15:41

Temperature (°C):	25.0	**Duration Used (s):**	60
Count Rate (kcps):	402.5	**Measurement Position (mm):**	4.65
Cell Description:	Glass cuvette with square aperture	**Attenuator:**	10

			Size (d.nm):	**% Intensity**	**Width (d.nm):**
Z-Average (d.nm):	325.2	**Peak 1:**	304.5	100.0	39.42
PdI:	0.186	**Peak 2:**	0.000	0.0	0.000
Intercept:	0.939	**Peak 3:**	0.000	0.0	0.000
Result quality :	Good				

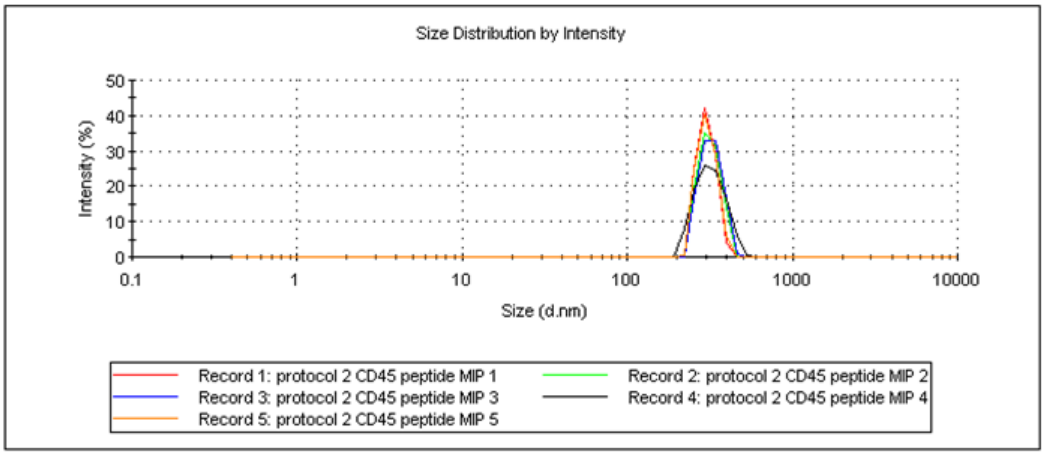

Figure 3.5. DLS analysis of nanoMIPs synthesised using the CD45 template containing amino acids cysteine and glycine and protocol 2.

The mean size of the nanoMIPs is 304.5 nm with a PDI of 0.186.

The differences observed in the physical characteristics between the two synthesised nanoMIPs (standard protocol versus protocol 2 containing fluorinated monomer) are intriguing. Firstly, the sizes of the particles are very different. It is possible that the difference in size was due to the composition of the monomers and cross linkers. For instance, in a recent work by Ma and colleagues (2017) in which the researchers synthesised a thermo-responsive fluorinated nanoMIPs via RAFT mediated aqueous polymerisation using poly(2,2,2-Trifluoroethyl) methacrylate (PTFEMA), there was a linear correlation between the concentration of the cross-linker EDGMA (EDGMA:PTFEMA ratio) and the size of the nanoMIP synthesised. Despite the fact that these particles are larger than the ones synthesised using conventional monomers, the observation that the nanoMIPs from protocol

2 has produced uniform particles with low PDI, however, is a significant one and deserves further investigations to find out whether these nanoMIPs are, indeed, better suited for imprinting proteins and peptides. In fact, as discussed in section 1.3.2, fluorinated methacrylate monomers are known to improve the polymerisation process and enhance the properties of synthesised polymers (Yao *et al*, 2014). It has been reported that copolymerisation of fluorinated monomers with conventional hydrocarbon monomers produces copolymers with remarkable properties such as low surface energy and thermal stability (Erol *et al,* 2009).

3.4.2 Determination of the size and dispersity of MIPs by Tunable Resistive Pulse Sensing (TRPS)

The size analysis using TRPS (qNano) shows that the MIPs synthesised are heterogeneous in that there are multiple populations of different sizes (Figure 3.6)

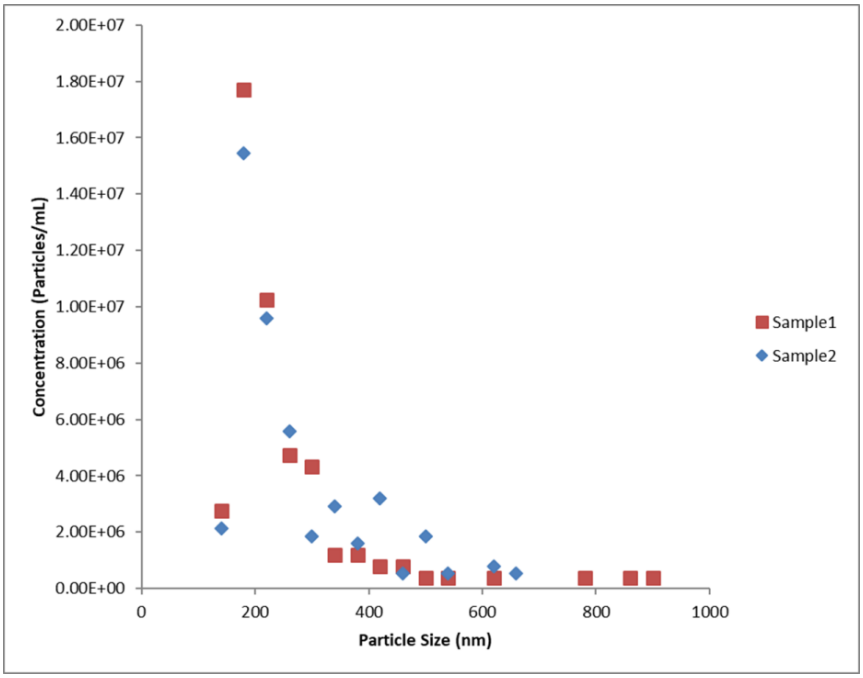

Figure 3.6. TRPS analysis of the size and dispersity of nanoMIPs synthesised in Cranfield.

Two aliquots (sample 1 and 2) of the nanoMIPs synthesised in Cranfield were analysed by TRPS. Both samples contained MIPs of varying sizes. The particle size of the predominant populations in both samples is 200-250nm

As the plot shows, the size of the nanoMIPs varies from 180nm to more than 800nm but the size of the predominant populations is 200-250nm. As mentioned, the advantage of TRPS is the ability to enumerate particles of a particular size. For example, the concentration of

nanoMIPs with a particle size of 200nm in sample 1 is $1.78x10^7$/ml and $1.58x10^7$/ml in sample 2. Low levels of very large particles are seen in sample 1. They probably represent agglomerates. A simple filtration through using a filter with pores smaller than 500 nm, could be sufficient to remove the agglomerate and leave the single nanoMIPs.

The results of the TRPS analysis of the size and dispersity of nanoMIPs synthesised in Leicester using the CD45 template containing amino acids cysteine and glycine are shown in Figure 3.7. Although the sizes of the particles of nanoMIP-1 (protocol 1) range from 82 nm to 390 nm, the vast majority of the particles are smaller than 200 nm in size. The predominant populations measure around 90-110 nm which is a good size for nanosensor applications. The concentration of the most predominant population (96 nm) is $9.1x10^8$/ml. The larger (>200 nm) particles are present in low concentrations (less than $1.0x10^8$/ml). These may represent clumps or agglomerates or impurities. Interestingly, the concentration of nanoMIP2 (protocol 2) is significantly higher than that of nanoMIP1. The predominant population is 110 nm in size and present at a concentration of $1.70x10^9$/ml. The nanoMIP2 particles also show heterogeneity of size but the majority of the populations measure less than 220 nm in size. The larger populations (>220 nm) are present in low concentrations (<$1.0x10^8$/ml) and may represent clumps or agglomerates or impurities. The TRPS plot shows that the nanoMIPs synthesised using the protocols 1 (magenta) and 2 (green) are heterogeneous in size.

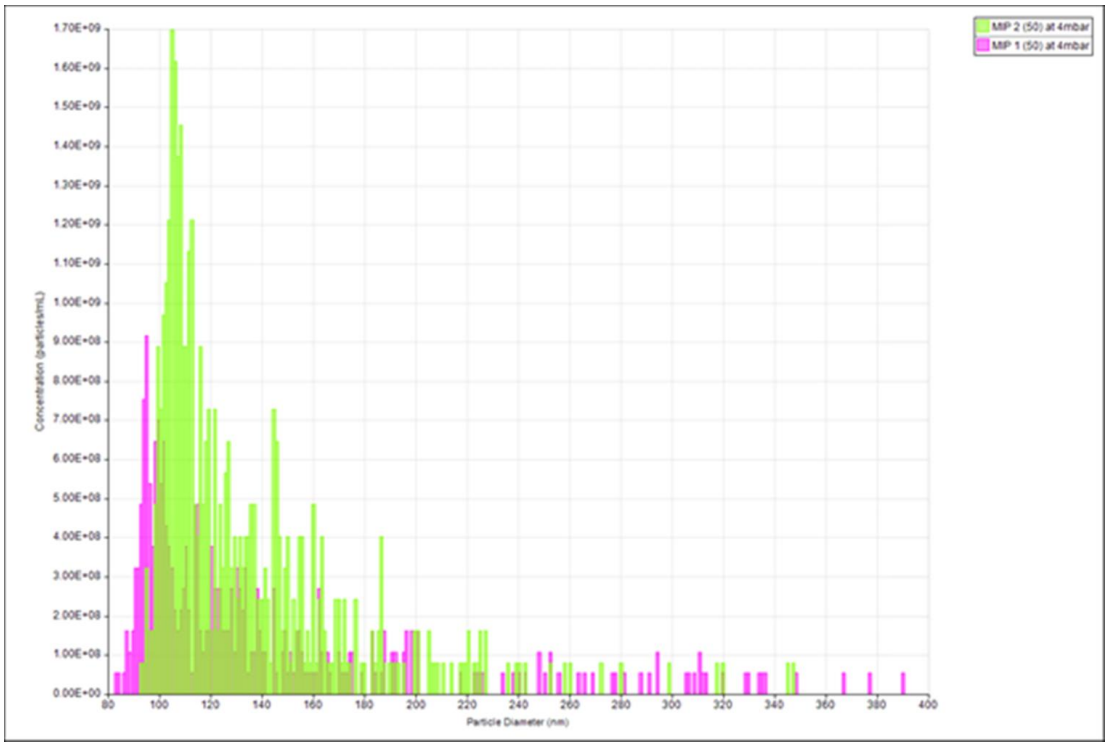

Figure 3.7. TRPS analysis of the size and dispersity of nanoMIPs synthesised in Leicester using the CD45 template containing amino acids cysteine and glycine

The majority of the nanoMIPs produced using protocol 1 (magenta) are below 200 nm in size with the dominant populations measuring 90-110nm. The concentration of the most predominant population (96 nm) is 9.1×10^{8}/ml. The majority of the nanoMIPs produced using protocol 2 (green) are below 220 nm in size with the dominant populations measuring 95-150nm. The predominant population is 110 nm in size and present at a concentration of 1.70×10^{9}/ml.

The differences in sizes of the nanoMIPs 1 and 2 recorded by DLS and TRPS are striking. The DLS measurement of the dominant population in nanoMIP1 is 187 nm whereas the TRPS measurement gives a value of 100 nm (90-110 nm). Similarly the size of the predominant population in nanoMIP2 by DLS analysis is 304 nm while the size of the dominant populations in TRPS measurement is 110 nm (100-120 nm). In other words, DLS appears to overestimate the size of nanoparticles. The explanation for this difference is that the two technologies are very different; TRPS by its basic principle (Coulter) is an exquisite technology capable of measuring particle by particle analysis, while the DLS technology relies on Brownian motion and can only provide an average size of a population. A direct microscopic (SEM or TEM) analysis would have been useful to determine the true size of the nanoMIPs and to draw conclusion as to which of the two modalities is the more accurate and informative technique for the size measurement of nanoMIPs. Any future work, therefore, must include parallel analysis using all three (EM, DLS and TRPS) modalities.

3.4.3 Determination of binding of nanoMIPs to CD45 protein by DLS

As shown in Figure 3.8, the average size of the nanoMIPs was 228 ± 17 nm. The results of the DLS measurements after 5 minutes incubation with CD45 protein (40µl/ml) show that the average size of the nanoMIPs had increased from 228 ± 17 nm to 405 ± 85 nm (Figure 3.8) suggesting that there was an interaction between the nanoparticles and the target protein. But it should be appreciated that one cannot be certain whether the size change was caused by specific binding of CD45 imprinted nanoMIPs and the CD45 protein or passive binding of protein to the nanoparticles (protein corona effect). It is well known that nanoparticles bind to proteins avidly (Monopoly et al, 2011; Piozzi et al, 2015). Since any non-specific binding between the particle and the template can significantly impair the diagnostic potential of the nanomaterial, it is imperative to establish the true nature of the nanoMIP-template protein interaction. A possible control that was not done here, but would have been useful to establish the nature of the interaction between the nanoMIP and the protein, could have been to repeat the experiment using a different protein with similar size. Nevertheless the DLS technique might not be the best modality to provide absolute evidence of the specific interaction between the epitope-made nanoMIPs and the protein. More sensitive and specific assays are required to confirm a true epitope-protein binding. One of the more specific techniques such as SPR, SERS or QCM may provide such an evidence. In addition to this, there is increasing evidence that TRPS is capable of studying nanoparticle-target interactions (Healey *et al*, 2019; Holton *et al*, 2018; Sivakumaran & Platt, 2017).

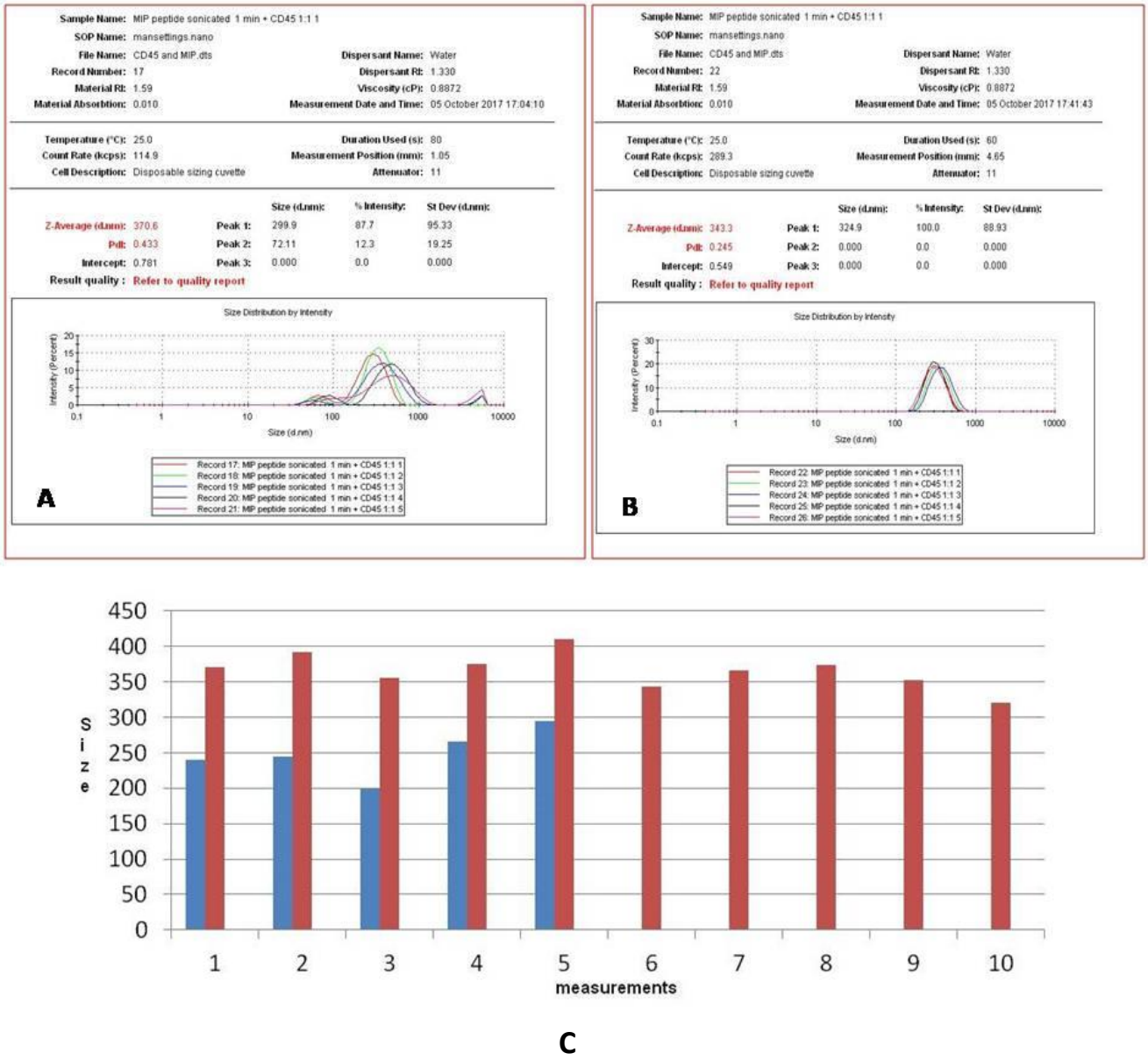

Figure 3.8. Study of nanoMIPs-CD45 protein interaction by DLS: Changes in the size of NPs.

Ten readings were made after incubating nanoMIPs in CD45 solution. The first five readings were obtained after 5 minutes incubation of nanoMIPs with CD45 protein (**A**). The average size of the nanoMIP is 380 nm. The readings 6-10 were obtained after 40 minutes incubation (**B**). The average size of the nanoMIPs has reduced to 351.

(**C**) Column diagram to illustrate the nanoMIP size changes following incubation with CD45 protein. For comparison, five measurements of 'neat' (not exposed to CD45 protein) are shown in blue. The measurements post-incubation is shown in brown.

It is interesting to note that the average size of the nanoMIPs reduced from 405 ± 85 nm to 351 after prolonged incubation. It is not very clear why the size had reduced but it may be the result of dissociation of weakly bound protein molecules from the nanoparticles. This phenomenon is often observed when nanoparticles are introduced into blood plasma or serum. When low affinity proteins bind to nanoparticles, they produce what is described as 'soft corona' (Pozzi *et al*, 2015). The proteins forming soft corona can spontaneously disassociate from the nanoparticle thus lowering the size of the nanoparticle protein complex. It is conceivable that a similar dissociation may have taken place when the CD45 imprinted nanoMIPs were incubated with the template protein for a longer period. The CD45 protein molecules that bound to the nanoMIPs with low affinity receptors may have dissociated from the complex. Blundell and colleagues (2016) have demonstrated this phenomenon using polymer nanoparticles incubated in human serum and TRPS.

It is also interesting to study the changes in polydispersity following incubation of the CD45 nanoMIPs with CD45 protein. The mean PDI of the nanoMIPs increased from 0.330 ± 0.022 to 0.470 + 0.056 (Figure 3.9) indicating that disorderly binding of CD45 protein to the nanoMIPs. The PDI of the nanoMIP-protein complex reduced significantly to 0.229 ± 0.045 following prolonged incubation indicating that any bound CD45 protein may have dissociated from the particle. However, it is not possible to explain why the PDI had dropped to a level that was even lower than the neat CD45 nanoMIPs. It may be that after a long incubation, some of the larger particle aggregates that were present in solution had precipitated and settled decreasing the PDI significantly.

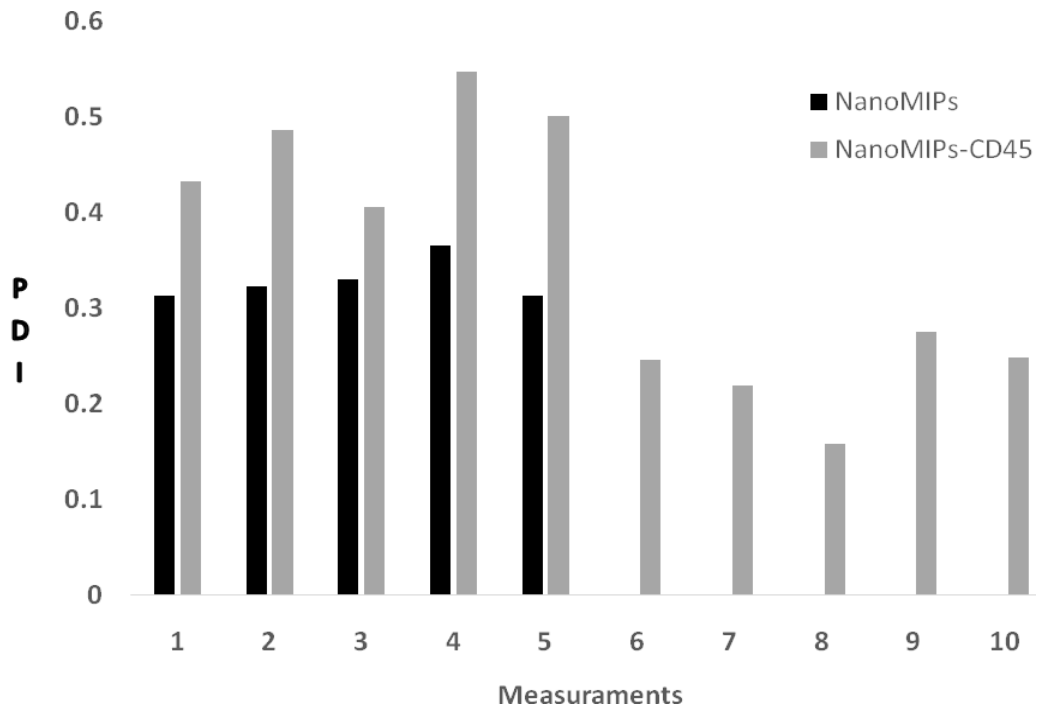

Figure 3.9. NanoMIPs-CD45 protein interaction: Changes in polydispersity Index (PDI)

Column diagram to illustrate the changes in the PDI following incubation with CD45 protein. For comparison, five measurements of 'neat' (not exposed to CD45 protein) are shown in black. The measurements post-incubation are shown in grey. The first five readings were obtained after 5 minutes incubation of nanoMIPs with CD45 protein. The average PDI is 0.4704. The readings 6-10 were obtained after 40 minutes incubation. The average PDI has reduced to 0.229.

The results of the DLS measurements after 5 minutes incubation shows that the average size of the nanoMIP has increased from 249 $\pm$ 35 nm to 380$\pm$ 21 nm suggesting that there was an interaction between the nanoparticles and the target protein. The interaction may be a passive binding of protein to the nanoparticles (protein corona effect) or a true epitope-protein binding. More sensitive and specific assay such as SPR analysis will need to be carried out to confirm a true epitope-protein binding. It is interesting to note that the average size of the nanoMIPs-CD45 complex reduced from 381 $\pm$21 nm to 347 $\pm$ 22 nm after prolonged incubation. It is not very clear why the size had reduced but it may be a result of dissociation of weakly bound protein molecules from the nanoparticles.

3.4.4 Determination of binding of nanoMIPs to CD45 protein by TRPS

The MIP-target binding experiments were carried out using diluted solutions of purified CD45 antigen. Since CD45 antigen is not used in routine immunocytochemistry or immunohistochemistry, the concentration of the CD45 solution was based on the concentrations of anti-CD45 antibody that are widely used in routine diagnosis. (Beckman Coulter datasheet for anti-CD45 antibody).

The first experiment done by TRPS to study the interaction between the nanoMIPs synthesised in Cranfield and CD45 protein did not show a significant interaction between the MIP and the protein. Even though this was a surprising finding, it did support the assertion that may be the size changes observed by DLS may have been a non-specific protein corona formation rather than a true receptor-ligand interaction. Furthermore, this result raised an important question as to why there was no discernible binding between the nanoMIPs and the target protein. It was postulated that the lack of interaction between the nanoMIP and CD45 protein might have been due to the 'polyclonal' nature of the MIP receptors as a result of random orientation of the template peptides on the silica beads. This inference prompted us to change the amino acid sequence of the peptide by adding a cysteine residue to one end of the peptide and use the SIA method to couple the template to the silica particles.

Significantly, the nanoMIP synthesised using cysteine containing peptide template produced not only a more uniform batch of particles with lower PDI as shown by the DLS and TRPS size data, they also demonstrated a specific binding between the nanoMIPs and the target protein. The TRPS experiments carried out to study the interactions between the nanoMIPs and two concentrations of CD45 protein showed that the size of the particles increased following incubation with CD45 protein (Figure 3.10). The dominant population of the nanoMIPs identified by TRPS measured 120 nm in size. There was another smaller population with a size of 140 nm. The TRPS size plot shows that there was no significant change in the size of the nanoMIPs incubated in a dilute solution (0.4µg/ml) of CD45 protein. However, The size of the nanoMIPs

incubated in a concentrated solution (40µg/ml) of CD45 protein increased significantly from 120-140 nm to 250 nm indicating that there was binding of target protein to the nanoMIPs. As was in the case of DLS analysis, one cannot be absolutely certain whether the increase in the size of the nanoMIPs after incubation with target protein is indicative of specific binding between the receptor and the target protein or is a result of passive adsorption (protein corona effect). A control binding experiment with a different protein of similar size can be done in the future to assess the specificity of the binding. However, the results of the experiments carried out to study the changes in the zeta potential of the nanoMIPs show more promising results.

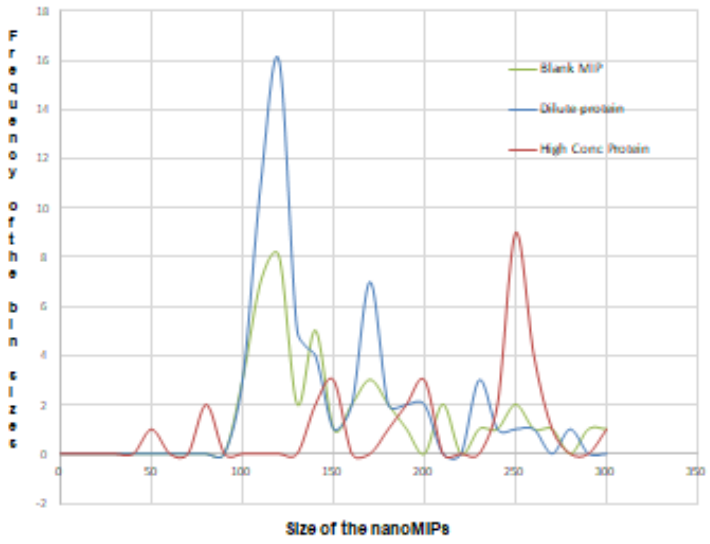

Figure 3.10. TRPS analysis of NanoMIPs-CD45 protein interaction: Changes in size

The size of the dominant population of the blank nanoMIPs is 120 nm. There is another smaller population with a size of 140 nm. There was no significant change in the size of the nanoMIPs following incubation with a dilute solution (1:100) of CD45 protein. The size of the nanoMIPs incubated in a concentrated solution (1:1) of CD45 protein, however, increased significantly to 250 nm.

The results of the experiments conducted to study binding of CD45 protein to the imprinted nanoMIPs show measurable changes in the zeta potential of the nanoMIPs following incubation with dilute (1:100) CD45 protein solution. The zeta potential of the nanoMIPs changed from -2mv to -11mv following exposure to the target protein

indicating that there was binding of the protein to the MIP particles (Figure 3.11).

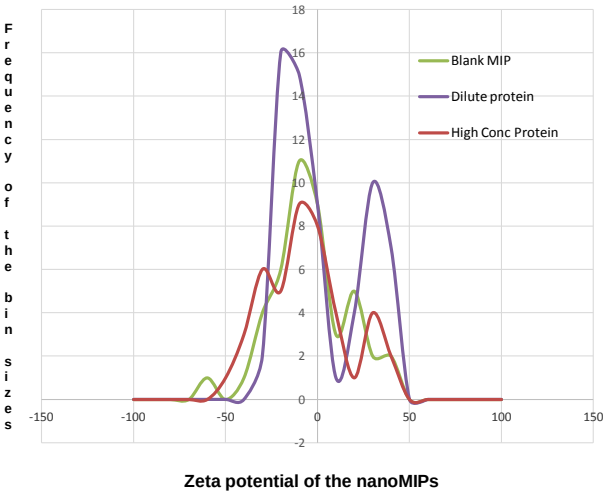

Figure 3.11. TRPS analysis of NanoMIPs-CD45 protein interaction: Changes in zeta potential

The zeta potential of the dominant population of the blank nanoMIPs is -2mv. The zeta potential of the nanoMIPs incubated in a dilute solution of CD45 protein reduced to -11mv indicating binding of CD45 protein to the MIPs.

Surprisingly, no discernible change in zeta potential was observed following incubation in concentrated (1:1) CD45 solution. One possible explanation for this observation could be steric hindrance but further experiments using varying concentrations of the target protein are needed to answer this question.

3.5 The relevance and significance of this research for MIP-based Cancer Diagnosis

Over the last two decades, several research groups have been very active in developing cheap and reproducible MIB-based bioassays for cancer diagnosis. A Medline search carried

out in September 2019 has come up with over 50 peer reviewed publications that are relevant to cancer diagnosis. Of which, the vast majority are related to the development of bioassays to detect 'disease markers' in body fluids such as plasma, serum, urine and bronchial secretions. The most commonly investigated biomarkers are prostate specific antigen (PSA) for prostate cancer (Brturk *et al*, 2015 & 2016; Jolly *et al*, 2016; Karami *et al*, 2019; Patra *et al*, 2015; Rebelo *et al*, 2014; Tang *et al*, 2018), alpha fetoprotein (AFP) for hepatocellular carcinoma (Karfa *et al*, 2016; Shen *et al*, 2016), carcinoembryonic antigen (CEA) for colorectal cancers (Moreira *et al*, 2016; Tavares *et al*, 2019), cancer antigen 125 for ovarian cancer (Viswanathan *et al*, 2012), nuclear matrix protein 22 for transitional cell carcinoma of the bladder (Lee *et al*, 2016), human chorionic gonadotropin (HCG) (Dabrowski *et al*, 2019), progastrin releasing peptide (ProGRP) (Qader *et al*, 2014; Rossetti *et al* 2017), carbohydrate antigen 15-3 (CA 15-3) for breast cancer (Ribeiro *et al*, 2018) and calcitonin for medullary carcinoma of the thyroid (Patra *et al*, 2015). Some researchers have focused on non-specific disease markers such as bilirubin (Cicek *et al*, 2016), neopterin (Sharma *et al*, 2016) and modified nucleosides (Dejous *et al*, 2016; Iwanowska *et al*, 2016; Martins *et al*, 2016), redox couples such as glutathione disulfide (Liu et al, 2019), deoxyadenosine (Scorrano *et al*, 2015), psueudouridine (Krstulja *et al*, 2017), neurone specific enolase (NSE) (Xing *et al*, 2019), sarcosine (Moein *et al*, 2015), nicotinamide adenine dinucleotide phosphate (NADP) and L-tyrosine (Moein *et al*, 2015).

It is noteworthy that, in terms of number of research publications, there have been very few articles that are related to cell/tissue based diagnosis of cancers. It should be emphasised that the standard modality of diagnosis of cancers including those of blood is cytological or histological. Although the biomarkers described above are useful in disease monitoring in some situations (e.g. PSA in prostate cancer), the cancer clinicians still rely on cell based (cytology) or tissue based (histology) diagnostic tests. In a bid to screen chronic lymphocytic leukaemia cells, El-Schich *et al* (2010) imprinted sialic acid and studied the expression of this molecule on the surface of the leukaemic cell by flow cytometry and fluorescent microscopy. Although the technical data provided by this group is interesting and signifies an important development towards MIP based cytology/histology, it should be stated that sialic acid expression is too non-specific for it to be useful in clinical diagnosis. A similar approach was employed by Wang and co-workers (2016). The researchers synthesised MIPs using sialic acid or fucose or mannose as templates and doped the resulting polymers with fluorescine

isothiocyanate for fluorescent imaging of human hepatoma cells and mammary cancer cells. They successfully label the cells using the tagged MIPs. Once again, the target templates used by the researchers are far too generic to be useful in clinical practice. Professor Haupt's group have also focused their attention on various carbohydrate molecules including glucuronic acid, acetyl neuraminic acid and sialic acid as the templates for MIP synthesis for cancer cell imaging. In one study, the researchers imprinted glucuronic acid and N-acetyl neuraminic acid and labelled them with green and red emitting quantum dots for multiplexed imaging (Demir *et al*, 2018; Panagiotopoulou *et al*, 2017). Ceccini and colleagues developed a nanoMIP against human vascular endothelial cell growth factor (VEGF) and coupled with quantum dots for cancer cell imaging (Ceccini *et al*, 2017). A novel dual-template epitope polymer for fluorescent imaging and targeted drug delivery to pancreatic cancer cells was developed by Jia and co-workers (Jia *et al*, 2019). The researches employed epitope imprinting using a peptide fragment of human fibroblast growth factor modified with glucose and bleomycin as templates. The imaging experiments *in vitro* showed that the MIPs specifically bind to BxPC-3 pancreatic cancer cells. They reported that the *in-vivo* experiments using xenograft models demonstrated inhibition of tumour cell growth by the MIP complex.

Although the above reports mark important technical advances in cell imaging, it must be pointed out that none of the above MIPs would be suitable for routine clinical diagnosis of cancers because of the non-specific nature of the target molecules used for molecular imprinting and it is very unlikely that their work will translate into clinical practice for cell/tissue based cancer diagnosis. It should be emphasised that an accurate determination of the lineage of the malignant cell is of paramount importance because it, not only facilitates the diagnosis of cancer, but also influences the treatment since the cancer therapy is heavily dependant on the type of tumour and the cell of origin. This is particularly so in the field of haematological malignancies such as leukaemias and lymphomas. For this reason, the current study using a lineage specific marker (CD45 antigen) as the template for MIP synthesis to differentiate blood cancers from non-haematological solid neoplasia is an important development because the CD45 imprinted MIPs have a real potential for use in cancer diagnostics carried out either by conventional cytochemistry/histochemistry or flow cytometry/fluorescent microscopy. To our best knowledge, there is no other published report describing a MIP to target a lineage specific marker for cancer cell imaging.

3.6 Conclusions and Future Work

This study was undertaken to investigate whether MIP nanoparticles synthesised using the solid-phase approach and epitope imprinting method have potential to replace antibodies in cancer diagnosis. Although the results obtained so far do not fully answer the question, the study has, however, provided a number of clues (both design and technical) to guide us to achieving this goal. The study has identified a suitable lineage specific marker (CD45 antigen) for the synthesis of a nanoMIP that could be useful in the laboratory diagnosis of blood cancers. This study has also identified a suitable epitope sequence to synthesise the template for imprinting. The results of this study prove that the solid-phase synthesis using a custom made polypeptide as the template (segment imprinting) is a logical approach. One important technical refinement was the immobilisation of the template protein to the silica beads in a single orientation *via* an amino acid with a thiol group (cysteine) and to use a SIA linker for peptide coupling. This modification resulted in the production of more uniform nanoMIPs with low PDI. Another significant observation of this study is that the use of fluorinated monomer in combination with the 'standard functional monomers' for the MIP synthesis has improved the quality of the nanoMIPs produced. This study has also re-emphasised the notion that the technique of DLS cannot be used as the only modality for the characterisation of synthesised nanoMIPs. This study has successfully explored, for the first time, the usefulness and applicability of the technique of tunable resistive pulse sensing (TRPS) for the characterisation of nanoMIPs. In fact, the preliminary results obtained in this study indicate that this technique may be superior to DLS for not only measuring the size of the particles, but also to study MIP-target interactions. The TRPS analysis of the changes in the zeta potential of the nanoMIPs has shown that the CD45 epitope imprinted nanoMIPs bind to the CD45 protein. Hence, this preliminary exploratory study has provided some encouraging results to support the original hypothesis that the molecularly imprinted nanoparticles may have a real potential for use in cancer diagnosis. However, it must be emphasised that further work is necessary to optimise the conditions for the synthesis of the nanoMIPs and to characterise the synthesised nanoparticles. It will also be necessary to employ a more sensitive and established techniques such as SPR, SERS or QCM to confirm nanoMIP-target protein binding and to establish the usefulness and applicability of TRPS for

the structural and functional characterisation of nanoMIPs. Finally, appropriate cell binding analysis will need to be carried out using fluorescent nanoMIPs prepared with a fluorescent monomer and this is compared with a traditional immunocytochemistry assay using fluorescent labelled anti-CD45 antibody.

CHAPTER 4 REFERENCES

Adams JC (1992). Biotin amplification of biotin and horseradish peroxidase signals in histochemical stains. J Histochem Cytochem., 40, 1457-1463.

Ahmad OS, Bedwell TS, Esen C, Garcia-Cruz A, Piletsky SA (2019). Molecularly imprinted polymers in electrochemical and optical sensors. Trends Biotechnol, 37, 3, 294-309.

Alexander C, Andersson H.S, Andersson LI, Ansell RJ, Kirsch N, Nicholls IA, O'Mahony J, Whitcombe MJ. (2006) Molecular imprinting science and technology: A survey of the literature for the years up to and including 2003. J. Mol. Recognit., 19, 106–180.

Alizadeh T, Akbari A. (2013). A capacitive biosensor for ultra-trace level urea determination based on nano-sized urea-imprinted polymer receptors coated on graphite electrode surface. Biosens. Bioelectron., 43, 321-327.

Altintas Z, Abdin MJ, Tothill AM, Karim K, Tothill IE (2016). Ultrasensitive detection of endotoxins using computationally designed nanoMIPs. Anal Chim Acta, 935:239-248.

Altintas Z, Gittens M, Guerreiro A, Thompson KA, Walker J, Piletsky S, Tothill IE (2015). Detection of waterborne viruses using high affinity molecularly imprinted polymers. Anal Chem, 87, 13, 6801-6807.

Altintas Z, Gittens M, Guerreiro A, Thompson KA, Walker J, Piletsky S, Tothill IE (2015). Detection of Waterborne Viruses Using High Affinity Molecularly Imprinted Polymers. Anal Chem., 87(13), 6801-6807.

Altintas Z, Pocock J, Thompson KA, Tothill IE (2015). Comparative investigations for adenovirus recognition and quantification: Plastic or natural antibodies? Biosens Bioelectron., 74:996-1004.

Ambrosini S, Beyazit S, Haupt K, Tse Sum Bui B (2013). Solid-phase synthesis of molecularly imprinted nanoparticles for protein recognition. Chem Commun (Camb). 2013 Aug 4;49(60):6746-8. doi: 10.1039/c3cc41701h.

Andersson LI, Muller R, Vlatakis G, Mosbach K. (1995). Proc Natl Acad Sci USA, 92:4788-4792.

Ansell RJ, Mosbach K (1998). Magnetic molecularly imprinted polymer beads for drug radioligand binding assay. Analyst, 123, 1611-1616.

Antuna-Jimenez D, Diaz-Diaz G, Blanco-Lopez MC, Lobo-Castanon MJ, Miranda-Ordieres AJ, Tunon-Blancp P (2012). Molecularly Imprinted Electrochemical Sensors: Past, Present and Future. In Molecularly Imprinted Sensors. Edited by Li S, Ge Y, Piletsky SA, Lunec J. Elsevir Publications. pp 1-34.

Arendt CW, Ostergaard HL (1997). Identification of the CD45-associated 116-kDa and 80-kDa proteins as the alpha- and beta-subunits of alpha-glucosidase II. J. Biol. Chem. 272 (20): 13117–25.

Arshady R (1992). Suspension, emulsion and dispersion polymerization: A methodological survey. Colloid and Polymer Science, 270 (8), 717-732.

Arshady R, Mosbach K (1981). Synthesis of substrate-selective polymers by host-guest polymerization. Makromol. Chem., 182, 687–692.

Avrameas S (1972). Enzyme markers: Their linkage with proteins and use in immunohistochemistry. Histochem J., 4: 321-330.

Baimani N, Aberoomand Azar P, Waqif Husain S, Ahmad Panahi H, Mehramizi A (2019). Ultrasensitive separation of methylprednisolone acetate using a photoresponsive molecularly imprinted polymer incorporated polyester dendrimer based on magnetic nanoparticles. J Sep Sci., 42(7):1468-1476. doi: 10.1002/jssc.201801093.

Bain BJ (2016). Preparation and Staining methods for blood and bone marrow films. Dacie and Lewis Practical Haematology (12th Edition). Edited by Lewis SM, Bain BJ, Bates I. Elsevir Publications. pp 50-60.

Bain BJ (2017). Leukaemia Diagnosis. Wiley Blackwell Publications.

Bedwell TS, Whitcombe MJ (2016). Analytical applications of MIPs in diagnostic assays: future perspectives. Anal Bioanal Chem., 408, 1735-1751.

Bengtsson H, Roos U, Andersson LI (1997) Anal Commun 34:233-235.

Benito-Peña, E.; Martins, S.; Orellana, G.; Moreno-Bondi, M.C. Water-compatible molecularly imprinted polymer for the selective recognition of fluoroquinolone antibiotics in biological samples. Anal. Bioanal Chem. 2009, 393, 235–245.

Berne BJ & Pecora R. Dynamic Light Scattering. With Applications to Chemistry, Biology and Physics. Dover Publications, New York.

Bers K, Eersels K, Van Grinsven B, Daemen M, Bogie JFJ, Hendricks JJA, Bouwmans EE, Puttmann C, Stein C, Barth S, Bos GMJ, Germaraad WTV, De Ceuinck W, Wagner P (2014) Langmuir 30:3631-3639.

Bi XD, Liu Z (2014) Facile preparation of glycoprotein-imprinted 96-well microplates for enzyme-linked immunosorbent assay by boronate affinity-based oriented surface imprinting. Anal Chem 86:959-966.

Biffis A, Graham NB, Siedlaczek G, Stalberg S, Wulff G. (2001). The synthesis, characterisation and molecular recognition properties of imprinted microgels. Macromol. Chem. Phys, 202, 163-171.

Blundell ELC, Healey MJ, Holton E, Mastana S, Sivakumaran M, Platt M (2016). Characterisation of the Protein Corona using. Tunable Resistive Pulse Sensing: Determining the Change and Distribution of a Particles Surface Charge. Anal Bioanal Chem, 408(21):5757-5768. doi: 10.1007/s00216-016-9678-6.

Bompart M, De Wilde Y, Haupt K (2010). Chemical nanosensors based on composite molecularly imprinted polymer particles and surface enhanced Raman scattering. Adv. Mater., 22, 2343-2348.

Bonini F, Piletsky S, Turner AP, Speghini A, Bossi A (2007). Surface imprinted beads for the recognition of human serum albumin. Biosens Bioelectron, 22, 9-10, 2322-2328.

Cáceres C, Canfarotta F, Chianella I, Pereira E, Moczko E, Esen C, Guerreiro A, Piletska E, Whitcombe MJ, Piletsky SA (2016). Does size matter? Study of performance of pseudo-ELISAs based on molecularly imprinted polymer nanoparticles prepared for analytes of different sizes. Analyst, 141(4):1405-1412.

Cai D, Ren L, Zhao H, Xu C, Zhang L, Yu Y, Wang H, Lan Y, Roberts MF, Chung JH, Naughton MJ, Ren Z, Chiles TC (2010). A molecular imprint nanosensor for ultrsensitive detection of proteins. Nature Chem, 5, 597-601.

Cai Y, Kang K, Li Q, Wang Y, He X (2018). Rapid and Sensitive Detection of Cardiac Troponin I for Point-of-Care Tests Based on Red Fluorescent Microspheres. Molecules, 23(5) doi: 10.3390/molecules23051102.

Canfarotta F, Lezina L, Guerreiro A, Czulak J, Petukhov A, Daks A, Smolinska-Kempisty K, Poma A, Piletsky S, Barlev NA (2018). Specific drug delivery to cancer cells with double-imprinted nanoparticles against epiderma growth factor receptor. Nano Lett, 18, 8, 4641-4646.

Canfarotta F, Poma A,Guerreiro A& Piletsky S**.** Solid-phase synthesis of molecularly imprinted nanoparticles. Nature Protocols, 11, 3, 2016, 443-455.

Canfarotta E, Smolinska-Kempisty K, Piletsky S (2017). Replacement of antibodies in pseudo-ELISAs: Molecularly imprinted nanoparticles for vancomycin detection. Methods Mol Biol, 1575, 389-398.

Carboni D, Flavin K, Servant A, Gouverneur V, Resmini M. (2000). The first example of molecularly imprinted nanogels with aldolase type I activity. Chem. Eur J., 14, 7059-7065.

Cecchini A, Raffa V, Canfarrota F, Signore G, Piletsky S, MacDonald MP, Cuschieri A (2017). In vivo recognition of human vascular endothelial growth factor by molecularly imprinted polymers. Nano Lett, 17, 4, 2307-2312.

Chen L, Wang X, Lu W, Wu X, Li J (2016). Molecular Imprinting: perspectives and applications. Chem Soc Rev., 45, 2137-2211.

Chen ZY, Hua ZD, Wang J, Guan Y, Zhao MP, Li YZ. (2007). Molecularly imprinted soluble nanogels as a peroxidase like catalyst in the oxidation reaction of homovanillic acid under aqueous conditions. Appl. Catal. A. 328, 252-258.

Chen Z, Xu L, Liang Y, Zhao M (2010). pH-Sensitive Water-Soluble Nanospheric Imprinted Hydrogels Prepared as Horseradish Peroxidase Mimetic Enzymes. Advanced Materials, 22(13), 1488-1492.

Chen Z & Ye L (2013). Molecularly Imprinted Nanoparticles. In 'Molecular Imprinting: Principles and Applications of Micro- and Nanostructured Polymers' Edited by Lei Ye. Pan Stanford Publishing Pte Ltd, pp 161-196.

Cheng Z, Wang E, Yang X. (2001). Capacitive detection of glucose using molecularly imprinted polymers. Biosens. Bioelectron, 16(3):179-185.

Chianella I, Guerreiro A, Moczko E, Caygill JS, Piletska EV, De Vargas Sansalvador IMP, Whitcombe MJ, Piletsky SA (2013). Anal Chem, 85:8462-8468.

Chronakis IS, Jacob A, Hagstrom B, Ye L (2006). Encapsulation and selective recognition of molecularly imprinted theophilline and 17b-estradiol nanoparticles within electrospun polymer nanofibres. Langmuir, 22, 8960-8965.

Chronakis IS, Milosevic B, Frenot A, Ye I. (2006). Generation of molecular recognition sites in electrospun polymer nanofibres via molecular imprinting. Macromolecules, 39, 357-361.

Cicek C, Yilmaz F, Ozgur E, Yavuz H, Denizli A (2016). Molecularly imprinted quartz crystal microbalance sensor (QCM) for bilirubin detection. Chemosensors, 4, 21.

Cirillo G, Lemma F, Puoci F, Parisi OI, Gurcio M, Spizzirri UG, Picci N. (2009). Imprinted hydrophilic nanospheres as drug delivery systems for 5-fluouracil sustained release. J Drug Target., 17, 72-77.

Coons AH, Creech HJ, Jones RN (1941). Immunological properties of an antibody containing a fluorescent group. Proceedings of the Society Experimental Biology and Medicine, 200-202.

Coulter WH. Means for counting particles in a fluid. *US patent 2,656,508* (20 October 1953).

Cutivet A, Schembri C, Kovensky J, Haupt K. (2009). Molecularly imprinted microgels as enzyme inhibitors. J. Am. Chem. Soc, 131, 14699-14702.

Cowen T, Karim K, Piletsky S. (2016). Computational approaches in the design of synthetic receptors - A review. Anal Chim Acta. 2016 Sep 14;936:62-74. doi: 10.1016/j.aca.2016.07.027.

Dabbs D (2018). Diagnostic Immunohistochemistry: Diagnostic and Theranostic Applications (5th Edition). Elsevere Publications.

Dabrowski M, Ziminska A, Kalecki J, Cieplak M, Lisowski W, Maksym R, Shao S, D'Souza F, Kuhn A, Sharma PS (2019). Facile fabrication of surface-imprinted macroporous films forchemosensing of human chorionic gonadotropic hormone. ACS App Mater Interfaces, 11, 9, 9265-9276.

De Boer T, Mol R, De Zeeuw RA, De Jong GJ, Sherrington DC, Cormack PAG, Ensing K. (2002). Spherical molecularly imprinted polymer particles: A promissing tool for molecular recognition in capillary electrokinetic separations. Electrophoresis, 23, 1296-1300.

Dejous C, Hallil H, Raimbault V, Lachaud JL, Plano B, Delepee R, Favetta P, Agrofoglio L, Rebiere D (2016). Love acoustic wave based devices and molecularly imprinted polymers as versatile sensors for electronic nose or tongue for cancer monitoring. Sensors, 16, 915.

Del Bruno JJ (2019). Molecularly Imprinted Polymers. Chem rev, 119, 94-119.

Demir B, Lemberger MM, Panagiotopoulou M, Medina Rangel PX, Timur S, Hirsh T, Tse Sum Bui B, Wegener J, Haupt K (2018). Tracking hyaluronan: Molecularly imprinted polymer coated carbon dots for cancer cell targeting and imaging. ACS Appl Mater Interfaces, 10, 4, 3305-3313.

Diltemiz ES, Keçili R, Ersöz A, Say R. (2017). Molecular Imprinting Technology in Quartz Crystal Microbalance (QCM) Sensors. Sensors, 17(3), 454. doi: 10.3390/s17030454.

Du XJ, Zhang F, Zhang HX, Wen YJ, Saren TY (2014) Food Agric Immunol 25:411-422.

Dvorakova G, Haschick R, Chiad K, Klapper M, Mullen K, Biffis A. (2010). Molecularly imprinted nanospheres by nonaqueous emulsion polymerisation. Macromol. Rapid Commun, 31, 2035-2040.

Eersels K, Diliën H, Lowdon JW, Redeker ES, Rogosic R, Heidt B, Peeters Cornelis P, Lux P, Reutelingsperger CP, Schurgers LJ, Cleij TJ, van Grinsven B (2018). A Novel Biomimetic Tool for Assessing Vitamin K Status Based on Molecularly Imprinted Polymers. Nutrients, 10, 751; doi:10.3390/nu10060751.

Eersels K, Van Grinsven B, Khorshid M, Somers V, Putmann C, Stein C, Barth S, Dilien H, Bos GMJ, Germaraad WTV, De Ceuninck W, Wagner P (2015) Langmuir 31:2043-2050.

Ellen L, Holthoff, Dimitra N. Stratis-Cullum and Mikella E. Hankus (2011). Article A Nanosensor for TNT Detection Based on Molecularly Imprinted Polymers and Surface Enhanced Raman Scattering. Sensors, 11, 2700-2714; doi:10.3390/s110302700

El-Schich Z, Abdulla M, Shinde S, Dizeyi N, Rosen A, Sellergren B, Wingren AG (2016). Different expression levels of glycans on leukaemic cells- a novel screening method with molecularly imprinted polymers (MIP) targeting sialic acid. Tumour Biol, 10, 13763-13768

EL-Sharif HF, Yapati H, Kalluru S, Reddy SM (2015). Highly selective BSA imprinted polyacrylamide hydrogels facilitated by a metal-coding MIP approachhighly selective BSA

imprinted polyacrylamide hydrogels facilitated by a metal-coding MIP approach. Acta Biomaterialia, 28, 121–127

Engvall E & Perlman P (1971). Enzyme-linked immunosorbent assay (ELISA). Qualitative assay of immunoglobulin G. Immunochemistry, 871-874.

Erol K, Kose K, Uzun L, Say R, Denizli A (2016). Polyethyleneimine assisted-two-step polymerization to develop surface imprinted cryogels for lysozyme purification. Colloids Surf B Biointerfaces, 146, 567-576**.**

Erol I, Sen O, Dedelioglu A, Cifci C (2009) Synthesis and characterisation of novel fluyorine-containing methacrylate copolymers: Ractivity ratios, themsl properties and antimicrobial activity. Journal of Applied Polymer Science, 114, 6, 3351-3359.

Erturk G, Hedstrom M, Turner MA, Denizli A, Mattiasson B (2015). Real-time prostate-specific antigen detectionwith prostate-specific antigen imprinted capacitivebiosensors. Anal Chim Acta, 891, 120-129.

Ertuk G, Ozen H, Turner MA, Mattiasson B, Denizli A. Microcontact imprinting based surface Plasmon resonance (SPR) biosensor for real time and ultrasensitive detection of prostate specific antigen (PSA) from clinical samples. Sens Actuators b, 224, 823-832.

Fang L, Chen S, Zhang Y, Zhang H (2011). Azobenzene-containing molecularly imprinted polymer microspheres with photoresponsive template binding properties, J. Mater. Chem., 7, 21, 2320-2329.

Flavin K, Resmini M. Imprinted nanomaterials: a new class of synthetic receptors. Anal Bioanal Chem, 393, 2, 437-444.

Frasconi M, Tel-Vered R, Riskin M, Wilner I (2005). Surface plasmon resonance analysis of antibiotics using imprinted boronic acid-functionalised Au nanoparticle composites. Anal. Chem., 82, 2512-2519.

Fu G-Q, Yu H, Zhu J (2008). Imprinting effect of protein-imprinted polymers composed of chitosan and polyacrylamide: a re-examination. Biomaterials, 29, 13, 2188-2142.

Gao D, Zhang Z, Wu M, Xie C,Guan G, Wang D. (2007). A surface functional monomer-directing strategy for highly dense imprinting of TNT at surface of silica nanoparticles. J Am. Chem. Soc, 129,7859-7866.

Ghasemzadeh N, Nyberg F, Hjerten S (2008). Highly selective artificial gel antibodies detection and quantification of biomarkers in clinical samples. I. Sphectrophotometric approach to design the calibration curve for the quantification. J Sep Sci, 31, 22, 3945-3953.

Ge Y, Butler B, Mirza F, Habib-Ullah S, Fei D (2013). Smart molecularly polymers: Recent developments and applications. Macromolecular Rapid Communications, 34 (11):903-15.

Ge, Y & Turner AP (2009). Molecularly imprinted sorbent assays: recent developments and applications. Chemistry, 17; 15(33):8100-8107.

Goldburg WI (1999). Dynamic Light Scattering. Am J Phys. 67, 12: 1152-1160.

Graniczxkowska K, Putz M, Hauser FM, DE Saeger S, Beloglazova NV. (2017). Capacitive sensing of N-formylamphetamine based on immobilized molecular imprinted polymers. Biosens. Bioelectron., 92, 741-747.

Guesdon JL, Terynck T, Avrameas S (1979). The use of avidine-biotin interaction in immunoenzymatic techniques. J Histochem Cytochem., 1131-1139.

Guo TY, Xia YQ, Hao GJ, Zhang BH, Fu GQ, Yuan Z (2005). Chemically modified chitosan beads as matrices for adsorptive separation of proteins by molecularly imprinted polymer. Carbohydr Pol, 62, 3, 214-221.

Gupta N, Shah K, Singh M (2016). An epitope-imprinted piezoelectric diagnostic tool for Neisseria meningitidis detection. J Mol Recognit., 12:572-579.

Haupt, K.; Mosbach, K. Molecularly imprinted polymers and their use in biomimetic sensors. Chem. Rev. 2000, 100, 2495–2504.

Hayden O, Bindeus R, Haderspock C, Mann K-J,Wirl B, DickertFL (2003). Mass sensitive detection of cells, viruses and enzymeswith artificial receptors. Sensors and Actuators B 91, 316–319.

Hayden O, Dickert FL (2001). Selective microorganism detection with cellsurface imprinted polymers. Adv. Mater., 12, 311–313.

He, C.; Long, Y.; Pan, J.; Li, K.; Liu, F., Application of molecularly imprinted polymers to solidphase extraction of analytes from real samples. J Biochem Bioph Meth 2007, 70, 133-150.

Heggeness MH & Ash JE (1977). Use of the avidin-biotin complex for thye localisation of actin and myosin with fluorescence microscopy. J Cell Biol., 73, 783-788.

Henriquez RR, Ito T, Sun L, Crooks RM (2004). The resurgence of Coulter counting for analyzing nanoscale objects. *Analyst*, 129, 478–482.

Hermiston ML, Xu Z, Weiss A (2003). "CD45: a critical regulator of signaling thresholds in immune cells". Annu Rev Immunol. 21: 107–137.

Hiratani H, Alvarez-Lorenzo C. (2002). Timolol uptake and release by imprinted soft contact lenses made ofc N,N-diethylacrylomide and methacrylic acid. J. Cont. Release, 83, 223-230.

Holmes N (2006). "CD45: all is not yet crystal clear". Immunology. 117 (2): 145–155.

Hoshino Y, Kodama T, Okahaata Y, Shea KJ. Peptideimprintedpolymernanoparticles: a plastic antibody. J Am Chem Soc. 2008; 130(46):15242-15243.

Hoshino Y, Koide H, Urakami T, Kanazawa H, Kodama T, Oku N, Shea KJ. (2010). Recognition, neutralisation and clearence of target peptides in the bloodstream of living mice by molecularly imprinted polymer nanoparticles: A plastic antibody. J. Am. Chem. Soc., 132, 6644-6645.

Hu XB, Li GT, Li MH, Huang J, Li Y, Gao YB, Zhang YH (2008). Ultrasensitive specific stimulant assay based on molecularly imprinted photonic hydrogel. Adv Func Mater 18:575-583.

Huang R, Kostanski LK, Filipe CDM, Ghosh R (2009). Environment-responsive hydrogel-based ultrafiltration membranes for protein bioseparation, J Membrane Science, 336, 42-49.

Hunt CE, Pasetto P, Ansell RJ, Haupt K (2006). A fluorescence polarisation molecular imprint sorbent assay for 2,4-D: a non-separation pseudo-immunoassay. Chem Commun 16:1754-1756.

Inoue J, Ooya T, Takeuchi T (2011). Protein imprinted TiO2- coated quantum dots for fluorescent proteinsensing prepared by liquid phase deposition. Soft Matter, 7, 9681-9684.

Iwanowska A, Yusa S, Nowakowska M, Szczubialka K (2016). Selective adsorption of modified nucleoside cancer biomarkers by hybrid molecularly imprinted adsorbents.J Sep Sci, 39, 15, 3072-3080.

Jang R, Kim KH, Zaidi SA, Cheong WJ, Moon MH. (2011). Analysis of phospholipids using an open-tubular capillary column with a monolithic layer of molecularly imprinted polymer in capillary electrochromatography-electrospray ionization-tandem mass spectrometry. Electrophoresis, 32(16):2167-2173.

Janiak DS, Ayyub OB, Kofinas P (2009). Effects of charge density on the recognition properties of molecularly imprinted polymeric hydrogels. Macromolecules, 42, 5, 1703-1709.

Janiak DS, Kofinas P (2007). Molecular imprinting of peptides and proteins in aqueous media. Anal Bioanal Chem, 389, 2, 399-404.

Ji Y, Yin I, Xu Z, Zhao C, Huang H, Zhang H, Wang C. (2009). Preparation of magnetic molecularly imprinted polymer for rapid determination of bisphenol A in environmental water and milk samples. Anal. Bioanal. Chem., 395, 1125-1133.

Jia C, Zhang M, Zhang Y, Ma ZB, Xiao NN, He XW, Li XW, Zhang YK (2019). Preparation of dual-template epitope imprinted polymers for targeted fluorescence imaging and targeted drug delivery to pancreatic cancer BxPC-3 cells. ACS Appl Mater Interfaces, 11, 35, 32431-32440.

Jiang GS, Zhong S, Chen L, Blakey I, Whitaker A (2011). Synthesis of molecularly imprinted organic–inorganic hybrid azobenzene materials by sol–gel for radiation induced selective recognition of 2,4-dichlorophenoxyacetic acid. Rad Physica and Chemistry, 80(2), 130-135.

Jing T, Du H, Dai Q, Xia H, Niu J, Hao Q, Mei S, Zhou Y. (2010). Magnetic moleculary imprinted nanoparticles for recognitionm of lysozyme. Biosens. Bioelectron., 26, 301-306.

Jolly P, Tamboli V, Harniman RL, Estrela P, Allender CJ, Bowen JL (2016). Aptamer–MIP hybrid receptor for highly sensitive electrochemical detection of prostate specific antigen. Biosensors and Bioelectronics, 75, 188–195.

Kan X, Geng Z, Zhao Y, Wang Z, Zhu JJ. (2009). Magnetic molecularly imprinted polymer for aspirin recognition and controlled release. Nanotechnol., 20, 165601.

Kanekiyo Y, Y, Naganawa R, Tao H (2003). pH-Responsive Molecularly Imprinted Polymers. Ang. Chem., 42(26), 3014-3016.

Karami P, Bagheri H, Johari-Ahar, Khoshsafar H, Arduini F, Afkhami A (2019). Talanta, 202, 111-122.

Karfa P, Madhuri R, Sharma PK (2016). A battle between spherical andcube-shaped Ag/AgCl naboparticle modified imprinted polymer to achieve femtogram detection of alpha feto protein. J Mater Chem, 4, 5534-5547

Kawamura A, Hata Y, Miyata T, Uragami T. (2012). Synthesis of glucose-responsive bioconjugated gel particles using surfactant-free emulsion polymerization. Colloids Surf B Biointerfaces, 99, 74-81.

Kempe M. (1996). Antibody-mimicking polymers as chiral stationary phases in HPLC. Anal. Chem., 68(11):1948-1953.

Kempe H, Kempe M (2006). Development and evaluation of spherical molecularly imprinted polymer beads. Anal Chem 78:3659-3666.

Ki CD, Chang JY. (2006).Preparation of a molecularly imprinted polymer nanocapsule with potential use in delivery applications. Macromolecules, 39, 3415-3419.

Kiernan JA (2008). Histological and Histochemical Methods: Theory and Practice. 4th ed. Bloxham, UK: Scion.

Kohler G & Milstein C (1975). Continous cultures of fused cells producing antibody of pre-defined specificity. Nature, 256: 495-497.

Kozak D, Anderson W, Vogel R (2011). Advances in Resistive Pulse Sensors: Devices bridging the void between molecular and microscopic detection. Nano Today, 6:531–545.

KrstuljaA, Lettieri S, Hall AJ, Roy V, Favetta P, Agrofoglio LA (2017). Tailor-made molecularly imprinted polymer for selective recognition of the urinary tumour marker pseudouridine. Macromol Biosci, 12. Doi: 10.1002/mabi.201700250.

Kubo T, Nomachi M, Nemoto K, Sano T, Hosoya K, Tanaka N, Kaya K. (2006). Chromatographic separation for domoic acid using a fragment imprinted polymer. Anal Chim Acta., 577(1):1-7.

Kulkarni SK (2014). Nanotechnology: Principles and Practices 3rd ed. Springer, New York.

Lee MH, Thomas JL, Chen YC, Chin WT, Lin HY (2013). The complete replacement of antibodies by protein-imprinted poly(ethylene-co-vinyl alcohol) in sandwich fluoroimmunoassays. Microchim Acta 180:1393-1399.

Lee MH, Thomas JL, Chang YC, Tsai YS, Liu BD, Lin HY (2016). Electrochemical sensing of nuclear matrix protein 22 in urine with molecularly imprinted poly(ethylene-co-vinyl alcohol) coated zinc oxide nanotrod arrays for clinical studies of bladder cancer diagnosis. Biosen Bioelectron, 79, 789-795.

Li H, Xu W, Wang N, Ma X, Niu D, Jiang B, Liu L, Huang W, Yang W, Zhou Z (2012). Synthesis of magnetic molecularly imprinted polymer particles for selective adsorption and separation of dibenzothiophene. Microchimica Acta, 179, 123-130.

Li S, Ge Y, Piletsky SA, Turner APF. (2011). A Zipper-Like On/Off-Switchable Molecularly Imprinted Polymer. Adv. Functional Meter., 21, 17, 3344-3349.

Li S, Ge Y, Tiwari A, Cao S. (2010). A Temperature-Responsive Nanoreactor**.** Small, 6, 21, 2453-2459.

Li Y, Yang QH, Zhang ZX, Wang XR.(2006). Protein recognition via surface molecularly imprinted polymer nanowires. Anal Chem.,78, 317-320.

Li Y, Zhao B, RenY, Xiao G, Wang X, Li CX. (2007). Water-assisted formation of novel molecularly imprinted polymer membranes with ordered porous structure. Polymer, 48, 6205-6209.

Liao S, Wang X, Lin X, Wu X, Xie Z. (2010). A molecularly imprinted monolith for the fast chiral separation of antiparasitic drugs by pressurized CEC. J. Sep. Sci., 33(14):2123-2130.

Lin CI, Joseph AK, Chang CK, Lee YD (2004). Molecularly imprinted polymer film on semiconductor nanoparticles analyte detection by quantum dot photoluminescence. J Chromatogr. A, 1027, 259-262.

Lin HY, Ho MS, Lee MH (2009). Instant formation of molecularly imprinted poly(ethylene-co-vinyl alcohol) quantum dot composite nanoparticles and their use in one-pot urinalysis. Biosens. Bioelectron., 25, 579-586.

Liu J, Deng Q, Yang K, Zhang L, Liang Z, Zhang Y. (2010). Macroporous molecularly imprinted monolithic polymer columns for protein recognition by liquid chromatography. J. Sep. Sci., 33 (17-18):2757-2761.

Liu J, Wang Y, Liu X, Yuan Q, Zhang Y, Li Y (2019). Novel molecularly imprinted polymer (MIP) multiple sensors for endogenous redox couples determination and their applications in lung cancer diagnosis. Talanta, 199, 573-580.

Liu M-F, Chen Y-L, Zhang C, Bo Z-X (2012). Stable superhydrophobic fluorine containing polyfluorenes. Chinese J Polymer Scinece, 30, 2, 308-315.

Lofgreen JE and Ozin GA (2014). Controlling morphology and porosity to improve performance of molecularly imprinted sol-gel silica. Chem. Soc. Rev., 43, 911–933.

López, M.M.C.; Pérez, M.C.; García, M.S.D.; Vilarino, J.M.L.; Rodríguez, M.V.G.; Losada, L.F.B. (2012) Preparation, evaluation and characterization of quercetin-molecularly imprinted polymer for preconcentration and clean-up of catechins. Anal. Chim. Acta, 721, 68–78.

Lu CH, Zhang Y, Tang SF, Fang ZB, Yang HH, Chen X, Chen GN (2012). Sensing HIV related protein using epitope imprinted hydrophilic polymer coated quartz crystal microbalance.Biosens Bioelectron. 2012 Jan 15;31(1):439-44. doi: 10.1016/j.bios.2011.11.008.

Ma J, Zhang L, Geng B, Azhar U, Xu A, Zhang S (2017). Preparation of Thermo-Responsive and Cross-LinkedFluorinated Nanoparticles via RAFT-MediatedAqueous Polymerization in Nanoreactors. Molecules 2017, 22, 152; doi:10.3390/molecules22020152.

Ma Y, Shen XL, Zeng Q, Wang HS, Wang LS (2017). A multi-walled carbon nanotubes based molecularlyimprintedpolymers electrochemical sensor for the sensitive determination of HIV-p24. Talanta, 164:121-127.

Maddock SC, Pasetto P, Resmini M. (2004). Novel imprinted soluble microgels with hydrolytic catalytic activity. Chem. Commun, 536-537.

Mahajan R, Rouhi M, Shinde S, Bedwell T, Incel A, Mavliutova L, Piletsky S, Nicholls IA, Sellergren B (2019). Highly Efficient Synthesis and Assay of Protein-Imprinted Nanogels by Using Magnetic Templates.Angew Chem Int Ed Engl., 58(3):727-730. doi: 10.1002/anie.201805772.

Mao Y, Bao Y, Gan S, Li F, Niu L. (2011). Electrochemical sensor for dopamine based on a novel graphene-molecular imprinted polymers composite recognition element. 28,1, 291-297.

Martins GV, Marques AC, Fortunato E, Sales MGF (2016). 8-hydroxy-2’-deoxyguanosine (8-OHdG) biomarker detection down to picomolar level on a plastic antibody film. Biosens Bioelectron, 86, 225-234.

Matsui J, Akamatsu K, Hara N, Miyoshi D, Nawafune H, Tamaki K, Sugimoto N (2005). SPR sensor ship for detection of small molecules using molecularly imprinted polymer with embedded gold nanoparticles. Anal. Chem., 77, 4282-4285.

Matsui J, Akamatsu K, Nishiguchi S, Miyoshi D, Nawafune H, Tamaki K, Sugimoto N. (2004). Composite of Au nanoparticles and molecularly imprinted polymer as a sensing material. Anal. Chem, 76, 1310-1315.

Mayes AG and Mosbach K. (1996). Molecularly imprinted polymer beads: Suspension polymerisation using a liquid perfluorocarbon as the dispersing phase. Anal. Chem., 68, 3769-3774.

McPhee W, Tam C, Pelton R (1993). Poly(*N*-isopropylacrylamide) Latices Prepared with Sodium Dodecyl Sulfate. J. Colloid and Interface Science, 156(1), 24-30.

Mendes AN, Filgueiras LA, Siqueira MRP, Barbosa GM, Holandino C, de Lima Moreira D, Pinto JC, Nele M (2017). Encapsulation of *Piper cabralanum* (Piperaceae) nonpolar extract in poly(methyl methacrylate) by miniemulsion and evaluation of increase in the effectiveness of antileukemic activity in K562 cells. Int J Nanomedicine, 12, 8363-8373. doi: 10.2147/IJN.S134756

Merighi A and Lossi L (Edit) (2015). Immunocytochemistry and Related Techniques. Humana Press, New York, USA.

Minoura N, Idei K, Rachkov A, Uzawa H, Matsuda K (2003). (Molecularly Imprinted Polymer Membranes with Photoregulated Template Binding, Chem. Mater., 15(25), 4703-4704.

Miyata T, Jige M, Nakaminami T, Uragami T (2006). Tumor marker-responsive behavior of gels prepared by biomolecular imprinting. PNAS, 103(5), 1190-1193.

Moczko E, Mirkes EM, Caceres C, Gorban AN, Piletsky S (2016). Fluorescence-based assay as a new screening tool for toxic chemicals. Sci Rep, 6, 33922. Doi: 10.1038/srep33922.

Moczko E, Poma A, Guerreiro A, Sansalvador IPV, CaygillS, Canfarrotta F, Whitcombe MJ, Piletsky S (2013). Surface-modified multifunctional MIP nanoparticles. Nanoscale, 5, 9, 3733-3741.

Mohajeri SA, Malaekeh-Nikouei B, Sadegh H. (2012). Development of a pH-responsive imprinted polymer for diclofenac and study of its binding properties in organic and aqueous media. Drug Development and Industrial Pharmacy, 38, 5, 616-622.

Moein MM, Jayanbakht M, Karimi M, Akbari-adergani B, Abdel-Rahim M (2015). A new strategy for surface modification of polysulfone membrane by in situ imprinted sol-gel method for the selective separation and screening of L-tyrosine as a lung cancer biomarker. Analyst, 140, 6, 1939-1946.

Moein MM, Abdel-Rehim A, Abdel-Rehim M (2015). On-line determination of sarcosine in biological fluids utilizing dummy molecularly imprinted polymers in microextraction by packed sorbent. J Sep Sci, 38, 5, 788-795.

Monopoli MP, Walczyk D, Campbell A, Elia G, Lynch I, Bombelli FB, Dawson KA (2011). Physical-Chemical aspects of protein corona: Relevance to in vitro and in vivo biological impacts of nanoparticles. J Am Chem Soc, 133(8):2525-2534. doi:10.1021/ja107583h.

Moreira FTC, Ferreira MJMS, Puga JRT, Sales MGF (2016). Screen-printed electrode produced by printed-circuit board technology. Aplication to cancer biomarker detection by means of plastic antibody as sensing material. Sens Actuators B Chem, 223, 927-935.

Munawar H, Smolinska-Kempisty K, Cruz AG, Canfarotta F, Piletska E, Karim K, Piletsky SA (2018). Molecularly imprinted polymer nanoparticle-based assay (MINA): application for fumonisin B1 determination. Analyst, 143, 14, 3481-3488.

Nakane PK & Pierce GBJ (1967). Enzyme labelled antibodies for the light and electron microscopic localization of tissue antigens. J Cell Biol., 33, 307-318.

Naklua W, Suedee R, Lieberzeit PA. (2016). Dopaminergic receptor-ligand binding assays based on molecularly imprinted polymers on quartz crystal microbalance sensors. Biosens Bioelectron. 2016, 81:117-24.

Nayak S, Lyon LA (2004) Photoinduced Phase Transitions in Poly(*N*-isopropylacrylamide) Microgels, Chem. Mater., 16(13), 2623-2627.

Nicholls IA, Andersson HS, Golker K, Henschel H, Karlsson BC, Olsson GD, Rosengren AM, Shoravi S, Suriyanarayanan S, Wiklander JG, Wikman S (2011). Rational design of biomimetic molecularly imprinted materials: theoretical and computational strategies for guiding nanoscale structured polymer development. Anal Bioanal Chem., 400(6):1771-86. doi: 10.1007/s00216-011-4935-1.

Panagiotopoulou M, Kunath S, Haupt K, Tse Sum Bui B (2017). Cell and tissue imaging with molecularly imprinted polymers. Methods Mol Biol, 1575, 399-415.

Pasetto P, Maddock SC, Resmini M (2005). Synthesis and characterisation of molecularly imprinted catalytic microgels for carbonate hydrolysis. Anal. Chim. Acta, 542, 66-75.

Patil Y, Ameduri B (2013). Avances in (co)polymerization of alkyl 2-trifluoromethacrylates and 2-(trifluoromethyl) acrylic acid. Prog Polym Sci, 38, 5, 703-739.

Patra S, Roy E, Madhuri R, Sharma PK (2015). Nano-inferter based imprinted sensor for ultra trace level detection of prostate-specific antigen in both men and women. Biosens Bioelectron, 66, 1-10.

Patra S, Roy E, Madhuri R, Sharma PK (2015). Imprinted ZnO nanostructure-based electrochemical sensing of calcitonin: a clinical marker for medullary thyroid carcinoma. Anal ChimActa, 853, 271-284.

Peeters M, Csipai P, Geerets B, Weustenraed A, Grinsven B, Thoelen R, Gruber J, De Ceuninck W, Cleij TJ, Troost FJ, Wagner P (2013). Heat-transfer-based detection of l-nicotine, histamine, and serotonin using molecularly imprinted polymers as biomimetic receptors. Anal Bioanal Chem 405: 6453-6460.

Perez N, Whitcombe MJ, Vulfson EN. (2001). Surface imprinting of cholesterol submicrometer core-shell emulsion particles. Macromolecules, 34, 830-836.

Perez-Moral N, Mayes AG (2007). Molecularly imprinted multilayer core-shell nanoparticles: A surface grafting approach. Macromol. Rapid Commun., 28, 2170-2175.

Piacham T, Josell A, Arwin H, Prachayasittikul V, Ye I. (2005). Molecularly imprinted polymer thin films on quartz crystal microbalance using a surface bopund photo-radical initiator. Anal. Chim. Acta. 536, 191-196.

Piletska E, Abd BH, Krakowiak AS, Parmar A, Pink DL, Wall KS, Wharton L, Moczko E, Whitcombe MJ, Karim K, Piletsky SA (2015). Magnetic high throughput screening system for the development of nano-sized molecularly imprinted polymers for controlled deliveryof curcumin. Analyst, 140, 9, 3113-3120.

Piletska E, Piletsky S, Karim K, Terpetschnig E, Turner A. (2004). Biotin-specific synthetic receptors prepared using molecular imprinting. Anal Chem Acta. 504, 1, 179-183.

Piletsky SA, Piletskaya EV, El'Skaya AV, Levi R, Yano K, Karube I (1997). Optical Detection System for Triazine Based on Molecularly-Imprinted Polymers.Anal Lett 30:445-455.

Piletsky SS, Rabinowicz S, Yang Z, Zagar C, Piletska EV, Guerreiro A, Piletsky SA (2017). Development of molecularly imprinted polymers specific for blood antigens for application in antibody-free blood typing. Chem Commun (Camb), 53, 11, 1793-1796.

Pinkus GS (1982). Diagnostic immunocytochemistry of paraffin-embedded tissues. Human Pathol., 13, 411-415.

Poma A, Guerreiro A, Whitcombe MJ, Piletska EV, Turner APF, Piletsksky SA. (2013). Solid-Phase Synthesis of Molecularly Imprinted Polymer Nanoparticles with a Reusable Template – “Plastic Antibodies”. Adv Funct Mater. 2013 June 13; 23(22): 2821–2827. doi:10.1002/adfm.201202397.

Pozzi D, Caracciolo G, Digiacomo L, Colapicchioni V, Palchetti S, Capriotti AL, Cavaliere C, Zenezini Chiozzi R, Puglisi A, Laganà A (2015). The biomolecular corona of nanoparticles in circulating blood media. Nanoscale. 2015;7:13958-13966. doi:10.1039/C5NR03701H.

Priego-Capote F, Ye L, Shakil S, Shamsi SA, Nilsson S. (2008). Monoclonal behavior of moleculsarly imprinted polymer nanoparticles in capillary electrochromatography. Anal. Chem., 80, 2881-2887.

Pucci F, Lemma F, Muzzalupo R, Spizzirri UG, Trombino S, Cassano R, Picci N. (2004). Spherical Molecularly Imprinted Polymers (SMIPs) via a Novel Precipitation Polymerization in the Controlled Delivery of Sulfasalazine. Macromolecular Science, 4(1), 22-26.

Qader AA, Urraca J, Torsetness SB, Tonnesen F, Reubsaet L, Sellergren B (2014). Peptide imprinted receptors for the determination of the small cell lung cancer associated biomarker progastrin releasing peptide. J Chroma, 1370, 56-62.

Qin L, He X-W, Jia M, Li W-Y, Zhang Y-K. (2010). A Thermosensitive Monolithic Column as an Artificial Antibody for the On-line Selective Separation of the Protein. Chemistry A European Journal, 17(5), 1696-1704.

Qin L, He X-W, Yuan X, Li W-Y, Zhang Y-K (2011). Molecularly imprinted beads with double thermosensitive gates for selective recognition of proteins. Anal. Bioanal. Chem., 399(10), 3375-3385.

Qian T, Yu C, Zhou X, Ma P, Wu S, Xu L, Shen J. (2014). Ultrasensitive dopamine sensor based on novel molecularly imprinted polypyrrole coated carbon nanotubes. 58, 237-241.

Rachkov A, Minoura N. (2000). Recognition of oxytocin and oxytocin-related peptides in aqueous media using a molecularly imprinted polymer synthesized by the epitope approach. J Chromatogr A. 2000 Aug 11;889(1-2):111-8.

Ramanavicienea A, Ramanaviciusa A (2004). Molecularly imprinted polypyrrole-based synthetic receptor for direct detection of bovine leukemia virus glycoproteins. Biosensors and Bioelectronics, 20, 1076–1082.

Rebelo TSCR, Santos C, Costa-Rodrigues J, Fernandes MH, Noronha JP, Sales MGF (2014). Novel prostate specific antigen plastic antibody designed with charged binding sites for an improved protein binding and its application in a biosensor of potentiometric transduction. Electrochim Acta, 132, 142-150.

Reimhult K, Yoshimatsu K, Risveden K, Chen S, Ye L, Krozer A (2008). Characterization of QCM sensor surfaces coated with molecularly imprinted nanoparticles. Biosens. Bioelectron., 23, 1908-1914.

Ribeiro JA, Pereira CM, Silva AF, Sles MGF (2018). Disposable electrochemical detection of breast cancer tumour marker CA 15-3 using poly(Toluidine Blue) as imprinted polymer receptor. Biosens Bioelectron, 109, 246-254

Rifaie-Graham O, Pollard J, Raccio S, Balog S, Rusch S, Hernández-Castañeda MA, Mantel PY, Beck HP, Bruns N (2019). Hemozoin-catalyzed precipitation polymerization as an assay for malaria diagnosis.Nat Commun, 10, 1:1369. doi: 10.1038/s41467-019-09122-z.

Riskin M, Tel-Vered R, Frasconi M, Yavo N, Willner I (2010). Stereoselective and chiroselective surface plasmon resonance (SPR) analysis of amino acids by molecularly imprinted Au-Nanoparticle composites. Chem. Eur. J., 16, 7114-7120.

Roberts GS, Kozak D, Anderson W (2010). Tunable nano/micropores for particle detection and discrimination: scanning ion occlusion spectroscopy. Small, 6(23), 2653-8.

Rossetti C, Switnicka-Plak MA, Gronhaug Halvorsen T, Cormack PA, Sellergren B, Reubsaet L (2017). Automated protein biomarker analysis: on-line extraction of clinical samples by molecularly imprinted polymers. Sci Rep, 7, 44298. Doi: 10.1038/srep44298.

Santos, M.G.; Vitor, R.V.; Andrade, F.L.; Martins, I.; Figueiredo, E.C. Molecularly imprinted solid phase extraction of urinary diethyl thiophosphate and diethyl dithiophosphate and their analysis by gas chromatography–mass spectrometry. J. Chromatogr. B 2012, 909, 70–76.

Schmidt RH, Mosbach K, Haupt K. (2004). A simple method for spin-coating molecularlyimprinted polymer films of controlled thickness and porosity. Adv. Mater., 16, 719-722.

Schweitz L, Spegel P, Nilsson S. (2000). Molecularly imprinted microparticles for capillary elctrochromatographic enantiomer separation of propranolol. Analyst, 125, 1899-1901.

Scorrano S, Mergola L, Di Bello MP, Lazzoi MR, Vasapollo G, Del Sole R (2015). Molecularly imprinted composite membranes for selective detection of 2-deoxyadenosine (2-DA) in urine samples. Int J Mol Sci, 16, 6, 13746-13759.

Sharma PS, Wojnarowicz A, Sosnowska M, Benincori T, Noworyta K, D'Sousa F, Kutner W, (2016). Potentiometric chemosensor for neopterin, a cancer biomarker, using electrochemically synthesised molecularly imprinted polymer as the recognition unit. Biosens Bioelectron, 77, 565-572.

Shen X, Ye L. (2011). Interfacial molecular imprinting in nanoparticle stabilized emulsions. Macromolecules, 44, 5631-5637.

Shen X Ma Y, Zeng Q, Tao J, Huang J, Wang L (2016). Molecularly imprinted electrochemical sensor for advanced diagnosis of alpha-fetoprotein. Anal Methods, 8, 823-832.

Shi H,Tsai WB, Garrison MD, Ferrari S, Ratner BD. Template-imprinted nanostructured surfaces for protein recognition. Nature. 1999; 398(6728):593-7.

Shi SR, Key ME, Kalra KL (1991). Antigen retrieval in formalin-fixed paraffin-embeded tissues: an enhancement method for immunohistochemical staining based on microwave oven heating of sections. J Histochem Cytochem, 39, 741-748.

Shi X, Wu A, Qu G, Li R, Zhang D (2007). Development and characterisation of molecularly imprinted polymers based on methacrylic acid for selective recognition of drugs. Biomaterials, 28, 3741–3749.

Shuguo, H.; Li, L.; Xiwen, H. Molecularly Imprinted Polymers: A New Kind of Sorbent with High Selectivity in Solid Phase Extraction. Prog. Chem. 2005, 17, 531–543.

Sivakumaran M, Canfarotta F, Piletsky S, Chianella I (2019). Molecularly Imprinted Polymers: Potential Applications in Medicine and Biotechnology. (manuscript in preparation)

Sivakumaran M & Platt M (2017). Tunable resistive Pulse Sensing: Potential applications in Nanomedicine. Nanomedicine (Lond). 2016 Aug;11(16):2197-214. doi: 10.2217/nnm-2016-0097.

Smolinska-Kempisty K, Ahmad OS, Guerreiro A, Karim K, Piletska E, Piletsky S (2017). New potentiometric sensorbased on molecularly imprinted nanoparticles for cocaine detection. Biosens Bioelectron, 96, 49-54.

Smolinska-Kempisty K, Guerreiro A, Canfarotta F, Cáceres C, Whitcombe MJ, Piletsky S. A (2016). Comparison of the performance of molecularly imprinted polymer nanoparticles for small molecule targets and antibodies in the ELISA format. Scientific Reports, 6:37638, DOI: 10.1038/srep37638

Song, X.; Li, J.; Wang, J.; Chen, L. Quercetin molecularly imprinted polymers: Preparation, recognition characteristics and properties as sorbent for solid-phase extraction. Talanta 2009, 80, 694–702.

Sowerby SJ, Broom MF, Petersen GB. Sens.Actuators, B, 2007, 123, 325

Spegel P, Schweitz L, Nilsson S. (2003). Molecularlyimprintedpolymers in capillary electrochromatography: recent developments and future trends. Electrophoresis, 22-23, 3892-3899.

Sreenivasan K (1999). On the application of molecularly imprinted poly(HEMA) as a template responsive release system, J Appl Polym Sci, 71(11), 1819-1821.

Sterberger LA, Hardy PH, Cuculis JJ, Meyer HG (1970), The unlabelled antibody enzyme method of immunohistochemistry: preparation and properties of soluble antigen-antibody complex (horseradish peroxidase-antiperoxidase) and its use in identification of spirochaetes. J Histochem Cytochem., 18, 315.

Sulitzky C, Rueckert B, Hall AJ, Lanza F, Unger K, Sellergren B. (2002). Grafting of molecularly imprinted polymer films on silica supports containing surface-bound free radical initiators. Macromolecules, 35, 79-91.

Sun S, Zhang M, Yijun L, Xiwen H (2013). Article A Molecularly Imprinted Polymer with Incorporated Graphene Oxide for Electrochemical Determination of Quercetin. Sensors, 13, 5493-5506; doi:10.3390/s130505493

Svarna KS, Layton C, Bancroft JD (2018). Bancroft's Theory and Practice of Histological Techniques (8th Edition). Elsevir Publications.

Swerdlow SH, Campo E, Harris NL, Jaffe ES, Pileri SA, Stein H, Thiele J. WHO Classification of Tumours of Haematopoietic and Lymphoid Tissues. Revised 4th Edition, 2017). IARC: Lyon 2017

Tai DF, Lin CY, Wu TZ, Huang JH, Shu PY (2006). Artificial receptors in serologic tests for the early diagnosis of dengue virus infection. Clin Chem., 52(8):1486-1491.

Takeuchi T, Hayashi T, Ichikawa S, Kaji A, Masui M, Matsumoto H, Sasao R (2016). Molecularly imprinted tailor-made functional polymer receptors for highly sensitive and selective separation and detection of target molecules. Chromatography, DOI: 10,15583/jpchrom.2016.007

Takeuchi T, Minato Y, Takase M, Shinmori H (2005). Molecularly imprinted polymers with halogen bonding-based molecular recognition sites. Tetrahedron Lett, 46, 9025-9027.

Tamayo FG, Casillas JL, Martan-Esteban A. (2005). Evaluation of new selective molecularly imprinted polymers prepared by precipitation polymerisation for the extraction of phenylurea herbicides. J Chrom.1069, 2, 173-181.

Tan CJ and Tong YW. (2007). Molecularly imprinted beads by surface imprinting. Anal. Bioanal. Chem. 389, 369-376.

Tang P, Wang Y, Huo J, Lin X (2018). Love wave sensor for prostate-specific membrane antigen detection based on hydrophilic molecularly-imprinted polymer. Polymers, 10, 5. Doi: 10.3390/polym10050563

Tang Q, Gong C, Lam MHW, Fu X (2011). Preparation of a photoresponsive molecularly imprinted polymer containing fluorine-substituted azobenzene chromophores. Sensors Actuators B, 156,1, 100-107.

Tavares APM, Truta LAANA, Moreira FT C, Carneiro LPT, Sales MGF (2019). Self-powered self-signalled autonomous electrochemical biosensor applied to carcinoembryonic antigen determination. BiosensBioelectron, 140, 111320. Doi 10.1016j.bios.2019.111320.

Taylor CR & Burns J (1974). The demonstratoion of plasma cells and other immunoglobulin-containing cells in formalin fixed, paraffin embedded tissues using peroxidase labelled antibody. J Clin Path., 27, 14-20.

Tiwari A, Deshpande SR, Kobayashi H, Turner AP. (2012). Detection of p53 gene point mutation using sequence-specific molecularly imprinted PoPD electrode. Biosens. Bioelectron., 35(1):224-229.

Ton XA, Acha V, Haupt K, Tse Sum Bui B (2012).Direct fluorimetric sensing of UV-excited analytes in biological and environmental samples using molecularly imprinted polymer nanoparticles and fluorescence polarization. Biosens Bioelectron 36:22-28.

Tuffaha MSA, Guski H, Kristiansen G (2018). Immunocytochemistry in Tumour Diagnostics (First Edition), Springer International Publications.

Turiel, E.; Martín-Esteban, A. Molecularly imprinted polymers for sample preparation: A review. Anal. Chim. Acta 2010, 668, 87–99.

Turkewitsch P, Wandelt B, Darling GD, Powell WS (1998). Fluorescent Functional Recognition Sites through Molecular Imprinting. A Polymer-Based Fluorescent Chemosensor for Aqueous cAMP. Anal Chem 70:2025-2030.

Surugiu I, Ye L, Yilmaz E, Dzgoev A, Danielsson B, Mosbach K, Haupt K (2000). An enzyme-linked molecularly imprinted sorbent assay. Analyst 125:125:13-16.

Vaihinger D, Landfester K, Krauter I, Brunner H, Tovar GEM. (2002). Molecularly imprinted polymer nanospheres as synthetic affinity receptors obtained by miniemulsion polymerisation. Macromol. Chem. Phys, 203, 1965-1973.

Verheyen E, Schillemans JP, van Wijk M, Demeniex MA, Hennink WE, van Nostrum CF (2011). Challenges for the effective molecular imprinting of proteins. Biomaterials, 32, 11, 3008-3020.

Viswanathan S, Rani C, Ribeiro S, Delarue-Matos C (2012). Molecular imprinted nanoelectrodes for ultrasensitive detection of ovarian cancer marker. Biosens Bioelectron, 33, 179-183.

Vlatakis G, Andersson L.I, Müller R, Mosbach K (1993). Drug assay using antibody mimics made by molecular imprinting. Nature, 361, 645–647.

Volkmann A& Brüggemann O (2006). Catalysis of an ester hydrolysis applying molecularly imprinted polymer shells based on an immobilised chiral template. React. Funct. Polym. 2006, 66, 1725–1733.

Vyberg M & Nielsen S (1998). Dextran polymer conjugate two-step visualisation system for immunocytochemistry: a comparison of En Vision+ with two three step avidin-biotin techniques. Applied Immunohistochemistry, 6(1): 3-10.

Walker JM(1994). The dansyl method for identifying N-terminal amino acids.Methods Mol Biol. 1994;32:321-8.

Walshe M, Howarth J, Kelly MT, O'Kennedy R, Smyth MR. The preparation of a molecular imprinted polymer to 7-hydroxycoumarin and its use as a solid-phase extraction material. J Pharm Biomed Anal. (1997). 16(2), 319-325.

Wan W, Biyikal M, Wagner R, Sellergren B, Rurack K (2013).Fluorescent Sensory Microparticles that “Light-up” Consisting of a Silica Core and a Molecularly Imprinted Polymer (MIP) Shell. Angew Chem Int Ed 52:7023-7027.

Wandera D, Wickramasinghe SR, Husson SM (2010). Stimuli-responsive membranes, J. Memb. Sci., 357, 5-35.

Wang JP, Tang WW, Fang GZ, Pan MF, Wang S (2011). Development of a Biomimetic Enzyme-linked Immunosorbent Assay Method for the Determination of Methimazole in Urine Sample. J Chin Chem Soc 58:463-469.

Wang L, Zhang ZJ (2008).Chemiluminescence imaging assay dipyridamole based on molecular imprinted polymer as recognition material. Sens Actuators B 133:40-45.

Wang L, Zhi K, Zhang Y, Liu Y, Zhang L, Yasin A, Lin Q (2019). Molecularly Imprinted Polymers for Gossypol via Sol^{-}Gel, Bulk, and Surface Layer Imprinting-A Comparative Study. Polymers, 11, 4. pii: E602. doi: 10.3390/polym11040602.

Wang S, Yin D, Wang W, Shen X, Zhu J-J, Chen H-Y, Liu Z (2016). Targeting and Imaging of Cancer Cells via Monosaccharide-Imprinted Fluorescent Nanoparticles. Scientific Reports, 6., 22757, DOI: 10.1038/srep22757.

Wang X, Wang L, He X, Zhang Y, Chen I. (2009). A molecularly imprinted polymer-coated nanocomposite of magnetic nanoparticles for estrone recognition. Talanta, 78, 327-332.

Watanabe M, Akahoshi T, Tabata Y, Nakayama D. (1998). Molecular Specific Swelling Change of Hydrogels in Accordance with the Concentration of Guest Molecules. J. Am. Chem. Soc., 120 (22), 5577-5578.

Weatherall E, Willmott GR (2015). Applications of tunable resistive pulse sensing. *Analyst*, 140, 3318-3334.

Wei ST, Molinelli A, Mizaikoff B (2006). Molecularly imprinted micro and nanospheres for the selective recognition of 17β-estradiol. Biosens Bioelectron 21:1943-1951.

Wenqiang Y, Li Y, Huang X (2014). Fluorinated poly(meth)acrylate: Synthesis and properties. Polymer 55 (2014) 6197e6211

Whitcombe MJ, Rodriguez ME, Villar P, , Vulfson EN. A new method for the introduction of recognition site functionality into polymers prepared by molecular imprinting- synthesis and characterisation of polymeric receptors for cholesterol. J.Am.Chem.Soc., 117, 7105-7111.

Wulff, G. Biorecognition in molecularly imprinted polymers. Concept, chemistry and application. In Molecular Interactions in Bio-separations; Ngo, T.T., Ed.; Plenum Press: New York, NY, USA, 1993; pp. 363–381.

Wulff G, Chong BO, Kolb U. (2006). Soluble single-molecule nanogels of controlled structure as a matrix for efficient artificial enzymes. Angew. Chem. Int. Ed, 45, 2955-2958.

Wulff, G.; Sarhan, A. The use of polymers with enzyme-analogous structures for the resolution of racemate. J. Angew. Chem. Int. Ed. 1972, 11, 341–345.

Xie C, Zhang Z, Wang D, Guan G, Gao D, Liu J (2006). Surface molecular self assembly strategy for TNT imprinting of polymer nanowire/nanotube arrays. Anal Chem. 78, 8339-8346.

Xing R, Wen Y, Dong Y, Wang Y, Zhang Q, Liu Z (2019). Dual molecularly imprinted polymer-based plasmonic immunosandwich assay for the specific and sensitive detection of protein biomarkers. Anal Chem, 91, 15, 9993-10000.

Yanez-Sedeno P, Campuzano S, Pingarron JM (2017). Electrochemical sensors based on magneticmolecularlyimprintedpolymers: A review. Anal Chim Acta. 2017 Apr 1;960:1-17.

Yang K, Berg BMM, Zhao C, Ye L. (2009). One-pot synthesis of hydrophilic molecularly imprinted nanoparticles. Macromolecules, 42, 8739-8746.

Yang YQ, He XW, Wang YZ, Li WY, Zhang YK (2014). Epitope imprinted polymer coating CdTe quantum dots for specific recognition and direct fluorescent quantification of the target protein bovine serum albumin.Biosens Bioelectron. 15;54:266-72. doi: 10.1016/j.bios.2013.11.004.

Yao W, Li Y, Huang X (2014). Fluorinated poly(meth)acrylate: Synthesis and properties. Polymer, 55 (2014) 6197e6211

Ye J, Chen Y, Liu Z (2014). A Boronate Affinity Sandwich Assay: An Appealing Alternative to Immunoassays for the Determination of Glycoproteins. Angew Chem Int Ed 53:10386-10389.

Ye L, Cormack PAG, Mosbach K. (1999). Molecularly imprinted monodisperse microspheres for competitive radioassay. Anal. Commun, 36, 35-38.

Ye L, Yilmaz E. (2005). Molecularly Imprinted Materials, Science and Technology, eds. Yan M and Ramstrom O., Part V 'Molecularly Imprinted Polymer Beads' Marcel Dekker, New York, pp. 435-454.

Yilmaz E, Ramstrom O, Moller P, Sanchez D and Mosbach K. (2002). A facile method for preparing molecularly imprinted polymer spheres using spherical silica templates. J. Mater. Chem., 12, 1577-1581.

Yoshida K, Kurogi T, Torisu T, Watanabe I, Murata H (2013). Effects of 2,2,2-trifluoroethyl methacrylateon properties of autopolymerized hard direct denture reline resins. Dent Med Journal, 32, 5, 744-752.

Yoshimatsu K, Reimhult K, Krozer A, Mosbach K, Sode K, Ye L (2007). Uniform molecularly imprinted microspheres and nanoparticles prepared by precipitation polymerization: The control of particle size suitable for different analytical applications. Anal Chim Acta 584:112-121.

Yoshimatsu K, Ye L, Lindberg J, Chrlonakis IS (2008). Selective molecular adsorption using electrospun nanofibre affinity membranes. Biosens. Bioelectron., 23, 1208-1215.

Yoshimatsu K, Ye L, Stenlund P, Chronakis I.S. (2008). A simple method for preparation of molecularly imprinted nanofiber materials with signal transduction ability. Chem, Commun., 2022-2024.

Zeng Z, Hoshino Y, Rodriguez A, Yoo H, Shea KJ. (Synthetic polymer nanoparticles with antibody-like affinity for a hydrophilic peptide. ACS Nano, 4, 199-204.

Zhang H. (2013). Application of controlled/'living' radical polymerization techniques in molecular imprinting. In 'Molecular Imprinting: Principles and Applications of Micro- and Nanostructured Polymers. Pan Stanford Publishing Pte Ltd, Singapore, pp 105-160.

Zhang Q, Wang Q, Zhan X, Chen F (2014). Synthesis and Performance of Novel Fluorinated Acrylate Polymers: Preparation and Reactivity of Short Perfluoroalkyl Group Containing Monomers. *Ind. Eng. Chem. Res.,*2014, 53 (19), pp 8026–8034 **DOI:** 10.1021/ie404217d

Zhang W, He X-W, Chen Y, Li WY, Zhang YK (2011). Composite of CdTe quantum dots and molecularly imprinted polymer as a sensing material for cytochrome c. Biosens Bioelectron, 26, 2553-2558.

Zhang Z, Liu J. (2016). Molecularly Imprinted Polymers with DNA Aptamer Fragments as Macromonomers. ACS Appl Mater Interfaces, 8(10):6371-8.

Zhao WF, Fang BH, Li N, Nie SQ, Wei Q, Zhao CS (2009). Fabrication of pH-responsive molecularly imprinted polyethersulfone particles for bisphenol-A uptake. J. Appl. Polym. Sci., 113(2), 916-921.

Zhao YY, Ma YX, Li H, Wang LY (2012). Composite QDs@MIP Nanospheres for specific recognition and direct fluorescent quantitation of pesticides in aqueous media. Anal Chem, 84:386-395.

Zhao Z, Teng Y, Xu G, Zhang T, Kan X (2013). Molecular Imprinted Polymer Based Thermo-Sensitive Electrochemical Sensor for Theophylline Recognition. Anal. Lett., 46(14), 2180-2188.

Zhou J, Gan N, Li T, Hu F, Li X, Wang L, Zheng L (2014). A cost-effective sandwich electrochemiluminescence immunosensor for ultrasensitive detection of HIV-1 antibody using magnetic molecularlyimprintedpolymers as capture probes. Biosens Bioelectron., 54:199-206.

Zhou WH, Lu CH, Guo XC, Chen FR, Yang HH, Wang XR. (2010). Mussel inspired molecularly imprinted polymer coating superparamagnetic particles for protein recognition. J. Mater. Chem, 20, 880-883.

Zimmerman SC, Wendland MS, Rakow NA, Zharov I, Suslick KS. (2002). Synthetic hosts by monomolecular imprinting inside dentrimers. Nature, 418, 399-403.

Zor E, Morales-Narváez E, Zamora-Gálvez A, Bingol H, Ersoz M, Merkoçi A. (2015). Graphene Quantum Dots-based Photoluminescent Sensor: A Multifunctional Composite for Pesticide Detection. ACS Appl Mater Interfaces. 16;7(36):20272-9.

Zrinyi M (2000). Intelligent polymer gels controlled by magnetic fields, Colloid and Polymer Science, 278 (2), 98-103.

Appendix 1

Examples of Lineage-specific antigens. (Source: Diagnostic Immunohistochemistry (Edited by Dabbs D, 2018); Theory and Practice of Histological Techniques (Editors Bancroft JD & Gamble M, 2002)

Cell type	Lineage specific antigen(s)
Leucocytes (white cells)	Common leukocyte antigen (CD45 antigen)
Myeloid cells	CD13, CD33, MPO
Monocytes	CD14
Precursor lymphoid cells (blasts)	TDT
B lymphocytes	CD19, CD20, CD21, CD22, CD23, CD79a, PAX5
T cells	CD2, CD3, CD4, CD5, CD7, CD8
T helper cells	CD4
T suppressor cells	CD8
Natural killer cells	CD56
Megakaryocytes	CD41, CD61
Erythroid cells	Glycophorin A
Plasma cells	CD138
Histiocytes	CD68
Epithelial cells	Cytokeratin, epithelial membrane antigen
Endothelial cells	CD31, CD34, Factor VIII, thrombomodulin
Mesenchymal tissue	S-100P, desmin
Liver cells	AE1/AE3, CK7, CK20, CAM5.2, 35BH11
Nerve cells	Neurofilament proteins (NFPs)
Neuroendocrine cells	Chromogranin A, synaptophysin, neuron-specific enolase,
Bone cells	Osteocalcin, osteonectin
Muscle cells	Desmin, vimentin, actins, myoglobin, myogenin, caldesmon
Skin cells	Keratin,
Prostate cells	PSA, PAP, PSMA, AMACR
Fibroblasts	Vimentin

Appendix 2

Examples of disease associated antigens. (Source: WHO Classification of Tumours of haemopoietic and Lymphoid Tissues 5th Edition (2018); Diagnostic Immunohistochemistry (Edited by Dabbs D, 2018).

Disease	Antigen expression
Acute promyelocytic leukaemia	PML-RARA fusion protein
Chronic myeloid leukaemia	BCR-ABL fusion protein
Hairy cell leukaemia	B-RAF, CD103, Cd11c, CD25, FMC-7
Mantle cell lymphoma	Cyclin D1
Follicular NHL	BCL2
Hodgkin lymphoma	CD15
Anaplastic large cell lymphoma	ALK, nucleophosmin, CD30
Lymphoblastic lymphoma, acute lymphoblastic leukaemia	CD10 (CALLA)
Aggressive NK cell leukaemia	FAS ligand
Large granular lymphocytic leukaemia	CD57, perforin
Adult T cell leukaemia/lymphoma	CCR4, FOXP3, CD25
Hepatosplenic T-cell lymphoma	TIA1, granzyme M
Mycosis fungoides	CLA
Angioimmunoblastic T cell lymphoma	CXCL13
Hodgkin lymphoma	CD15, CD30
Histiocytic sarcoma	CD68, CD163, lysozyme
Langerhans cell tumour	CD1a, langerin, S100, vimentin
Follicular Dentritic cell sarcoma	KiM4p, clusterin
Breast cancer	BRCA, CEA, EMA,
Colon cancer	Cytokeratin 20, CEA
Prostate cancer	PSA, PAP, PSMA, AMACR
Lung cancer	Cytokeratin 7, CEA, EMA,
Ovarian cancer	Cytokeratin 7
Endometrial cancer	Cytokeratin 7, EMA
Liver cancer	AE1/AE3, CK7, CK20, CAM5.2,
Skin cancer	Cytokeratin 5/6, EMA,
Gastric cancer	CEA
Germ cell tumours	CK, EMA, PLAP, AFP
Thyroid cancer	Thyroglobulin
Neuroendocrine tumour	CAM5,2, CK7, Chromogranin A, synaptophysin,
Renal cancer	RCC, vimentin,

Appendix 3

Examples of Smart MIPs for potential biotechnology applications

Class of SMART MIP	Template	Suggested application	Reference
Thermosensitive			
	Adrenaline	Recognition	Watanabe *et a*l, J. Am. Chem. Soc., 1998, 120, 5577-
	Theophylline	Sensor	Zhao *et a*l, Anal. Lett., 2013, 46, 2180-2188.
	Lysozyme	Separation	Qin *et al,* Chem. Eur. J., 2011, 17, 1696-1704.
	Cefalexin	Drug release	Pan *et al*, Appl. Surf. Sci., 2013, 287, 211-217.
	Myoglobin	Sensors, assays	Turan *et al*, Macromol. Biosci., 2009, 9, 421-428.
	Dopamine	Electrophoresis	Suedee *et al*, J. Chrom. A, 2006, 1114, 2339-249.
pH responsive			
	Sulphasalazine	Drug delivery	Puoci *et al,* Macromol. Biosci., 2004, 4, 22-26.
	Omeprazole	Drug delivery	Suedee *et al*, J. C. Release, 2010, 142, 122-131.
	Insulin	Drug delivery	Li *et al*, Adv. Mater. Lett., 2010, 1, 4-10.
	Doxorubicin	Drug delivery	Zhang *et al*, J. Pharm. Sci, 2014, 103, 643-651.
Magnet responsive			
	Sildenafil	Extraction	Ding *et al*, 2011. J Hazard Mater., 15;191:177-83.
	Ofloxacin	Separation	Qu *et al*, 2010 J Chromatogr A. ;1217(39):6115-21.
	Lysozyme	Extraction	Jing *et al,* 2011, Anal Chim Acta;692(1-2):73-9.
	BSA	Separation	Zhang *et al,* 2011, Anal Bioanal Chem;401:2855-63.
	Sulfadiazine	Detection	Lu *et al*, 2012,Anal Chim Acta; 718:84-91.
	Oxytetracycline	Separation	Chen *et al*, 2009, J Chromatogr A, 1;1216:3710-9.
	Ciprofloxacin	Extraction	Chen *et al*, 2010, Anal Chim Acta, 3;662(1):31-38.
	Streptomycin	Sensor	Liu *et al*, 2013, Biosens Bioelectron,15;41:551-556
	BSA	Extraction	Tan *et a*l, 2008, Anal Chem 1;80(3):683-92.
	Benzyl penicillin	Sensor	Hu *et al*, 2011, Anal Chim Acta, 18;698(1-2):61-8.
Photoresponsive			
	Dansylamide	Detection	Minoura *et al*, 2003, Chem. Mater., 15, 4703-4704
	Paracetamol	Detection	Gong *et al*, 2008,
	Ibuprofen	Detection	Li *et a*l, 2013

	Guanine	Detection	Li *et al*, 2015
Biomolecule responsive			
	Hydrocortisone	Drug delivery	Sreenivasan, 1999
	Alpha fetoprotein	Sensing	Miyata *et a*l, 2006
	Glucose	Sensing	Kawamura *et a*l, 2012
Ionic Strength responsive			
	NaCl	Separation	*Huang et al*, 2009
Multiresponsive			
Thermo/magnetic	Sulphamethazine	Drug release,	Xu *et a*l, J. Hazard. Mater., 2012, 233, 48-56.
Thermo/magnetic	BSA	Separation, drug delivery, sensing	Li *et al*, Biosens. Bioelectron., 2014, 51, 261-267.
Ph/thermo	glycoprotein	Sensing, separation	Gao *et al*, Colloids Surf. A, 2013, 433, 191-199.
Thermo/salt	Bovine serum albumin	Sensors, delivery, controlled release	Hua *et a*l, Langmuir, 2008, 24, 5773-5780.
Thermo/salt/ biomolecule	lysozyme	Synthetic receptor	Chen *et al*, J. Mol. Recognit., 2008, 21, 71-77.
Photo/thermo/ph	propranolol	Drug delivery, bioanalysis	Ma *et al*, Chem. Commun., 2012, 48, 6217-6219.

Appendix 4
Molecularly imprinted polymers for biomolecules

Type of Biomolecule	Example	Reference
Vitamins	Ascorbic acid	Prasad *et al* (2008) J Chromatogr A, 1198-1199:59-66.
	Folic acid	Quaglia *et al* (2001) J Am Chem Soc., 123(10):2146-54.
	Pyridoxine	Alizadeh T (2008) Anal Chim Acta, 623(1):101-8
Hormones	Corticosteroids	Ramstrom *et al* (1996) Chem Biol., 3(6):471-7.
	17β Oestradiol	Ma *et al* (2011) Biosens Bioelectron., 26(5):2791-5.
	Estrogen	Buszewski *et al* (2010). Anal Bioanal Chem., 397(7):2977-86.
	Testosterone	Zhang *et al* (2014). Anal Chem., 463:7-14.
	Ephedrine	Ramstrom *et al* (1996). J Mol Recognit., 9(5-6):691-6.
	Insulin	Moein *et al* (2014). Talanta, 121:30-6.
Neurotransmitters	Dopamin	Lakshmi *et al* (2009) Anal Chem, 81(9):3576-84.
	Catechol	Lakshmi *et al* (2009) Anal Chem, 81(9):3576-84.
	Serotonin	Okutucu *et al* (2008) Talanta, 76(5):1153-8.
	Cholecystokinin	Ji *et al* (2015). Biomed Chromatogr, 8:1280-9.
Metabolites	AMP	Dejous *et al* (2016). Sensors, 16(6). doi: 10.3390/s16060915.
	ATP	Plewa *et al* (2012). J Med Chem., 55(20):8712-20.
	Creatinine	Subrahmanyam et al (2001) Biosens Bioelectron 16, 631-7.
	Uric acid	Prasad *et al* (2007). J Chromatogr A, 1173(1-2):18-26.
	Bilirubin	Syu *et al* (2005). Biomaterials, 22, 4684-92
	Urea	Alizadeh T (2010) Anal Chim Acta, 669(1-2):94-101
Biomarkers	CEA125	Buyuktiryaki *et al* (2017). Talanta, 167:172-180.
	PSA	Jolly *et al* (2016) Biosens Bioelectron, 75:188-95.
	Beta 2 microglobulin	Yang *et al* (2017) J Chromatogr, 1494:18-26.
	Neopterin	Sharma *et al* (2016) Biosens Bioelectron, 77:565-72.
	ProGRP	Rossetti *et al* (2017) Sci Rep, 7:44298.
	Alpha fetoprotein	Karfa *et al* (2016) Biosens Bioelectron, 78:454-63.
		Karimian *et al* (2014) Biosens Bioelectron, 59:160-5.
Sugars	Glucose	Parmpi & Kofinas (2004) Biomaterials, 25(10):1969-73.
	Fructose	Rajkumar *et al* (2008) Talanta, 76(5):1119-23.
	Galactose	Okutucu *et al* (2009) Talanta, 78(3):1190-3.
Lipids	Cholesterol	Hwang *et al* (2002). J Chroimatogr A, 962(1-2):69-78.
	LDL	Chunra *et al* (2016). Anal Chem., 88(2):1419-25.
	Phospholipids	Pegoraro *et al* (2008). Biosens Bioelectron., 24(4):748-55.

Aminoacids/	Tryptophan	Monier *et al* (2015). J Colloid Interface Sci., 445:371-9.
Peptides/	Phenylalanine	Casey *et al* (2010). Biosens Bioelectron., 26(2):703-9
Proteins	Glycoproteins	Shi *et al* (1999) Nature, 398(6728):593-7.
	Albumin	Shi *et al* (1999) Nature, 398(6728):593-7.
	Immunoglobulin G	Shi *et al* (1999) Nature, 398(6728):593-7.
	Lysozyme	Shi *et al* (1999) Nature, 398(6728):593-7.
	Ribonuclease	Lin *et al* (2006). Biosens Bioelectron., 22(4):534-43.
	Protein C	Seifner *et al* (2009) Anal Chim Acta, 651(2):215-9.
	Red cell antigens	Deng *et al* (2013). Sensors, 13, 12994-13004.
	Haemoglobin	Wu *et al* (2010). Analyst, 135(10):2523-7.
	Myoglobin	Kugimiya *et al* (2001). Biosens Bioelectron, 9-12:1059-62.
	Sialic acid	Jing *et al* (2010), Biosens Bioelectron, 26(2):301-6.
	Lysozyme	Lin *et al* (2006). Biosens Bioelectron., 22(4):534-43.
	Endotoxin	Bossi *et al* (2001). Anal Chem, 73(21):5281-6.
	Histamin	Trikka *et al* (2012). Aminoacids, 43(5):2113-24.
	Cytochrome C	Zhang *et al* (2011). Biosens Bioelectron., 26(5):2553-8.
	Interferon ά 2a	Rodrigues *et al* (2013). J Chromatogr A, 1318:43-8.
	ProGRP	Rossetti *et al* (2014). 86(24):12291-8.
	Atropine	Abbasifar *et al* (2016). J Fluoresc., 26(5):1645-52.
	Hyaluran	Panagiotopoulou *et al* (2017) Biosens Bioelectron., 88:85-93.
	sTfR	Liu *et al* (2015). Anal Chem., 87(21):10910-9.
	VEGF	Cecchini *et al* (2017). Nano Lett., 17(4):2307-2312.
	Chondroitin sulphate	Baydemir G (2016). Artif Cells Nanomed Biotechnol., 2016;44(2):610-7.
Nucleic acids	dsDNA	Ogiso *et al* (2006) Biomaterials, 27(22):4177-82.

Appendix 5
Molecularly imprinted polymers for drugs

Class of drug	Example	Reference
Antibiotics	Chloremphenicol	Suarez-Rodriquez *et al* (2001) Biosens Bioelectron,16, 955-61.
	Penicillin G	Cederfur *et al* (2003). J Comb Chem., 5(1):67-72.
	Amoxicillin	Yin *et al* (2010). J Chromatogr A, 1217(33):5420-6.
	Ampicillin	Yin *et al* (2010). J Chromatogr A, 1217(33):5420-6.
	Tetracycline	Hou *et al* (2016). Talanta, 146:34-40.
	Oxytetracycline	Moreira *et al* (2010). Bioisens Bioelectron., 26(2):566-74.
	Doxycycline	Li *et al* (2015). Analyst, 140(13):4702-7.
	Vancomycin	Korposh *et al* (2014). Analyst, 139(9):2229-36.
	Nitrofurantoin	Athikomrattanakul *et al* (2009), Biosens Bioelectron, 25:82-7.
	Erythromycin	Lian *et al* (2012). Biosens Bioelectron, 38(1):163-9.
	Azithromycin	Zhou *et al* (2016). PLoS., 11(1):e0147002.
	Ciprofloxacin	Okan *et al* (2017). Biosens Bioelectron., 88:258-264.
	Norfloxacin	Wang *et al* (2013). Anal Bioanal Chem., 405(8):2525-33.
	Sulphonamides	Chen *et al* (2016). J Sep Sci., 39(24):4866-4875.
	Sulfadiazine	Lu *et al* (2012). Anal Chim Acta, 718:84-91.
	Vancomycin	Chianella *et al* (2013). Anal Chem., 85(17):8462-8.
	Cefotaxime	Yang *et al* (2014). Biosens Bioelectron., 53:447-52.
	Dapsone	Lu *et al* (2012). Anal Bioanal Chem., 404(1):79-88.
Antiviral drugs	Zidovidine	Duy *et al* (2009). J Chromatogr B, 877:1101-8.
	Acyclovir	Wu *et al* (2013). J Chromatogr A, 1285:124-31.
Antiprotozoal drugs	Metronidazole	Xiao *et al* (2016). Bioisens Bioelectron., 81:54-60.
Anti-cancer drugs	Sunitinib	Pellizonni *et al* (2016) Biosens Bioelectron, 86:913-9.
	Tamoxifen	Ray *et al* (2016) Anal Bioanal Chem., 408(7) 1855-1861.
	Methotrexate	Liu *et al* (2009). J Chromatogr A, 1216(44):7533-8.
	Ifosfamide	Bali Prasad *et al* (2017). Biosens Bioelectron., 94:1-9.
Anti-diabetic drugs	Metformin	He *et al* (2006). Anal Bioanal Chem., 385(1):128-33.
	Glibenclamide	Lahsini *et al* (2013). Acta Pharm., 63(2):265-75.
Bronchodilators	Theophylline	Vlatakis *et al* (1993). Nature, 361(6413):645-7.
	Salbutamol	Li *et al* (2017). Biosens Bioelectron., 90:210-216.
Tranquilisers	Diazepam	Vlatakis *et al* (1993). Nature, 361(6413):645-7.
	Benzodiazepines	Figueiredo *et al* (2011). Analyst, 136(18):3753-7.
Antidepressants	Amitriptyline	Santos *et al* (2017). Talanta, 163:8-16.
Antiepileptics	Phenytoin	Bereczki *et al* (2001). J Chromatogr A, 930(1-2):31-8.

	Carbamazepine	Beltran *et al* (2007). Anal Chim Acta, 597(1):6-11.
Analgesics	Salicylic acid Paracetamol	Sreenivasan K (2007). Anal Chim Acta, 583(2):284-8. Liu *et al* (2010). Appl Biochem Biotechnol., 160(2):328-42.
Cardiotropic drugs	Digoxin	Gonzalez *et al* (2008). Biosens Bioelectron., 23(11):1754-8.
Hormone analogues	17β-estradiol Methyl testosterone	Xiao *et al* (2017). Food Chem., 221:82-86. Saadaoui *et al* (2016). J Mol Recognit., doi: 10.1002/jmr.2594
Immunomodulators	Mycophenolate	Yin *et al* (2006). J Chromatogr B, 844(1):142-7.
Narcotics	Methamphetamine Tramadol	Romero Guerra *et al* (2009). Analyst, 134(8):1565-70. Afkhami *et al* (2013). Biosens Bioelectron., 44:34-40.
Antihypertensives	Propranolol Atenolol Beta blockers	Gurtavo *et al* (2013). Anal Bioanal Chem., 405(1):287-95. Iacob *et al* (2015). Anal Chem., 87(5):2755-63. Santos *et al* (2015). Analyst, 140(8):2696-703.
Anticoagulants	Heparin	Li *et al* (2013). Anal Biochem, 434(2):242-6.
Anti-inflammatory drugs	Mefenemic acid Naproxene	Madrakian *et al* (2015). Bioisens Bioelectron., 68:712-8. Tahmasebi *et al* (2016). J Chromatogr., 1470:19-26.